Appendix D

UC Davis Air Monitoring Report

Final Report of
Nishi Property Particulate Measurements

Prepared for
Tim Ruff
of
Norcal Land,

by

Dr. David E. Barnes
Department of Physics
University of California, Davis
Davis, CA 95616

April 25, 2014

Printed on Recycled Paper

I. ASSIGNMENT

I was asked to conduct a preliminary study of particulates using the methods developed by the UC Davis DELTA Group, especially utilizing the ability to collect and analyze separately, the ultra-fine component of PM 2.5. The purpose of this study was to help assess potential impacts on the Nishi property, due to its proximity to interstate 80. The results of the study would be a report, to include a brief interpretation of the data, including all detectable elemental and mass concentrations available using the DELTA Group analysis techniques. Final data would include providing concentrations of PM10, PM2.5 and, ultra-fine (0.09 to 0.0 μm) total mass and elemental components (if detected using the applied techniques).

One goal of this study was to provide measurements and analysis on a short time frame. There were two reasons for this. The primary being the impact of concern is ultra-fine components from the nearby freeway, impacts of this nature are biggest during our strong winter inversions. The time of year and weather forecasts suggested that potential for these conditions would vastly decrease very soon. The second reason was to provide some preliminary data that might allow the overall project to continue to progress, by using data specific to the property location for the Environmental Impact Report.

II. SITE SELECTION

The property is located adjacent to interstate 80 which borders to the south and east, the UC Davis campus (proper) to the west and north and the City of Davis to the east and north, see Figure 1. Note the freeway generally passes to the south of the property and angled from southwest to slightly north of east.

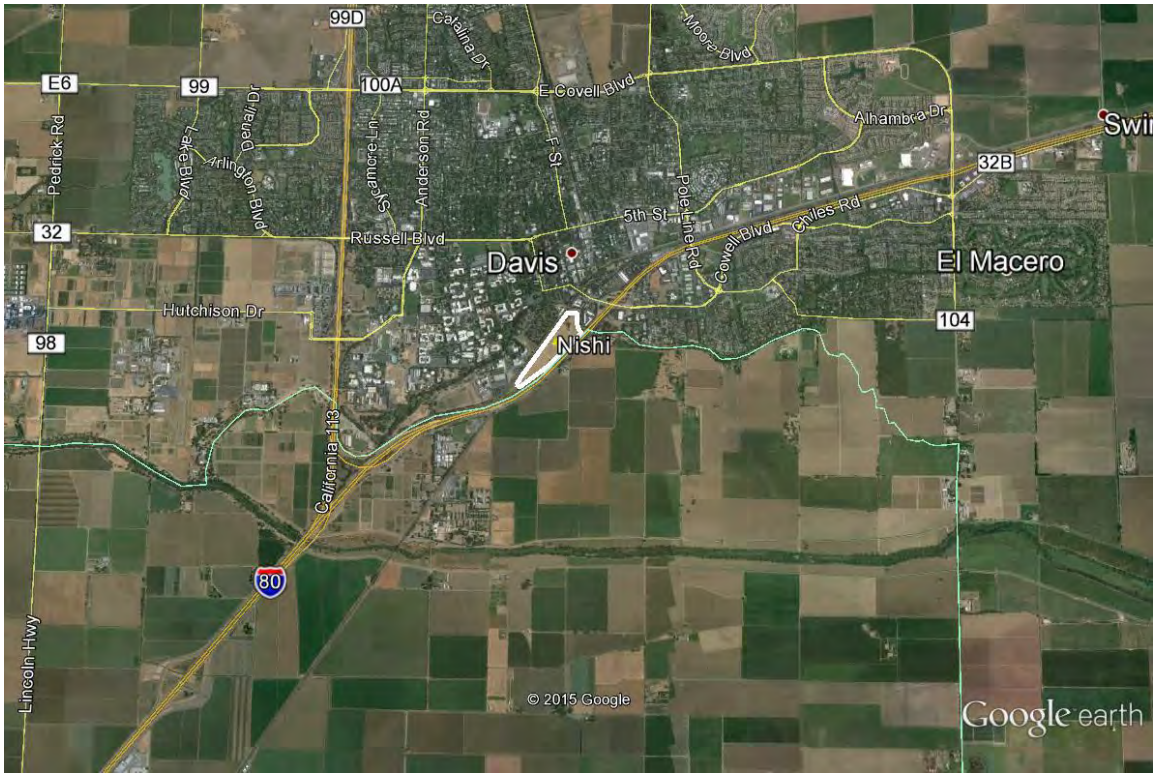

Figure 1 Overview of Nishi property and Interstate 80.

I visited the property and nearby areas with Tim Ruff to determine the most feasible and appropriate site location. We had had several preliminary conversations primarily dealing with the logistics required of a site, but also discussed potential locations on and adjacent to the Nishi property. We visited the area and determined a location immediately east of the property, near Olive Drive would provide the facilitation necessary for siting. Although the Olive Drive site (OlDr) location was not on the property, the position with respect to the freeway was analogous to the middle of the property and therefore should provide comparable results, Figure 2.

Given the project timeline, this was the only viable site, as any other site would have involved facilitation efforts. Additionally, the analysis exposure procedures had already begun on a batch of samples at ALS. With this in mind I scheduled these samples into the active analysis queue and ran the deployment as long as possible without the current synchrotron analysis window closing. The synchrotron analysis is run in large batches which occur approximately every 4 to 6 months due to scheduling logistics.

Figure 2 Relationship between Nishi property and Olive Drive sampling location.

As Figure 2 shows the sampling location is slightly closer to the freeway than the center of the property. The distances are 118 meters and 138 meters to freeway center respectively. These distances are well within the expected influence of freeway particulates, especially considering recent changes in measured distances of influence for ultra-fine particles Hu (2009), and the growing concerns with the increased effective toxicity of ultra-fine particles, Lippmann (2009).

The freeway tends to loop around the property, Figure 1 and Figure 2, thus giving slightly more exposure directions for air movement, than a straight section of freeway would. One can see the potential freeway impacting directions could involve air that moves to the property from the east, southeast, south and south west, in degrees on the compass from 90º to 225º.

III. SUMMARY ANALYSIS, INTERPRETATION AND RESULTS

One requirement of the study is to generate a set of data that could be utilized for evaluation, while meteorological conditions (inversions) still existed that might be more favorable for detection of near roadway emissions. The validated data for the study extends from February 3, 6:20 PM to February 13, 9:20 PM. So we have over a week worth of data which includes a weekend and therefore the extra exposure involved with the heavier traffic at those times.

Beta Mass including ultra-fines

The second purpose was to include the measurement of the ultra-fine size mode using the prototype continuous ultra-fine filter system (9th stage). Figure 3 shows particulate matter mass for PM10, PM2.5 and ultra-fines, 0.09 µm to 0.0 µm. There is strong correlation with time to PM2.5 and PM10, this is certainly the result of such clean conditions overall.

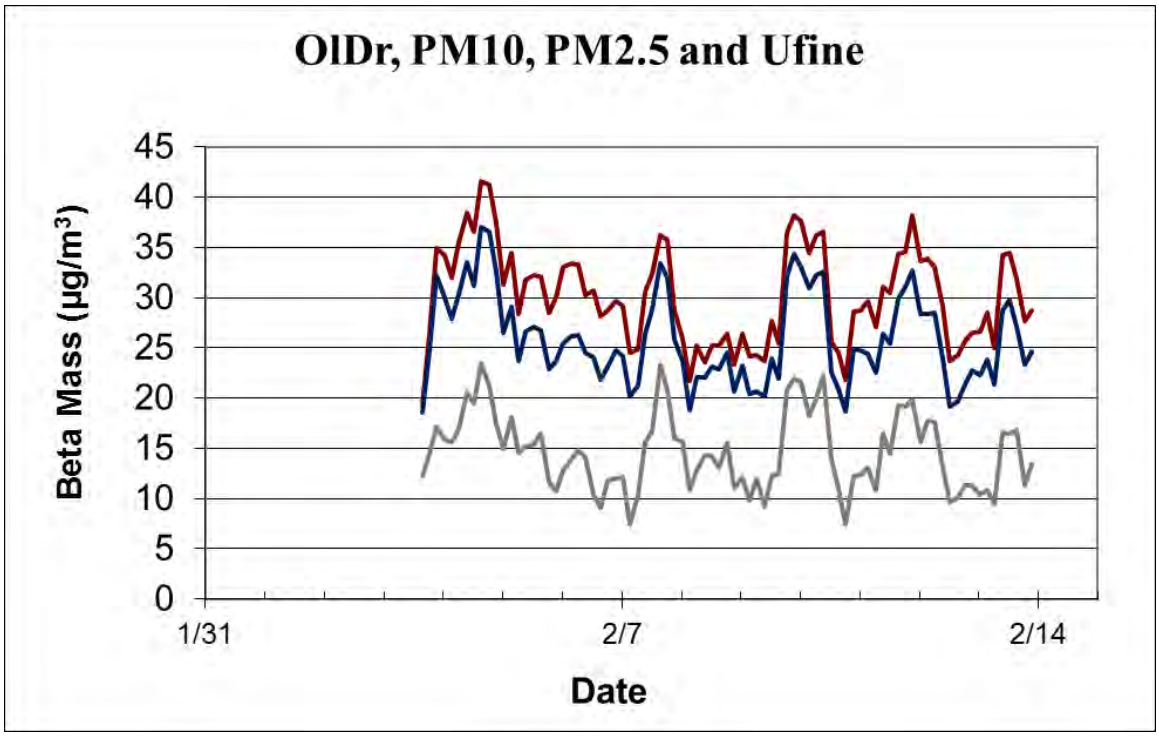

Figure 3. PM10, PM2.5 and Ultra-fine mass

It is not unusual for the ultra-fine mass to be a large fraction of PM2.5, but often it does not correlate with PM2.5 in either time or composition. The first test of the 9th stage, in Sacramento in winter 2009, also had large mass ratios.

Note:
The total mass concentration allows for direct calculation of constituent concentrations for every sample. To clarify, each data point, of each size mode represents an independent aerosol sample for which a concentration of a given element can be calculated.

Included in the digital files (see Attachment 7) are the beta mass concentrations for the study representing over 700 individual mass sample concentrations across 9 size modes.

S-XRF Analysis

Ultra-fine signature in elemental data

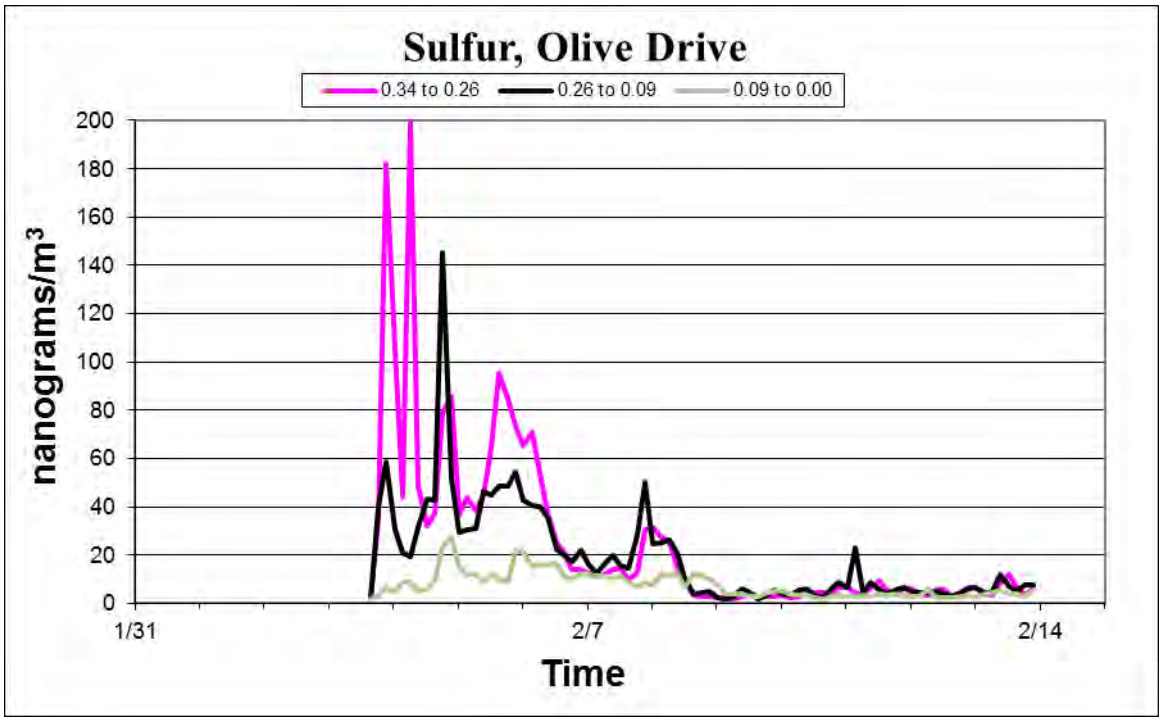

Figure 4. Three finest size modes of sulfur

The presence of sulfur in stage 8 and 9 is an indication that even though conditions were clean overall we can detect ultra-fine signatures associated with roadway traffic. The lack of sulfur in this size range during the later portion of the study is due to unfavorable meteorology for measurement, namely higher wind speeds and wind directions that do not bring emissions from the freeway.

Ultra-fine element concentrations

A recent paper reported ultra-fine species data from Watt Avenue in Sacramento. This is a good set of data for comparison as it is local, and includes both spring and winter (inversion) conditions. The paper showed meteorological differences between winter inversion conditions and spring conditions profoundly affect the ability to detect potential local emission issues, Cahill (2014).

Table 5 below compares concentrations for ultra-fine elements from the current OIDr study to those found downwind of a heavily traveled secondary road. The table has the OIDr concentrations in the center, with the spring and winter data

on either side, followed subsequently by the ratio of OlDr concentrations to each data set.

	Ratio OlDr to Spring ArMi	Spring ArMi (ng/m^3)	OlDr (ng/m^3)	Winter ArMi (ng/m^3)	Ratio OlDr to Winter ArMi
Calcium	**9.1**	**0.41**	**3.77**	**2.58**	**1.46**
Sulfur	0.3	**32.25**	**9.72**	**9.78**	**0.99**
Potassium	**1.6**	2.90	**4.61**	5.00	**0.92**
Chromium	**5.5**	0.01	0.07	0.21	0.33
Manganese	**33.3**	**0.04**	**1.33**	**0.33**	**4.10**
Iron	0.4	**1.20**	0.50	**7.28**	0.07
Nickel	**4.4**	**0.08**	0.33	**2.88**	0.11
Copper	**3.2**	**0.10**	0.32	**2.03**	0.16
Zinc	**1.6**	**0.50**	0.80	**3.20**	0.25
Arsenic	-	0.08	nd	0.10	-
Selenium	-	0.06	nd	0.04	-
Bromine	0.5	0.45	0.23	0.29	0.77
Lead	**1.2**	0.35	0.43	0.41	**1.07**

Table 1 Comparison of Nishi ultra-fine metals to Watt Avenue study, both winter and spring.

Five of eleven ultra-fine metal concentrations are comparable or greater than the winter concentrations which were known to be influenced by inversion conditions.

Comparing the sum of the elements in the ultra-fine mode to PM2.5 and PM10 there is a large fraction (Figure 5, percent ultra-fine/PM2.5 dotted line) which comes in the ultra-fine mode when source contributions and meteorology come together.

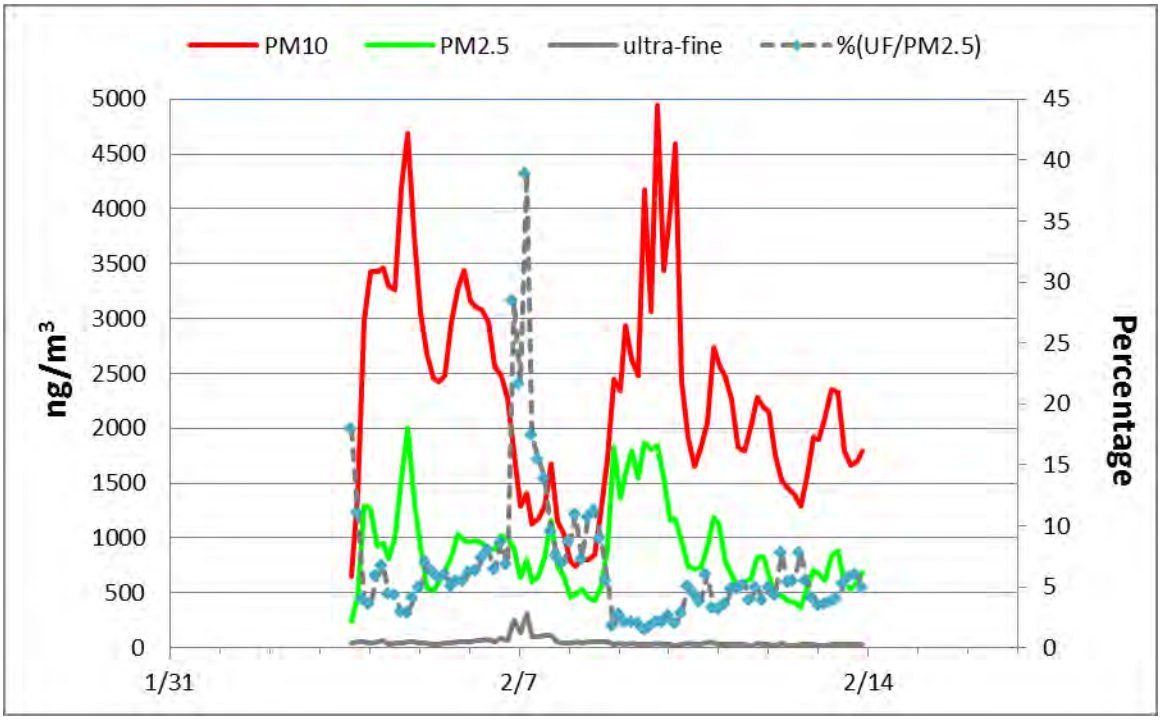

Figure 5. Summed elements for PM10, PM2.5, ultra-fines and the ratio Uf/PM2.5

This peak in ultra-fine elements extends from Friday afternoon to late Saturday. This is the time most likely to be affected by weekend traffic. This is the only time during the study the site was exposed to the weekend traffic and it shows up clearly as the largest concentrations in the ultra-fine signal.

Note:
All of the S-XRF concentrations data included in the digital files will be provided in the form of Excel spread sheets, Attachment 7. The elemental concentrations for the study represent over 13,000 separate elemental concentrations across 9 size modes.

Meteorology

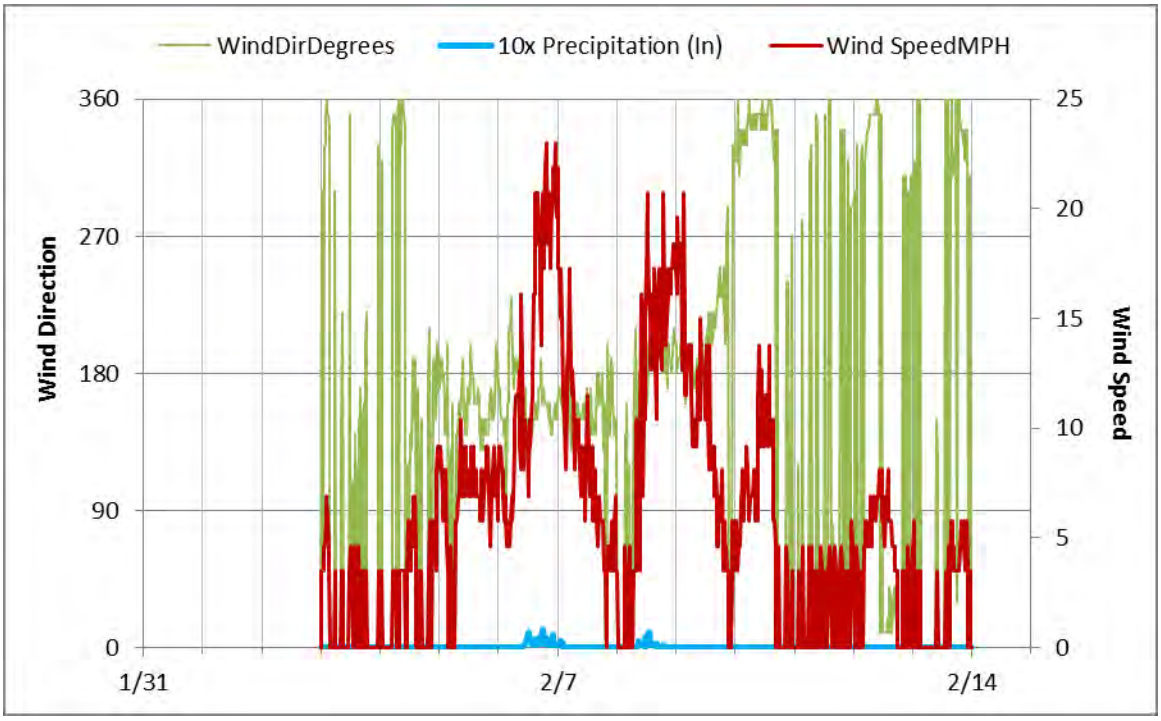

Figure 6. Wind Direction, Wind Speed, and Rain

Wind Direction, Wind Speed, Rain

Best detection would occur for winds speeds below 5 mph (right axis), optimum detectable wind direction is 135º to 180º, rain removes particles, ultra-fines less efficiently but these concentrations will also be continually reduced.

The general observations for the meteorology: wind direction was most favorable for detection about 30% of the time. During those times the wind speed was less than 6 mph less than 25% of the time. From early on the 5th to the 10th the slower winds occurred mostly late at night and in the early mornings when traffic impacts are reduced.

Based on the meteorological data optimum exposure for the sampling site to detect freeway emission occurred less than 10% of the time. This conclusion was corroborated by the HYSPLIT trajectories and the local AQI data.

Given the meteorological conditions during the Olive Drive study, the comparison to Watt avenue concentrations is surprising. It is not surprising that the emissions are generally more than the spring conditions for the Watt avenue study, because this freeway carries more traffic. It is a concern that several species are comparable to the strongly inversion influenced concentrations of the winter data.

IV. PROJECT PLAN AND BACKGROUND

To include as a data source to the Environmental Impact report with respect to the development of this site, I was asked to utilize DELTA technologies to characterize emissions from the adjacent freeway that could impact the Nishi property. In order to accomplish this I would do/provide the following:

1. Collect samples through the use of a DRUM (Davis Rotating-drum Unit for Monitoring) Sampler.
2. Collect samples with a continuous ultra-fine filter. A prototype system designed by the UC Davis DELTA group to allow separation of the ultra-fine size mode for separate analysis and characterization.
3. Analyze collected samples for concentrations of mass by beta gauge and elemental concentrations by Synchrotron-XRF
4. Provide a brief report summarizing results, including concentration data for all validated analyses, on all samples.
5. In addition, because these technologies are not broadly known I will also provide a context for how these measurements have been used in prior studies.

Importance of Aerosol Characterization as a Function of Time

Despite the fact that the 8-DRUM sampler takes 48 separate samples to equal a single 24 hour $PM_{2.5}$ Federal Reference Method (FRM) filter, the results for mass are identical to within a few percent, as seen in a yearlong side by side study for the California Air Resources Board in Sacramento (Cahill et al, 2011a).

However, the additional samples allow the DRUM to follow and correlate to the meteorology. This is of primary importance for characterizations as meteorology can have the greatest impact on observed aerosols at a specific location.

The DELTA DRUM technology and analysis is capable of providing a clear signature of a potential source in aerosols and can validate source identification with concentration changes as a function of distance and particle size distributions.

Importance of Aerosol Characterization as a Function of Size

The particle size distribution of aerosols evolves with distance from the particles source(s) this changes the aerosol concentration size profile with time. Thus particle size is a critical component of aerosol characterization. The evolution of source constituent profiles provides another tool to separate confounding sources from a specific source of interest.

Size also effects deposition (not expected to be important in this study). Almost all atmospheric aerosols are eventually removed from the atmosphere by deposition, either by dry or wet processes (Seinfeld and Pandis, 1998). If the aerosol has sufficient mass and the aerosol contains toxic contaminants of concern, the deposition process can lead to surface contamination resulting in exposure through ingestion via hand to mouth contact. Aerosols consisting of solid particulate matter, which contain certain heavy metals, and have sufficient mass to settle close to a source can result in a deposition at concentrations that exceed DTSC's regulatory thresholds (California Code of Regulations, title 22, section 66261.24).

Information must be gained on the types and concentrations of toxic materials in the atmosphere segregated by size, since size dominates the calculation of settling velocity and later deposition rates (Seinfeld and Pandis, 1998). Information on the sources of a potentially airborne deposited waste is enormously aided by information on the airborne material before deposition, as then all the tools of meteorology, particle size, and composition can be brought to bear to identify sources. Table 2 below identifies some size classifications of particulate matter and their corresponding size ranges.

Particulate Matter	Size Range
Very Coarse	10 – 35 µm
Coarse	2.5 – 10 µm
Fine	< 2.5 µm
Very Fine	< 0.25 µm
Ultra-Fine	< 0.10 µm

Table 2. Size Classifications of Particulate Matter

Sources which potentially produce aerosol particles containing toxic constituents must be evaluated with respect to deposition rates (i.e. size characterization). In order to properly protect surrounding areas from potential hazardous waste disposal issues, source evaluation must include particle size and composition characterization. It is important to include even larger sizes than PM_{10}, when the coarsest modes (10 – 35 µm, 2.5 – 10 µm) contain a significant contribution of a toxic material.

The DRUM sampler (and the Continuous Ultra-fine filter) and associated analyses allow the DELTA Group to measure quantitatively the elemental content and mass as a function of size and time thus more fully characterizing aerosols and providing data that allows correlation to health impacts e.g. Cahill (2011b) .

V. SAMPLE COLLECTION METHODOLOGIES

8-DRUM Sampler

The DRUM sampler consists of 8 rotating drums that are wrapped with a Mylar® substrate then coated with a thin layer of Apiezon-L grease (Wesolowski et al, 1978, Cahill 1979). The substrate (Mylar® and grease) is well characterized and provides a uniform, contaminant free background for high sensitivity analysis. The rotation rate of the substrate was set for 4 mm/day, which allows for 5½ weeks of sample collection without substrate change. All DRUM samples are particulate matter samples collected by impaction onto this type of clean/coated Mylar® substrates. An 8-DRUM sampler contains eight substrates to allow collection of ambient particulate aerosols into eight different size modes. Once collection is complete each of the eight substrates holds a record (samples) of the aerosol particles for a given size range, (Raabe et al, 1988), as a function of time sampled.

Continuous Ultra-fine sampler

The ultra-fine filter system was designed to be in-line with a DRUM sampler so the filter is capturing the particles remaining below the well-defined size modes of the 8-DRUM. The photo, Figure 3, shows the Teflon filter is mounted on an archival frame while in the unit and does not need remounting once sampling is completed. The system pictured is the original prototype; the system used in this study is functionally equivalent. One can clearly see the time evolution of the dark deposit at the right end of the frame (For sample photos of current study, see Attachment 4.)

Figure 7. Continuous Ultra-fine sampling system (DRUM stage 9)

Meteorological Data

The first level meteorological data required for aerosol assessments is simple wind speed, wind direction and precipitation. The data examined for these analyses come from online resources, such as weather underground, local air districts and a UC Davis/NOAA weather site.

VI. ANALYTICAL TECHNIQUES

Soft Beta Ray Transmission

The UC Davis DELTA Group measures mass concentration using Beta particles. Radioactive elements in general emit different types of radiation when they decay. Depending on the element, this radiation will be some combination of alpha particles (Helium nuclei), Beta particles (high energy electrons), neutrons, and gamma rays. A property that is common to all of these radioactive by-products is that their flux decreases exponentially as it travels through matter.

The element Nickel-63 (^{63}Ni) decays by emitting a 67 kiloelectron volt (keV) electron. These electrons are at a similar energy as those in the beam of electrons in an old-style cathode ray tube in a TV or computer monitor. Since the flux of these particles decreases in a predictable manner as it passes through matter, it is possible to measure the mass of a thin deposit on a uniform substrate.

Specifically, a detector is placed facing a ^{63}Ni source. A series of standards, with known aerial densities, are placed between the source and detector to calibrate the system. It is known that the flux of beta particles will obey the equation $I = I_0 e^{-\alpha m}$ where I_0 is the flux of particles with no sample between the source and detector, α is a coefficient specific to 67 keV electrons and m is the aerial density of the sample. The aerial density of the sample is then calculated to be: $m = -\frac{1}{\alpha} \ln \frac{I}{I_0}$.

Synchrotron X-Ray Fluorescence (S-XRF)

The UC Davis DELTA Group uses two synchrotrons, the Advanced Light Source (ALS) located at the Lawrence Berkeley National Laboratory, and the Stanford Synchrotron Radiation Lightsource (SSRL) located at the SLAC National Accelerator Laboratory.

X-ray fluorescence is a fundamental and widely used method for quantitatively measuring the amounts of all elements heavier than sodium. It relies on an x-ray beam knocking an electron from an atom, which then immediately decays by emitting an x-ray characteristic of that particular element. Each x-ray spectrum is unique, and thus determinations are definitive.

S-XRF has been developed and extensively used for 100s of thousands of aerosol samples since 1997 at the ALS, Lawrence Berkeley NL. An initial x-ray beam passes through the sample, knocking electrons out of the atoms, which then fills the vacancy by dropping in another electron and giving off the extra energy as a characteristic x-ray. Each element has a unique set of characteristic x-rays, which are then detected by modern energy dispersive x-ray detectors and data reduction programs. The system is calibrated by standards, including both commercial standards and Standard Research Materials (SRMs) from the

National Bureau of Standards, now National Institute for Standards and Technology (NIST).

In the Advanced Light Source (ALS), Lawrence Berkeley NL, the UC Davis DELTA Group has sponsored Beam Line 10.3.1 for the purpose of the most sensitive possible x-ray analyses of thin (< 100 μg/cm^2) aerosol samples. The analyses are based on a 14 keV polarized x-ray "white" beam collimated to typically 0.5 mm. Among the many choices necessary to achieve this capability, the analyses are done in a vacuum chamber, and the detector is optimized to handle high count rates of low energy x-rays, 1 keV to about 12 keV. It has achieved sensitivities in the femtogram/m^3 range in size and time resolved aerosol samples.

We also utilize a second system, the design of the SSRL capability was driven by the need to handle medium and heavy transition metals not available from the ALS, many of which are toxic, in the range from about 6 keV to 38 keV. The analyses are currently done in helium, not vacuum, and the detector is optimized for higher energy x-rays. The facility can handle samples of almost any size, a capability which is not available at the ALS.

Both systems have the capability to analyze aerosols impacted onto a Mylar® strip about 17 cm long, delivered by a rotating drum impactor which collects aerosols continuously as a function of time, typically for 5½ weeks. By collimating the beam to 0.5 mm, time resolution of 3 hour is achieved on standard 4 mm/day deposits.

Table 3 lists the title 22 elements, including regulatory thresholds, and the S-XRF facility capabilities and detectable limits for each element.

Metals and compounds	STLC mg/L	TTLC wet mg/kg	ALS, White beam ppm	SSRL, 38 keV ppm
Antimony	15	500	na	0.2
Arsenic	5.0	500	0.2	1.6
Barium	100	10,000	na	0.8
Beryllium	0.75	75	na	na
Cadmium	1.0	100	na	0.6
Chromium VI	5	500	na	na
Chromium, Cr III	5	2500	0.2	0.2
Cobalt	80	8,000	0.4	0.6
Copper	25	2,500	0.2	0.4
Flouride salts	180	18,000	na	na
Lead	5.0	1,000	1.3	1.6
Mercury	0.2	20	1.0	0.2
Molybdenum	350	3,500	6.6	0.4
Nickel	20	2,000	0.4	0.2
Selenium	1.0	100	0.2	0.2
Silver	5.0	500	na	0.2
Thallium	7.0	700	na	0.2
Vanadium	24	2,400	0.2	0.3
Zinc	250	5,000	0.4	0.6

Table 3. Title 22 elements of concern, regulatory thresholds and S-XRF capability.

The key advantage of S-XRF is that the polarization and intensity of the x-ray beams from synchrotrons give far better sensitivity than standard x-ray methods, while retaining the advantage of seeing a large suite of elements simultaneously and quantitatively.

Thus, not only are toxic elements like lead and other title 22 elements possible to measure, but many other trace and abundant elements can also be measured. It is important to note that this is not simply useful in identifying sources, but is an absolute necessity for this purpose. In general, a single element rarely constitutes, nor could be easily attributed to a single source.

The accuracy and precision of the analyses are confirmed using standard foils. Below we show the NIST (NBS) Standard Reference Materials (SRM) 1832 and 1833. These values are NIST certified. Also, note that UC Davis was one of the 5 certifying laboratories chosen by NIST.

Standards						
NBS (NIST)		**SRM 1832**		**Area**		
		1.73	Mg	37 mm foil	Areal	
	Atomic #	Elements	(%m/m)		Density	
Sodium	11	Na	6.6	0	14.2	$\mu g/cm^2$
Aluminum	13	Al	7.5	0.7	16.1	$\mu g/cm^2$
Silicon	14	Si	19.7	0.6	42.4	$\mu g/cm^2$
Argon	18	Ar	1	0	2.2	$\mu g/cm^2$
Calcium	20	Ca	11.8	0.8	25.4	$\mu g/cm^2$
Vanadium	23	V	2.4	0.3	5.2	$\mu g/cm^2$
Manganese	25	Mn	2.5	0.3	5.4	$\mu g/cm^2$

Cobalt	27	Co	0.61	0.04	1.3	µg/cm^2
Copper	29	Cu	1.4	0.1	3.0	µg/cm^2
NBS (NIST)		**SRM 1833**		**Area**		
		1.556	Mg	37 mm foil	Areal	
		Elements	(%m/m)		Density	
Silicon	14	Si	21.9	1.4	42.4	µg/cm^2
Argon	18	Ar	1	0	1.9	µg/cm^2
Potassium	19	K	11.2	1.1	21.7	µg/cm^2
Titanium	22	Ti	7	1	13.5	µg/cm^2
Iron	26	Fe	8.4	0.3	16.3	µg/cm^2
Zinc	30	Zn	3.3	0.3	6.4	µg/cm^2
Lead	82	Pb	13.4	0.7	25.9	µg/cm^2
					Areal	
Micromatter Inc certified					Density	
Cadmium selenide		CdSe	46.8	µg/cm2	46.8	µg/cm^2
Cadmium	48	Cd			31.17	µg/cm^2
Selenium	34	Se			15.58	µg/cm^2
Antimony	51	Sb	50.8	µg/cm2	50.8	µg/cm^2

Table 4. Standards used in the S-XRF analyses

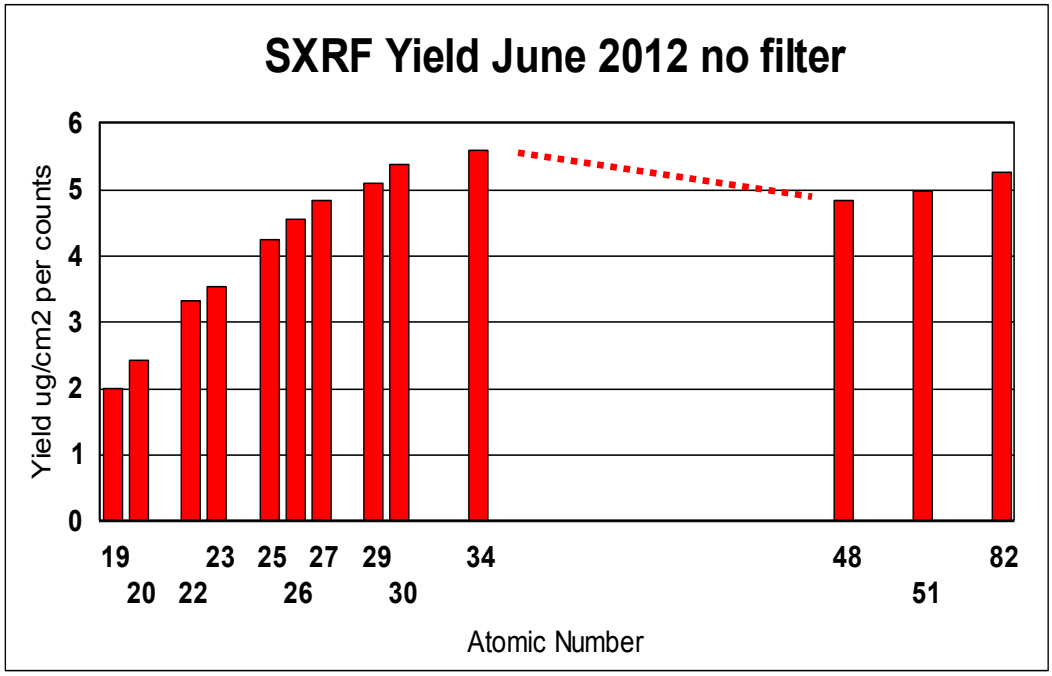

Figure 8. Yield curve for the tailored white beam based on NIST SRM and Micromatter Inc. standards.

The gap from Z = 35 to Z = 47 was caused by lack of standards, but atomic theory demands smooth transitions element to element (dashed line).

VII. SAMPLING ACTIVITIES

The timeframe of the deployment was from February 3, to February 21, 2015. This was extended beyond the initial week to provide as much data as possible, within the available timeline. The normal 5 ½ week duration was superseded so that the S-XRF analysis could be completed within the current analysis window.

The sampling site (OlDr) was setup on Tuesday, February 3, 2015 with the following two sampling systems, an 8-DRUM cascade impactor and in-line, a Continuous Ultra-fine sampler (9^{th} stage). The system was started (vacuum pump turned on) at 6:20 PM.

The site was visited one week after deployment, Tuesday, 2/10/2015 at 15:45. The systems were observed to be running well, motion, flow and vacuum systems checks were good.

On Saturday, February 21, 2015 the site was visited for shutdown of the site. The 8-DRUM had rotated as expected, based on the elapsed time and the preset rotation rate (4mm/day). The flow was then measured and found too low. After further inspection the 9^{th} stage was found to have stopped prematurely. Normally the ultra-fine filter is mechanically moved across in front of its orifice, Figure 7. This allows the filter to retain a time signature of deposited particles.

Because the motion stopped the ultra-fine particles build up in one location on the filter strip and eventually adversely affect the system flow. This explained the low flow reading. This was the system state, the deposit was short but otherwise the ultra-fine deposit looked normal.

The vacuum pump was shut down at 5:15 PM and the site was removed. The length of the deployment was about 1 day short of an automatic mid-deployment protocol movement that would have placed an in-situ blank on the Mylar® substrate. For longer deployments this blank helps with timing.

After site removal the sampling systems were taken to the DELTA Group laboratory at UC Davis with the samples inside. Other operational and quality assurance checks are made once the samplers (with samples) are back in the laboratory. In this case this will include accurate determination if possible of the length of time the system was improperly functioning.

In the laboratory in Physics by measuring the ultra-fine deposit length to center of stop peak, the time the continuous ultra-fine system stopped was determined to be 2/14/15 4:25 AM.

Because of the buildup of materials where the system stopped, data for the ultra-fines was affected before the stop so any data affected by the stop peak accumulation were also discarded. The material on the 9th stage near the peak does not affect the deposits and data on the 8-DRUM stages before the actual stop time on the 9th stage. This is because the corresponding deposits are no longer in the active deposition area due to drum rotation within each stage.

However, the 8-DRUM data after the ninth stage stopped has larger error due to variable flow restriction. It is difficult to accurately determine how quickly the effect would occur and what its variability may be. For this reason the data after the continuous after-filter system stopped should be ignored for primary analysis.

After the 9th stage stalled the flow effect is variable, but the final flow measured was 6.4 l/m, this corresponds to an error at the 8 stage cut-point (sizing) of more than 30% which is too large to consider sizing to be valid in the 8-DRUM system. For this reason, **only concentration data before the 9th stage stopped can be considered valid**. The validated data for the study extends from February 3, 6:20 PM to February 13, 9:20 PM

VIII. ANALYTICAL RESULTS

Archiving and validation of DRUM and Ultra-fine samples

After removing sample substrates from the sampler, sampler operations are checked for consistency to pre-field operations, which includes flow characteristics and electro-mechanical function. Prior to mounting the DRUM samples onto labeled analysis/archival frames, the collected sample dimensions were measured to verify expected lengths. Deposits were also examined visually to detect any anomalies during sample collection and to examine and confirm imbedded time markers (if any). The ultra-fine substrate is pre-mounted to its archival frame so it is simply removed from the system ready for initial measurements. All further analyses are done directly on the frame mounted deposits. For each DRUM sampler, information from these evaluations, e.g. sampler flow or timing is included in Attachment 3: Summary Notes from Archiving and Beta Sample Analysis.

Beta Mass Analysis

All archived DRUM and Ultra-fine samples were analyzed for particle mass concentration in 3 hour increments by soft beta ray transmission. Each archival frame contains a deposit of the material (aerosol particles) from a single size mode; therefore, the plots of mass concentration below provide a characterization of how the mass is distributed across different size regimes as a function of time sampling. The graphs that follow are the eight size modes from

the 8-DRUM sampler and the ninth size mode from the continuous ultra-fine sampler, all from site OlDr.

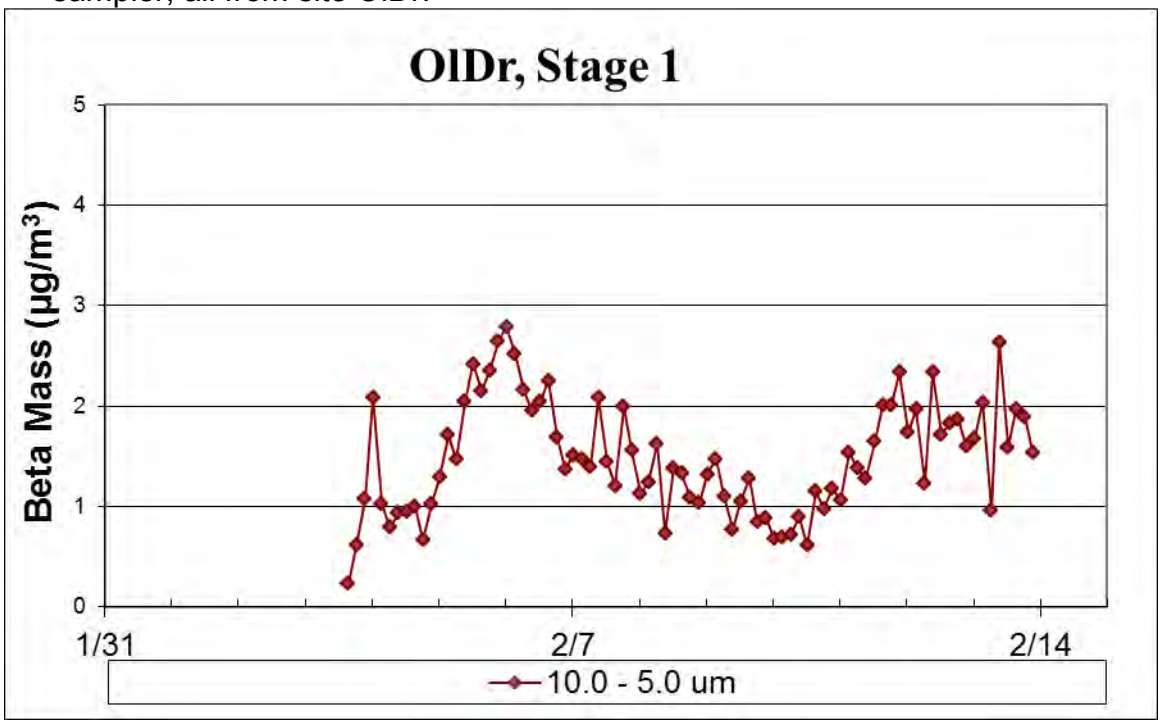

Figure 9. Mass concentration versus date for Stage 1, 10.0 to 5.0 µm size range

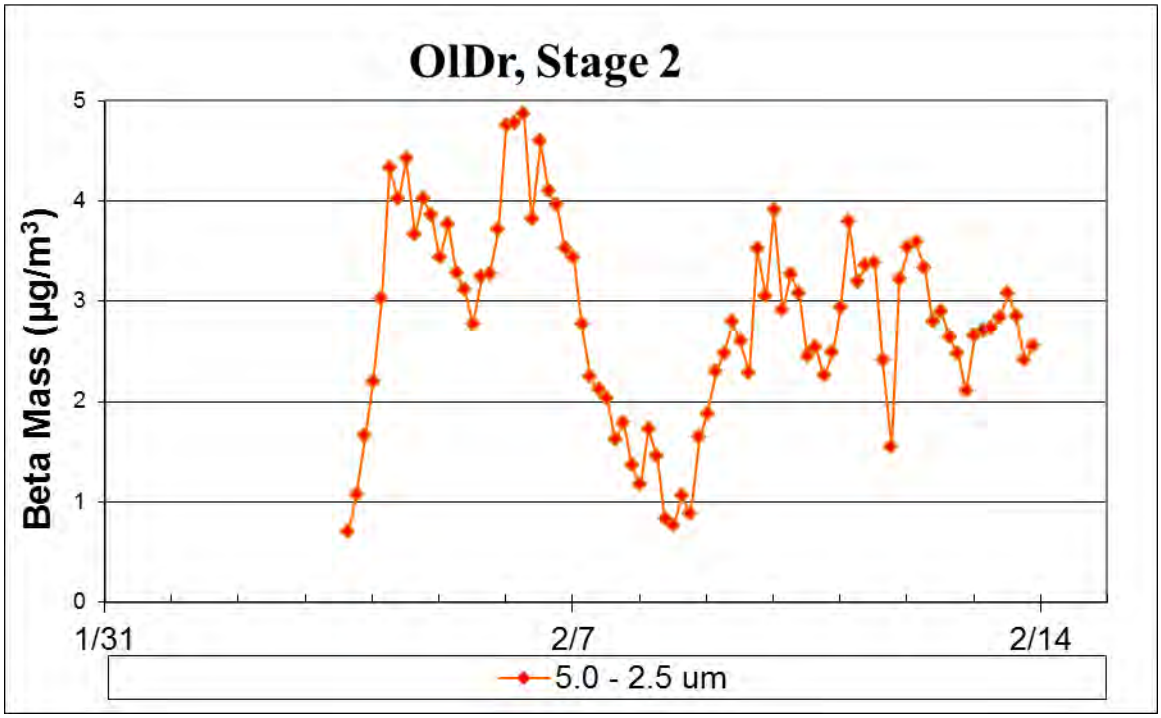

Figure 10. Mass concentration versus date for Stage 2, 5.0 to 2.5 µm size range

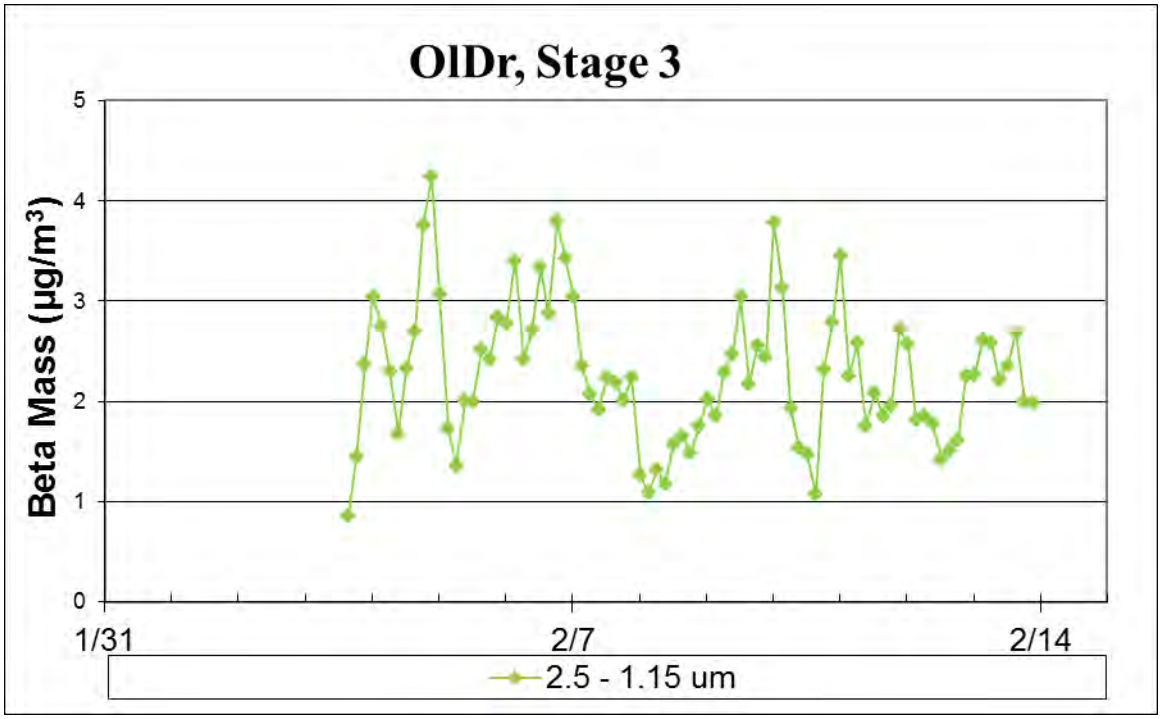

Figure 11. Mass concentration versus date for Stage 3, 2.5 to 1.15 µm size range

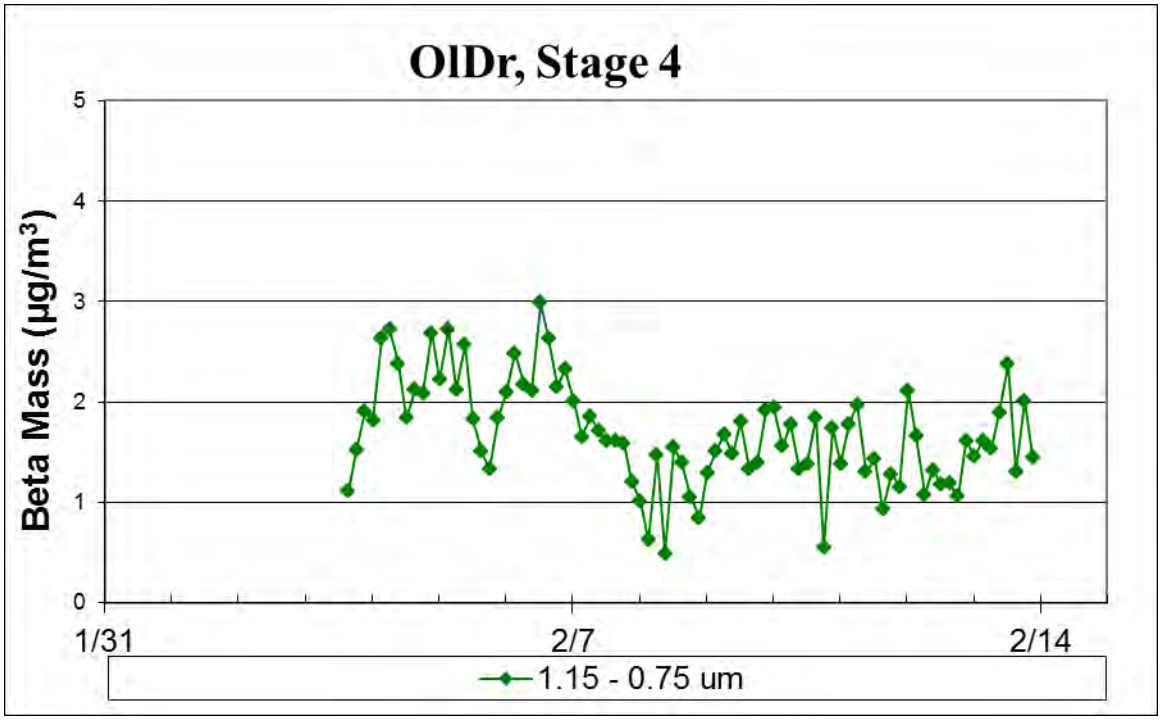

Figure 12. Mass concentration versus date for Stage 4, 1.15 to 0.75 µm size range

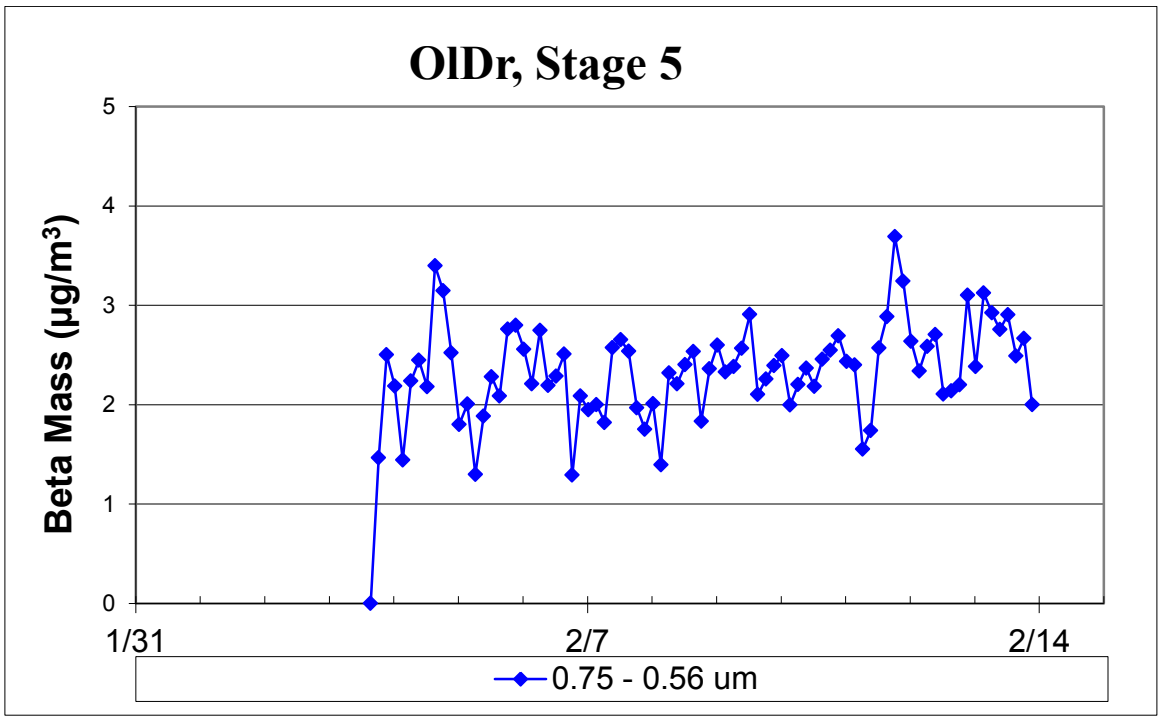

Figure 13. Mass concentration versus date for Stage 5, 0.75 to 0.56 µm size range

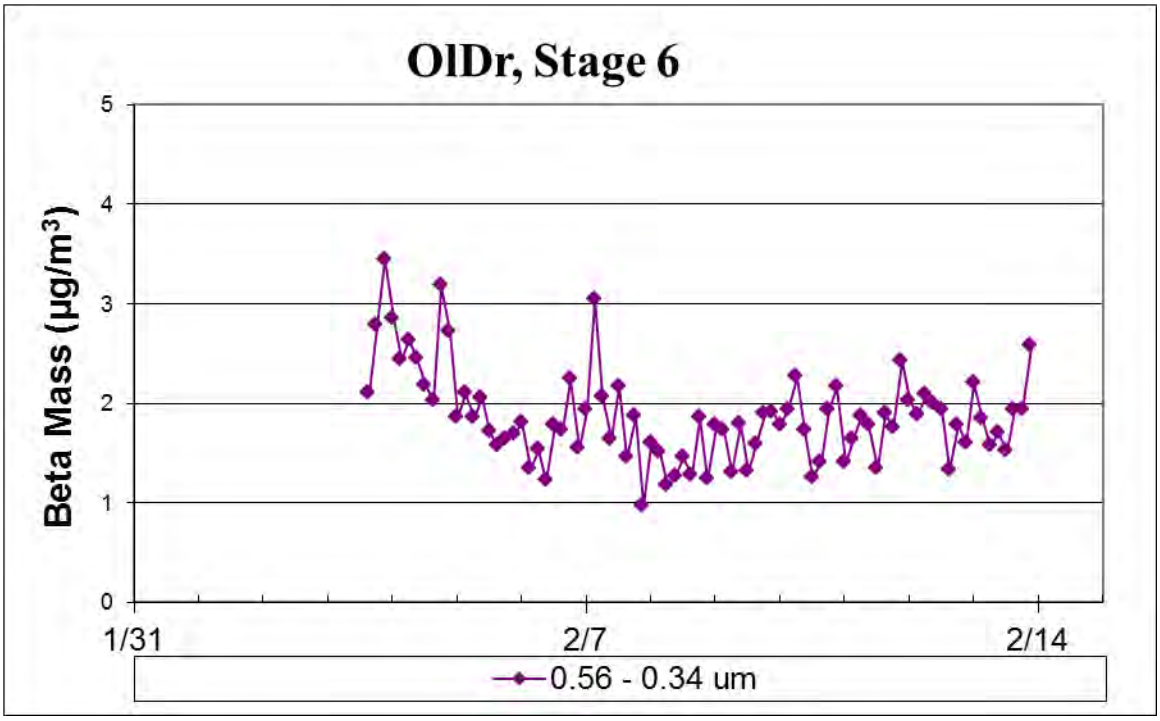

Figure 14. Mass concentration versus date for Stage 6, 0.56 to 0.34 µm size range

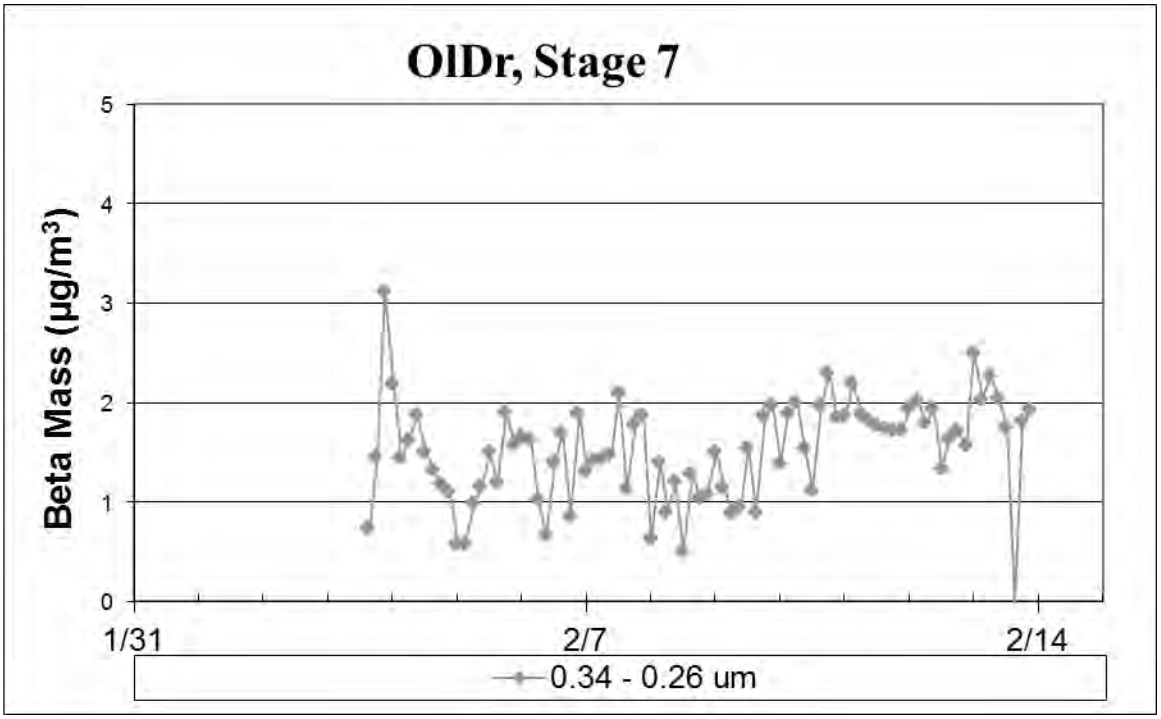

Figure 15. Mass concentration versus date for Stage 7, 0.34 to 0.26 µm size range

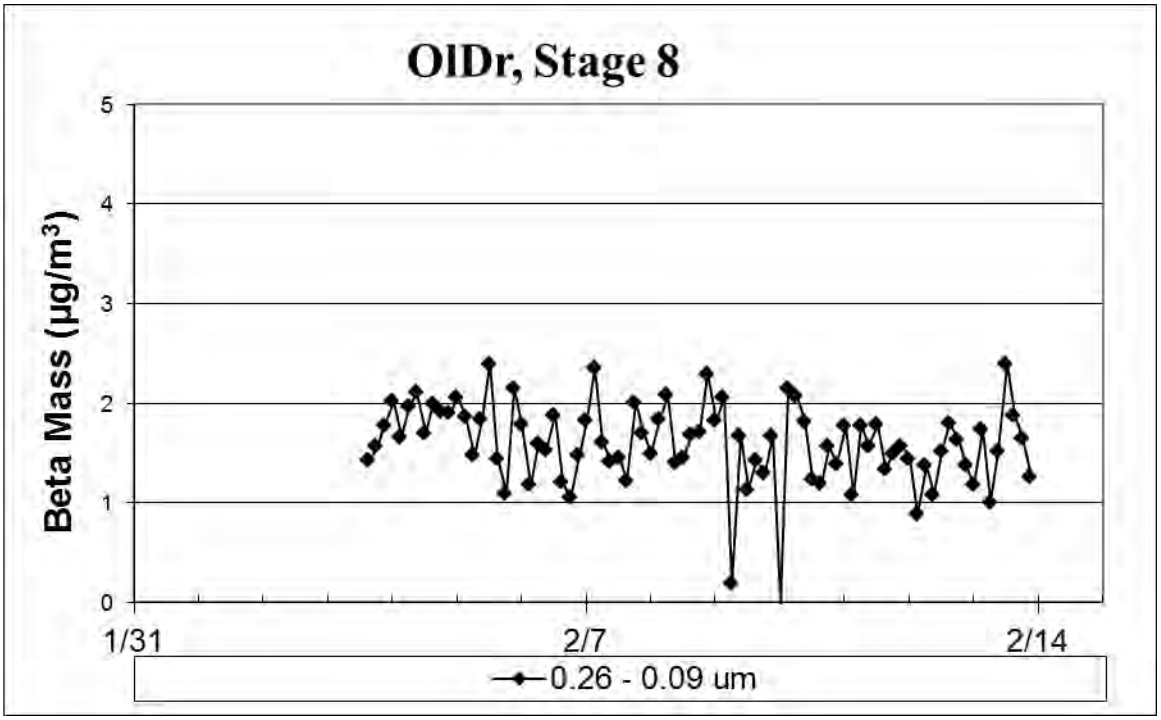

Figure 16. Mass concentration versus date for Stage 8, 0.26 to 0.09 µm size range

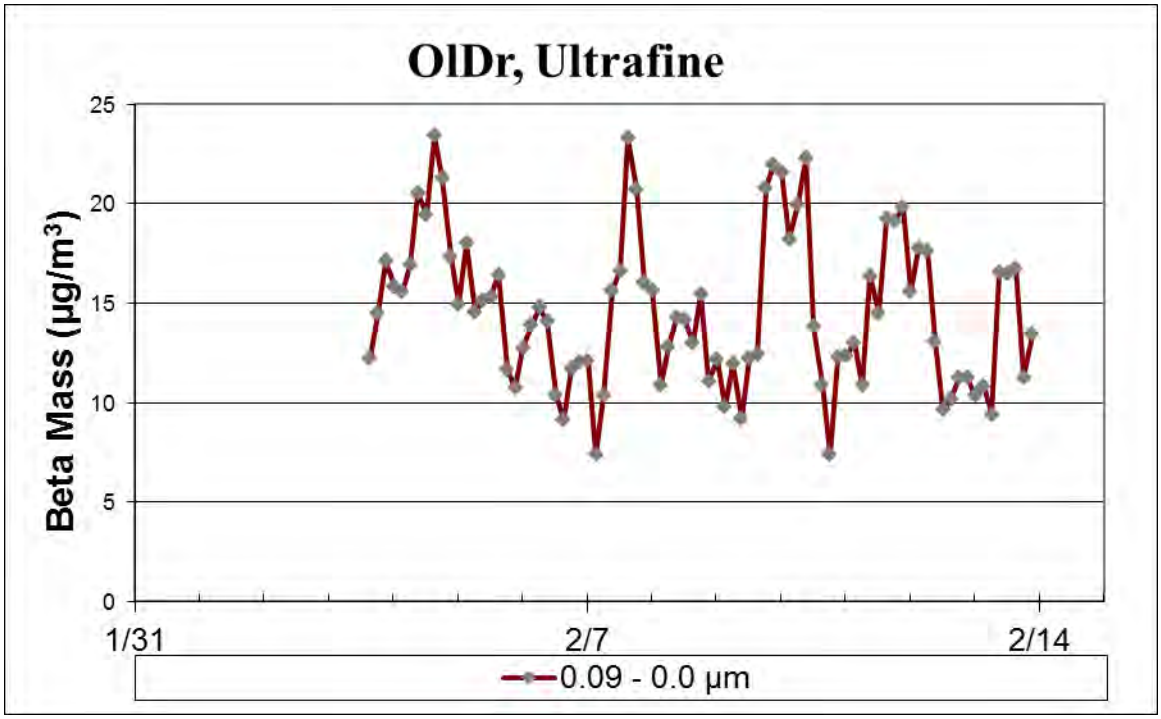

Figure 17. Mass concentration versus date for Stage 9, 0.09 to 0.0 µm size range

Now we look at the standard views for particulate matter PM10 and PM2.5. To that we add the component of mass of particular interest in this study, mass from the ultra-fine stage, 0.09 µm to 0.0 µm, Figure 18. Notice the correlation in time to PM2.5 and PM10, this is certainly the result of such clean conditions overall. It is not unusual for the ultra-fine mass to be a large fraction of PM2.5, but often it does not correlate with PM2.5 in either time or composition. The first test of the 9th stage, in Sacramento in winter 2009, also had large mass ratios, Figure 19.

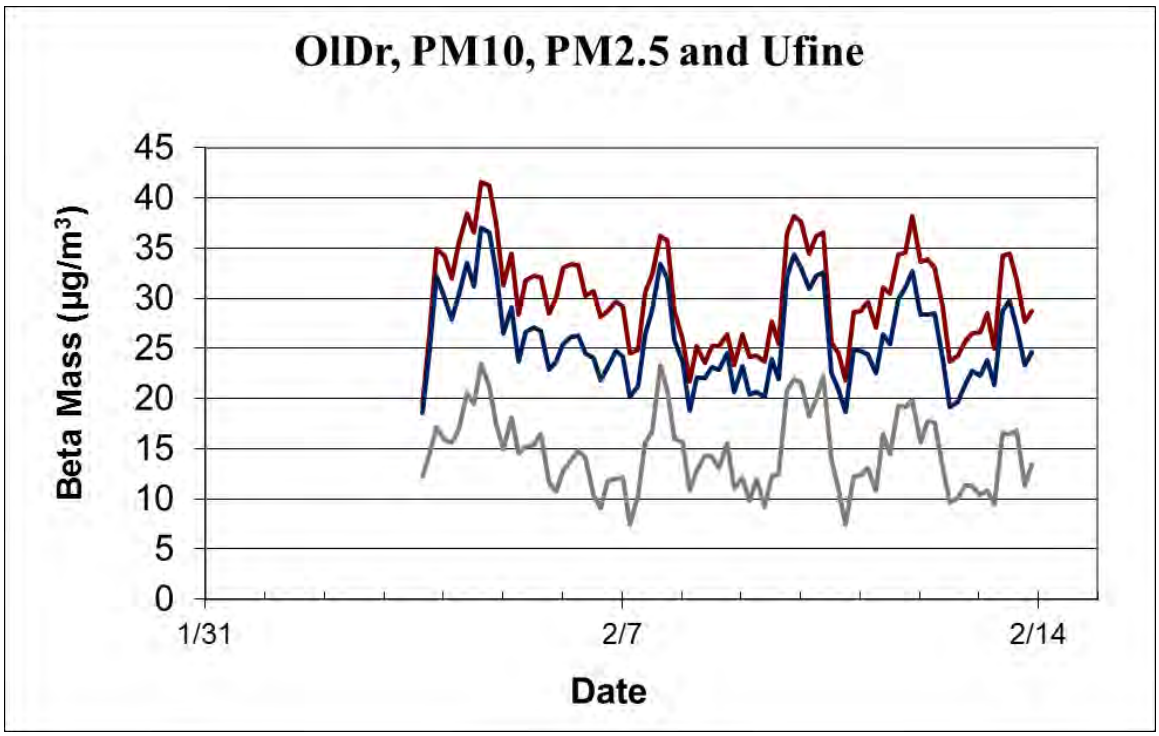

Figure 18. PM10, PM2.5 and Ultra-fine mass

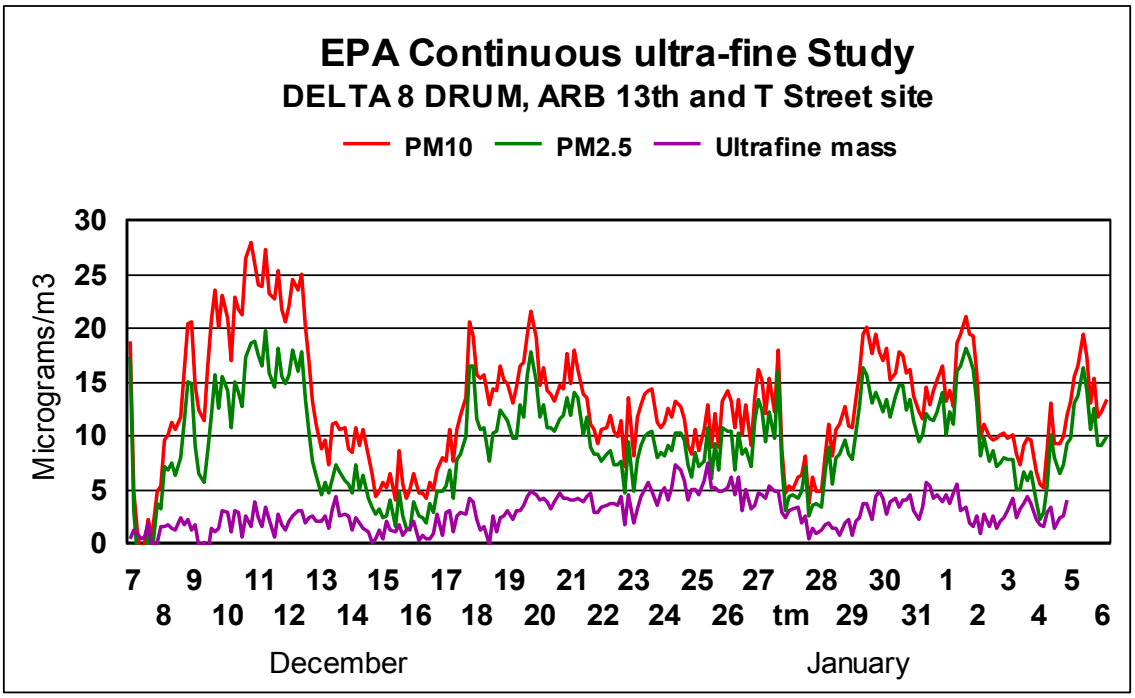

Figure 19. Ultra-fine contribution to mass in early test of ultra-fine system

The total mass concentration also allows for direct calculation of constituent concentrations for every sample. To clarify, each data point, of each size mode represents an independent aerosol sample for which a concentration of a given element (if detected by S-XRF) can be calculated.

For any aerosol sample the size profile is a function of the sources which originally produced the particles and, therefore, a particle size profile is as important in characterizing aerosols as elemental composition. In considering equivalency of two aerosols, it is not enough to say that there is a certain total concentration of a given element in the two samples. Equivalency requires that the aerosols must also show the same concentration of that element within each size mode.

Note:
Included in the digital files (Attachment 7) are the beta mass concentrations for the study representing over 700 individual mass sample concentrations across 9 size modes.

S-XRF Analysis

The DRUM samples were analyzed on the UC Davis DELTA Group beam line 10.3.1 of the Advanced Light Source, Lawrence Berkeley National Laboratory. The sensitivity and quality assurance of S-XRF is shown in Attachment 2, DRUM Quality Assurance Protocols.

The four plots in Figure 20 are examples of elemental concentrations versus time and size (four different size mode plots) from the Olive Drive site. Shown are elements aluminum (Al), silicon (Si), potasssium (K), calcium (Ca), iron (Fe) and sulfur (S) which, except for sulfur are generally soil constituents in coarse size modes. Examine the plots going from stage 1 (10.0 to 5.0 μm), stage 2 (5.0 to 2.5 μm), stage 3 (2.5 to 1.15 μm) and stage 4 (1.15 to 0.75 μm).

Notice that the ratio of these elements changes within each graph as a function of time. When you observe a change in ratios between elements within the same size mode that is aerosol of a different character (i.e. different source, different influences). Notice stage 1 and stage 2 look very similar. That results from these elements being representative of soils, and soils dominate these size modes. sulfur becomes more important by stage four where it corresponds to accumulation mode sulfate particles.

Notice also at a given time across the sequence of four plots, you will observe compositional changes with size. This is the result of particle sizes being tied to the particle formation process. So, in essence looking across size modes inherrantly is looking across diffferent source signatures.

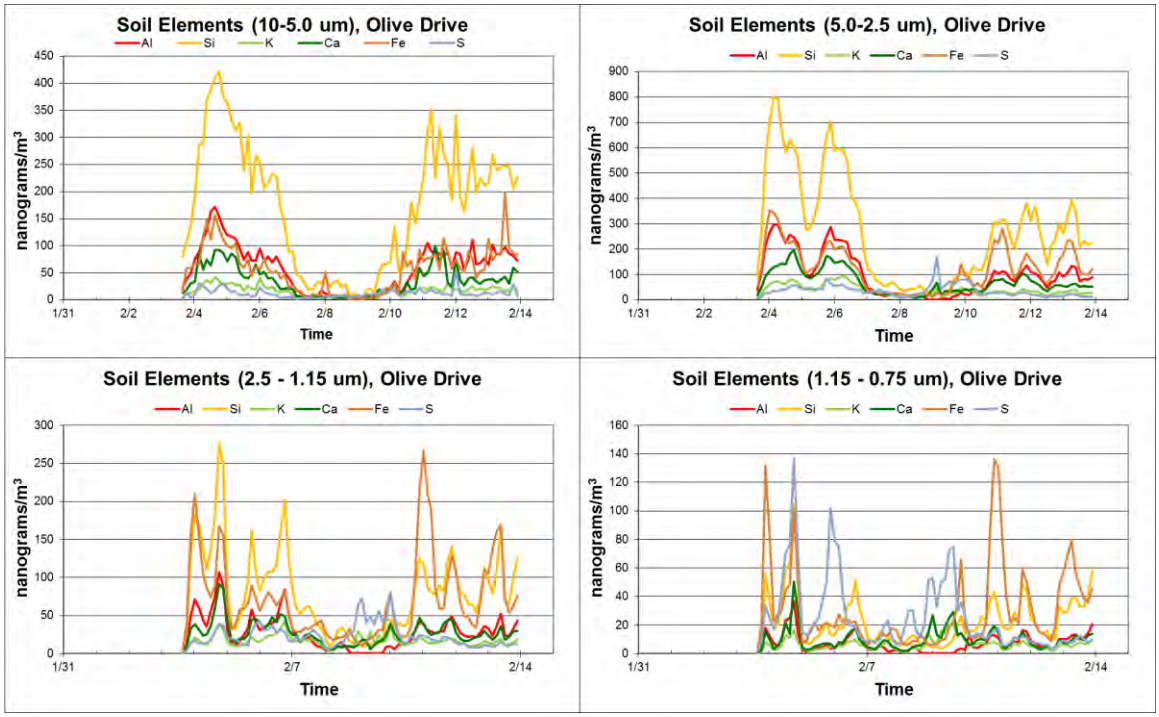

Figure 20. Soil Elements (plus S) versus Time, for four coarsest size modes

Ultra-fine signature in elemental data

Now let's look at the size mode of greatest interest in this study and whether we see evidence of roadway emissions. For that we can look at sulfur in the finest size modes, Figure 21. In stage 8 (0.26 to 0.09 µm) and stage 9 (0.09 to 0.0 µm) sulfur is representative of roadway emissions. Stage 7 (0.34 to 0.09 µm) is often overwhelmed by the influence of accumulation mode sulfates but in this study it tracks well with stage 8 and 9, this is likely due to the overall clean conditions of the study.

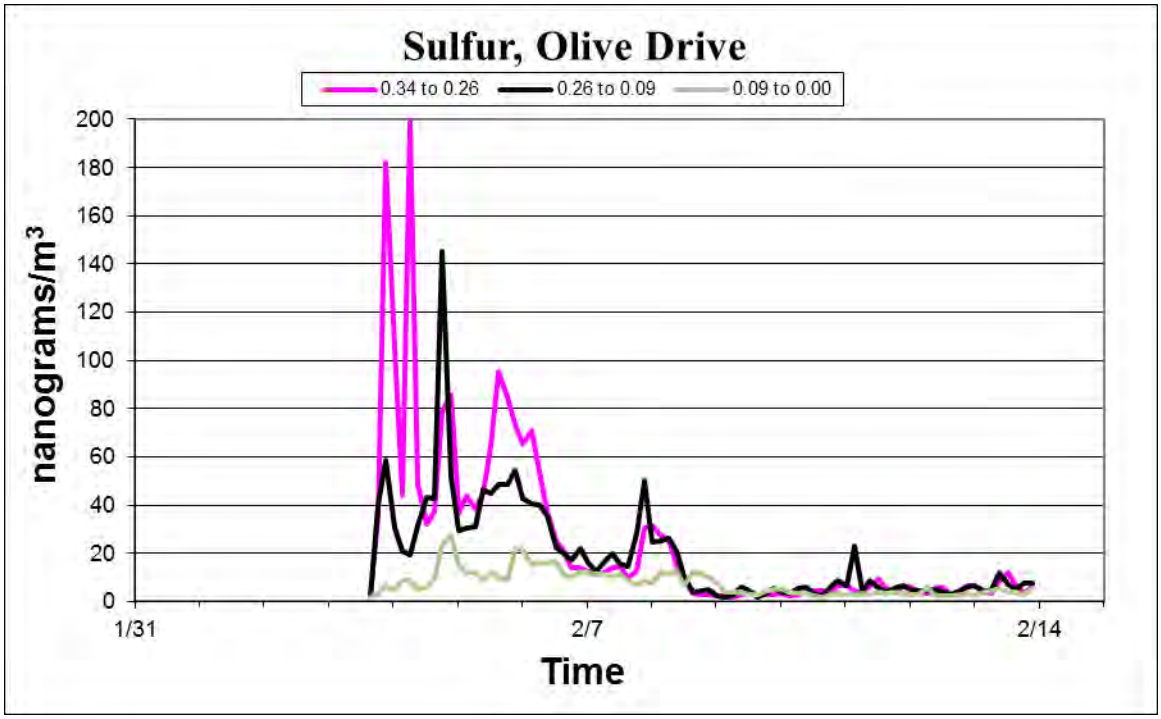

Figure 21. Three finest size modes of sulfur

The presence of sulfur in stage 8 and 9 is an indication that even though conditions were clean overall we can detect ultra-fine signatures associated with roadway traffic.

Ultra-fine elements compared to local heavily traveled secondary road

A recent paper generated a list of observed elements in the ultra-fine mode and measured the concentrations Cahill (2014). Since it is data from Sacramento and includes both spring and winter (inversion) conditions this is a good set of data for comparison. The paper showed meteorological differences between winter inversion conditions and spring conditions profoundly affect the ability to detect potential local emission issues.

Table 5 below compares concentrations for ultra-fine elements from OlDr to those found downwind of a heavily traveled secondary road in Sacramento, Cahill (2014). The table has the OlDr concentrations in the center, with the spring and winter data on either side, followed subsequently by the ratio of OlDr concentrations to each data set.

The paper used a 4 week average, since we did not have that much data; a comparison to one week of data was used. The OlDr concentrations are based on the first full week of data, starting on the first full day 2/4/2015. The four week average concentrations from the paper were divided by four to get a one week average for comparison.

	Ratio OlDr to Spring ArMi	Spring ArMi (ng/m^3)	OlDr (ng/m^3)	Winter ArMi (ng/m^3)	Ratio OlDr to Winter ArMi
Calcium	**9.1**	**0.41**	**3.77**	**2.58**	**1.46**
Sulfur	0.3	**32.25**	**9.72**	**9.78**	**0.99**
Potassium	**1.6**	2.90	**4.61**	5.00	**0.92**
Chromium	**5.5**	0.01	0.07	0.21	0.33
Manganese	**33.3**	**0.04**	**1.33**	**0.33**	**4.10**
Iron	0.4	**1.20**	0.50	**7.28**	0.07
Nickel	**4.4**	**0.08**	0.33	**2.88**	0.11
Copper	**3.2**	**0.10**	0.32	**2.03**	0.16
Zinc	**1.6**	**0.50**	0.80	**3.20**	0.25
Arsenic	-	0.08	nd	0.10	-
Selenium	-	0.06	nd	0.04	-
Bromine	0.5	0.45	0.23	0.29	0.77
Lead	**1.2**	0.35	0.43	0.41	**1.07**

Table 5 Comparison of Nishi ultra-fine metals to Watt Avenue study, both winter and spring.

The comparison shows the concentrations of eight out of eleven of these ultra-fine elements seen during the Nishi study are significantly larger than that seen in spring conditions in the Watt Avenue study. In fact five out of eleven are comparable or more then the winter concentrations which were known to be influenced by inversion conditions, which would make the levels higher.

Given the favorable meteorological conditions, i.e. conditions that would tend to reduce measurable freeway emission levels, this result is surprising. It is not surprising that the emissions are generally more than the spring conditions for the Watt avenue study, because this freeway carries more traffic. It is a concern that several species are comparable to the strongly inversion influenced concentrations of the winter data.

If we consider the sum of the elements measured in the ultra-fine mode to that in PM2.5 and PM10 there is a relatively large fraction (Figure 22, percent ultra-fine/PM2.5 dotted line) which comes in the ultra-fine mode when source contributions and meteorology come together.

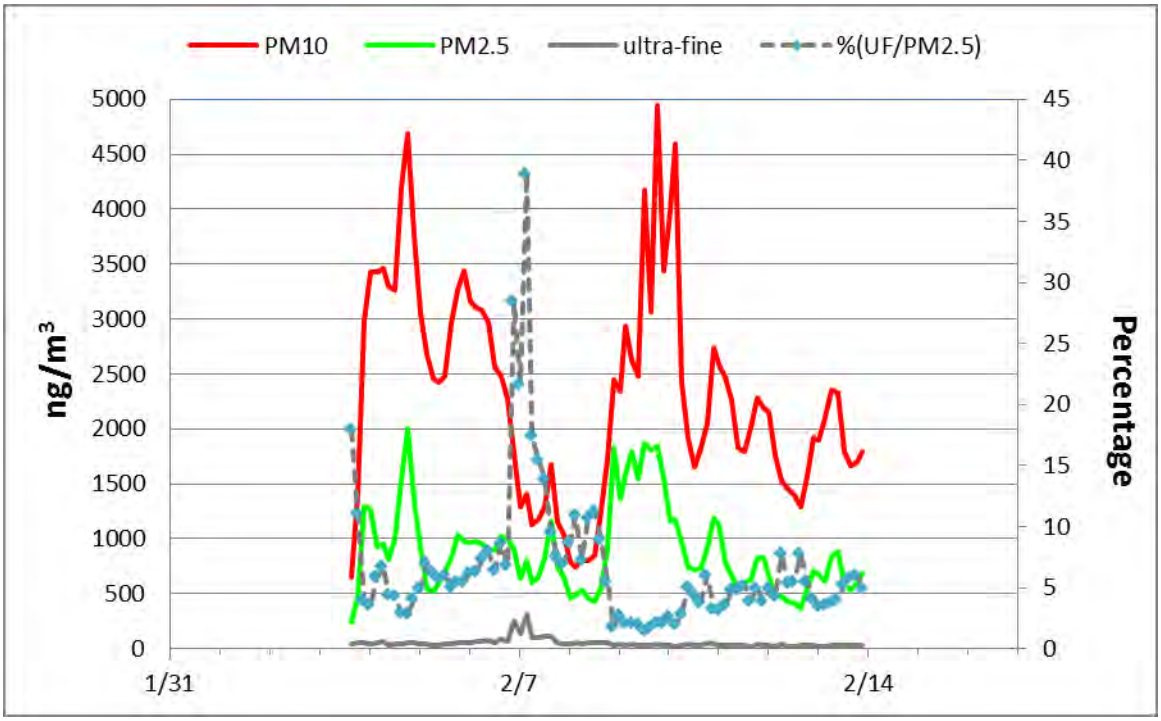

Figure 22. Summed elements for PM10, PM2.5, ultra-fines and the ratio Uf/PM2.5

This peak in ultra-fine elements at 2/7 extends from Friday afternoon to late Saturday. This is the time most likely to be affected by weekend traffic. This is the only time during the study the site was exposed to the weekend traffic and it shows up clearly as the largest concentrations in the ultra-fine signal.

The overall PM values are coming down at the time the ultra-fines are peaking. This is due to the fact that rain does not remove ultra-fines quite as efficiently as larger particles. So the rise while PM is falling is directly consistent with the different particle size behaviors during rain, see Figure 23.

Note that this is a sum of detectable elements only and cannot be compared directly with the mass concentrations. (What is missing primarily is the large mass contributions of lighter elements which make-up organics and oxides, namely hydrogen, carbon, and oxygen.)

Note:
All of the S-XRF concentrations data included in the digital files will be provided in the form of Excel spread sheets, Attachment 7. The elemental concentrations

for the study represent over 13,000 separate elemental concentrations across 9 size modes.

Meteorological Results

Meteorological data was utilized to determine what periods of the deployment might best represent a signature of the freeway at the sampling site. In larger studies, an upwind sampling site can provide actual baseline data for direct comparison (the concentrations of the baseline site can be subtracted from the concentrations of the downwind site). In this study however, we could not have deployed two such sites in the timeframe available, given the short timeline goal. Meteorology is however, always the basis which determines the intervals of greatest interest for characterizations.

Two types of meteorological sources were used to obtain the data to evaluate the likelihood of aerosol impact from the freeway: local weather from the University AP site utilizing weather underground, and NOAA READY HYSPLIT trajectory modeling.

Wind Direction, Wind Speed and Rain

Wind Direction

For favorable detection we are interested in times when the wind direction would bring the air across the freeway directly to the site in the shortest distance. The best wind directions to see an influence would be from the south or southeast as these are most direct (shortest distance) to the measurement site. On the graph this is the green line between 135º and 180º.

However in looking at the site overview, Figure 1, Page 4, air moving in from the southwest around the south to the east also crosses the freeway, this may allow more detection opportunity but with more distance there is more concentration fall-off possible.

In Figure 23 wind direction is represented by a green line, the left vertical axis is in units of degrees which means 0º = North, 90º = East, 180º = South, and 270º = West, then 360º is back to North.

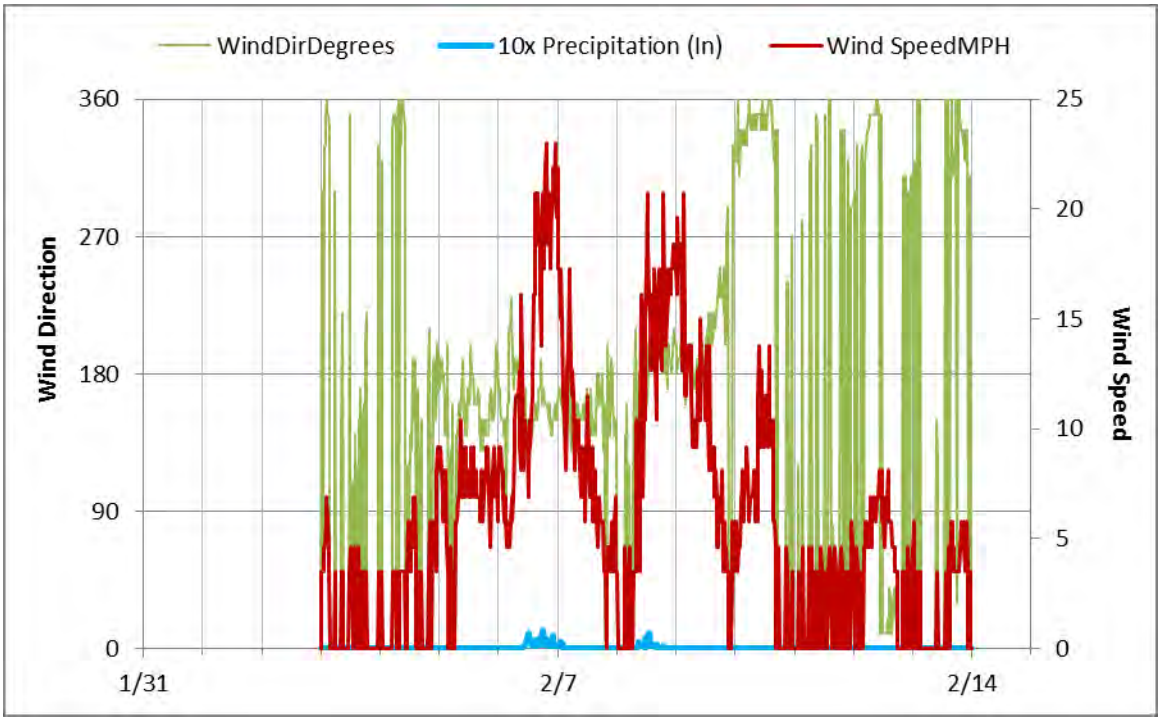

Figure 23. Wind Direction, Wind Speed, and Rain

Wind Speed
Higher wind speed means more dilution of a source by the crossing air volume. If there are no winds the local emission will "pile-up" near the source. Therefore easiest detection will occur if wind velocities are low. Wind Speed is indicated by the red line, Best detection would be the red line below 5 mph (right axis).

Rain
Rain tends to remove particles from the air, so during rain any build-up is reduced and levels will be lower. Larger particles are removed more efficiently than ultra-fine but these concentrations will also be continually reduced.

So considering the meteorology during the study, I can make the following observations: wind was from the south or southwest about 30% of the time. During those times the wind speed was less than 6 mph less than 25% of the time. From early on the 5th to the 10th the slower winds occurred mostly late at night and in the early mornings when traffic impacts are reduced. Optimum exposure for the sampling site to detect freeway emission occurred less than 10% of the time.

Additional Air Quality Data

In order to corroborate whether these aerosol measurements are indicative of relatively clean conditions for most of the deployment interval, I checked the Air Quality Index (AQI) during the time of the study.

The most significate effects from local sources are most easily measured during periods of low air movement and especially our winter inversions as they trap local emissions. If such conditions exist the AQI should also suffer.

The data in Table 6 below were taken from the spare the air web site. These data are from a station identified as “UC Davis campus”. The AQI, in this case is referenced to PM2.5 mass.

http://www.sparetheair.com		
sacramento region		Site
		Davis UCD Campus
		Max PM2.5 AQI
Saturday	1/31/2015	18
Sunday	2/1/2015	91
Monday	2/2/2015	67
Tuesday	2/3/2015	63
Wednesday	2/4/2015	87
Thursday	2/5/2015	63
Friday	2/6/2015	55
Saturday	2/7/2015	39
Sunday	2/8/2015	41
Monday	2/9/2015	38
Tuesday	2/10/2015	26
Wednesday	2/11/2015	35
Thursday	2/12/2015	28
Friday	2/13/2015	48
Saturday	2/14/2015	31
Sunday	2/15/2015	35
Deploy Average =		**47.5**
	Good Rating is 50 or below	
Moderate rating is between 50 and 100		

Table 6. Air Quality Index during OlDr study from 2/3 to 2/13

The local AQI data shows we had good air during almost the entire study. In fact the highest reading during the study (boxed data) was 87 on the first full day of the study (Wednesday, Feb. 4th). It is also the only reading above the halfway point of the moderate AQI range of 50 to 100. Seven of the 11 days were in the good air range of AQI (0-50), and the average over the study is 47.5, this was “good” air and thus unlikely to have had many inversion impacts.

Thus AQI, overall low mass and elemental concentrations and meteorology suggests, the study interval was not a strong inversion period.

Separation of source interferences using measured air trajectory

While local meteorology is very useful to determine immediate on-to-site wind direction, regional wind patterns are also important to identify potential upwind sources, or establish downwind impacted areas. For this we used HTSPLIT, Draxler (2012), Rolph (2012) and Attachment 6. Trajectories were determined for particles arriving at 7 AM and 5 PM for the days of the study. These times were chosen above other times of day as these represent the likely times of highest traffic impact.

Figure 1 below shows the direction from which the given trajectory moved onto the Nishi property, for each trajectory end time 7 AM and 5 PM, on every day of the study.

Figure 24 Direction entering Nishi for each modeled HYSPLIT Trajectory

So the positons of the points along the time axis are the times during the highest daily traffic impact (chosen as 7AM and 5PM), and the vertical axis is the angle the trajectory enters the property at that time. The angles corresponding to the most direct exposure are 180º and 135º. All of these occurred during the first six days of the study. Even further, considering the broader exposure angles 90º to 225º, all but one occurs within the first 6 days.

LIST OF ATTACHMENTS

The S-XRF elemental analysis was performed at the Advanced Light Source, Lawrence Berkeley National Laboratory by Dr. Yongjing Zhao, standards calibrations and data reduction also by Dr. Zhao, University of California, Davis.

All field preparation, sample preparation, beta mass attenuation analysis, remaining elemental data analysis, and report generation and project management performed by Dr. David E. Barnes.

SIGNATURE

_____

David E. Barnes
DELTA Group, Project Scientist
University of California, Davis

IX. REFERENCES

Cahill, T.A., David E. Barnes, Nicholas J. Spada, Seasonal variability of ultra-fine metals downwind of a heavily traveled secondary road, Atmospheric Environment 94, 173 – 179 (2014), doi:10.1016/j.atmosenv.2014.05.025 (PDF in soft copy)

Cahill, Thomas A. Comments on surface coatings for lundgren-type impactors. Aerosol Measurement. Dale A. Lundgren, Editor. University Presses of Florida, Pp. 131-134 (1979).

Cahill, T. A., David E. Barnes, Earl Withycombe , and Mitchell Watnik, Very Fine and Ultra-Fine Metals and Ischemic Heart Disease in the California Central Valley 2: 1974 – 1991, Aerosol Science and Technology 45, 1135-1142 (2011a).

Cahill, T. A., David E. Barnes, Nicholas J. Spada, Jonathan A. Lawton, and Thomas M. Cahill, Very Fine and Ultra-Fine Metals and Ischemic Heart Disease in the California Central Valley 1: 2003 – 2007, Aerosol Science and Technology 45, 1125-1134 (2011b).

Draxler, R.R. and Rolph, G.D., 2012. HYSPLIT (HYbrid Single-Particle Lagrangian Integrated Trajectory) Model access via NOAA ARL READY Website (http://ready.arl.noaa.gov/HYSPLIT.php). NOAA Air Resources Laboratory, Silver Spring, MD.

Hu S., Fruin S., Kozawa K., Mara S., Paulson S., Winer A.M., A wide area of air pollutant impact downwind of a freeway during pre-sunrise hours. Atmospheric Environment; 43:2541–2549, (2009).
Lippmann, Morton, Semi-continuous speciation analysis for ambient air particulate matter: an urgent need for health effects studies. J. Expo. Sci. Epidemiol. Stud. 19, 235-247 (2009)

Raabe, Otto G., David A. Braaten, Richard L. Axelbaum, Stephen V. Teague, and Thomas A. Cahill. Calibration Studies of the DRUM Impactor. Journal of Aerosol Science. 19.2:183-195 (1988).

Rolph, G.D., 2012. Real-time Environmental Applications and Display sYstem (READY) Website (http://ready.arl.noaa.gov). NOAA Air Resources Laboratory, Silver Spring, MD.

Seinfeld, J.H, and Pandis, S.N., Atmospheric Chemistry and Physics: From Air Pollution to Climate Change, Wiley Interscience (1998).

Wesolowski, J.J., W. John, W. Devor, T.A. Cahill, P.J. Feeney, G. Wolfe, R. Flocchini. Collection surfaces of cascade impactors. In X-ray fluorescence

analysis of environmental samples. Dzubay, T., Editor. Ann Arbor Science, Pp. 121-130 (1978).

Attachment 1: Curriculum Vita for David E. Barnes, Ph.D.

Project Scientist/Manager, DELTA Group,
One Shields Ave, University of California, Davis, CA 95616
E-mail: debarnes@ucdavis.edu

PROFESSIONAL PREPARATION

1993 **Ph.D. in Physics**, University of California, Davis
1987 **M.S. in Physics**, University of California, Davis
1982 **B.S. in Physics, B.S. in Oceanography**, Humboldt State University, Arcata, Calif.

PROFESSIONAL EXPERIENCE

2007-June 2014 Assistant Project Scientist III - V, JMIE, University of California, Davis
2005-2007 Post-Doc/Researcher/Project Manager, CEMS Dept., UC Davis
2003-2004 Researcher/Lecturer, Physics Dept., University of California, Davis
2000-2002 Process Development Engineer, CSpeed Corp., Santa Clara, CA
1998-2000 Microfabrication Process Engineer, Consulting, Davis, CA
1998 Sputter Process Engineer, HMT Technology, Fremont, CA
1997 Senior Advisory Yield Engineer, Seagate Recording Media, Milpitas, CA
1995-1997 Manager, Microfabrication Facility, ECE Dept., UC Davis, CA
1988-1995 Lecturer, Researcher, Research Assistant, Physics Dept., UC Davis

AEROSOLS RESEARCH STUDIES (DELTA GROUP)

A. I have been Projects Manager for all DELTA Group programs, 2005 – 2014. I also have been a Research Scientist with 8 peer reviewed publications and 15 research projects, including development of a new S-XRF beam line at SSRL, SLAC, Stanford. Below is a partial list of the funded studies that I have managed, including being primarily responsible for all field and day-to-day activities for these contracts, with T. A. Cahill, P.I. or co-P.I. with Prof. Jim Shackelford (Chem. Eng./MS) or Geoff Schladow (TERC).

1) Aerosols on the Greenland Ice Cap, Summit site, NSF Polar , 2003 – 14, 185 K
2) Continuous measurement of ultra-fine aerosols, near roadways and Indoor/Outdoor
   a) (OAPQS/ORD, Additional funding analysis/publication 2011 – 13, $20K
   b) (OAPQS/ORD, Detroit, NEXUS study) EPA 2010 – 11, $25 K
   c) (OAPQS/ORD, Cleveland study) EPA 2009 – 10, $24.4 K
3) Design and Development of Extension of S-XRF Analysis capabilities for Improved Aerosol Characterization Technology, UAF 2009 – 11, $20K
4) Antioch Dunes National Wildlife Refuge, Study of Aerosols to access Impacts on endangered species, Costs shared analysis, personnel 2012 – 13, few K
5) Deposition of toxic aerosols in California CA DTSC 2009 – 12, $350 K
   a) Aerosols from a Wilmington car shredder 2009 – 11
   b) Aerosols from the BNSF rail yard, San Bernardino 2010 – 11
   c) Aerosols near the Exide battery recycling plant 2010 – 12
   d) Aerosols impacting salt ponds in Redwood city 2011 – 13
6) Design and Development of Better Aerosol Characterization Technology, UAF, 2009 – 11, $200^{+}K
7) Field Sampling Support And Mass/Chemical Analyses Using DRUM Technology
   a) AK – Dept. of Environmental Conservation, subcontract through University of Alaska, Fairbanks, sampling related to Regional Haze Rule 2009 – 2010, $150K

8) Effect of off-road vehicles on PM_{10}, Oceano Dunes, San Luis Obispo, APCD, 2008-2010, $118 K
9) Aerosol Research Studies and Educational Programs with Breathe Calif.
   a) Smoke at Del Paso Manor SMAQMD, BCSET 2009 – 2010, $26 K
   b) Impact of near roadway aerosols SMAQMD, BCSET 2007 – 2009, $50 K
   c) Comparison of DRUM sampler with ARB FRMs, Breathe California/ARB, volunteer effort, 2007 – 2008
10) Aerosol Measurements for El Paso Asthma study, NIH 2008 – 2011. $52 K
11) Aerosols from the Roseville rail yard, BCSET, EPA Region IX, 2005 – 2008, $26 K
12) Central Valley aerosols and ischemic heart disease, BCSET, Legacy Law Group, 2008 – 2009, $26K
13) Fine particulate pollution at Lake Tahoe, TERC, EPA Region IX, 2006 – 2009, $180
14) Aerosols before and after Ice-Slicer™ Applications to Highway 50 at South Lake Tahoe, Cal Trans Storm Water Studies, 2005 – 2006, 73 K

Related Peer Reviewed Articles

T.A. Cahill, David E. Barnes, N. J. Spada, J. A. Lawton, and T. M. Cahill, **Very Fine and Ultra-Fine Metals and Ischemic Heart Disease in the California Central Valley 1: 2003 – 2007**, Aerosol Science and Technology, Special Issue on Air Pollution and Health: Bridging the Gap from Sources to Health Outcomes, Vol. 45, No. 9, Sept. 2011

T. A. Cahill , David E. Barnes, E.Withycombe, and M. Watnik , **Very Fine and Ultra-Fine Metals and Ischemic Heart Disease in the California Central Valley 2: 1974 – 1991** , Aerosol Science and Technology, Special Issue on Air Pollution and Health, Vol. 45, No. 9, Sept. 2011

T. A. Cahill, T. M. Cahill, David E. Barnes, N. J. Spada and R. Miller, **Inorganic and organic aerosols downwind of California's Roseville rail yard**, Aerosol Science and Technology, Special Issue on Air Pollution and Health, Vol. 45, No. 9, Sept. 2011

C. F. Cahill, P. G. Rinkleff, J. Dehn, P. W. Webley, T. A. Cahill, David E. Barnes, **Aerosol measurements from a recent Alaskan volcanic eruption: Implications for volcanic ash transport predictions**, Journal of Volcanology and Geothermal Research 198 (2010) 76–80,

R. VanCuren, T. A. Cahill, J. Burkhart, David E. Barnes, Y. Zhao, K. Perry, S. Cliff, and J. Mcconnell. **Aerosols and their sources at Summit Greenland – First results of continuous size- and time-resolved sampling**. Atmospheric Environment, 52: 82-97 doi:10.1016/j.atmosenv.2011.10.047

Peter Jenniskens (NASA), …Thomas A. Cahill, David E. Barnes, Jonathan Lawton (UCDavis), … and 66 additional authors, **Radar enabled recovery of Sutter's Mill Meteorite, a unique carbonaceous chondrite regolith breccia**, Science Magazine 338:1583-1587 (2012) doi: 10.1126/science.1227163, (10/2012)

S.R. Barberie, T.A. Cahill, C.F. Cahill, T.M. Cahill, C.R. Iceman, D.E. Barnes. **UC Davis XIPline ("zipline") end-station at the Stanford Synchrotron Radiation Lightsource: Development and experimental results.** Nucl. Instrum. Meth. Phys. Res. A: Accelerators, Spectrometers, Detectors and Associated Equipment 729:930-933 (2013) doi:10.1016/j.nima.2013.08.043

T. A. Cahill , David E. Barnes, N. J. Spada, **Seasonal variability of ultra-fine metals downwind of a heavily traveled secondary road**, Atmospheric Environment, 94 (2014)173-179, doi:10.1016/j.atmosenv.2014.05.025

Attachment 2: Overview of DRUM Quality Assurance Protocols

Summary of Quality Control and Quality Assurance procedures and validations
Validations in peer reviewed literature

Background:

The University of California, Davis designed and built rotating drum impactors, with the UC Davis 8 DRUM the dominant design. This sampler uses the principle of Lundgren et al 1967 to impact aerosols onto sticky surfaces in 8 size modes, selected aerodynamically by a series of smaller and smaller slot orifices. The impaction surfaces are slowly rotating drums, allowing collection of aerosols continuously over extended periods, typically 5 weeks. This allows use of focused beam analytical techniques to analyze for mass, optical behavior, and elemental composition with typical time resolution from 1 hr to 3 hr. Thus, the 8 DRUM collects typically 2,500 aerosol samples in a 5 week period, at the rate of 48 samples /day (3 hr time resolution, 8 size cuts). These can be directly compared with meteorological information source activities, etc. to identify sources in a way impossible for a 24 hr averaging Federal Reference Method (FRM) filter.

The 8 DRUM is a diagnostic tool and not meant to be a replacement for FRM sampling . However, it is important that data from the 8 DRUM can be compared to FRM data to obtain maximum relevance to regulatory needs. In this summary, we will provide some of the tests that support the accuracy and precision of 8 DRUM sampling and analysis. These will be presented in several categories:

1. Information from peer reviewed publications in the refereed literature,
    a. Sample collection and analysis for mass
        i. Sample analysis and analysis for mass
        ii. Elements by XRF and S-XRF analysis
2. Data required by the US EPA in Qapp/QC documentation required for EPA-funded research studies, and
3. Data from legal actions vetted by depositions and discovery actions.

i. DRUM sizing

An extremely important point is that Marple (1974) established analytical solutions for the size cuts of cascade impactors for both jetted and slotted designs. These were extensively validated at the U. Minnesota (Rao, thesis 1979 among others) which means that unlike many other types of samples (MOUDI, ..) any validations are merely confirmations of a validated theory. After the DRUM sampler was invented, the size cuts in sample collection were independently validated in a peer reviewed paper Raabe et al (1988).

Raabe, Otto G., David A. Braaten, Richard L. Axelbaum, Stephen V. Teague, and Thomas A. Cahill**. Calibration Studies of the DRUM Impactor.** *Journal of Aerosol Science.* 19.2:183-195 (1988).

Two different methods were used to establish the cut points. The results are given below in Table 1 Recently, the initial cut point was validated against an EPA FRM PM_{10} inlet during and extensively and formally peer reviewed EPA/SLOAPCVD funded study of dust at Oceano

Dunes , and the final two cut points were re-confirmed by the University of Alaska, summer, 2008.

Table 7 Parameters of the DELTA DRUM Slotted Drum Impactor

The width of the mass at full width, half maximum, W mass, represents the measured footprint of a non-rotating DRUM, accurate to about ± 15%. This results in a resolution in time using a 42 day rotation period (4 mm/day) given in T (hr). The after filter was not used in this work.

Stage No.	W (s) cm	L Cm	S cm	P out kPa	Re	u out m/s	ECD ae, μm	W (d) μm	ΔTime hr
1	0.360	0.6	1.44	101.3	2231	7.7	5.0	750	4.5
2	0.163	0.6	0.65	101.1	2810	17.1	2.5	500	3.0
3	0.073	0.6	0.29	100.2	3195	38.3	1.15	300	1.8
4	0.049	0.6	0.20	98.3	3331	58.3	0.75	265	1.6
5	0.038	0.6	0.15	94.9	3416	77.4	0.56	240	1.4
6	0.026	0.6	0.11	86.8	3575	122.2	0.34	245	1.8
7	0.024	0.6	0.10	75.1	3692	156.0	0.26	180	0.9
8	0.021	0.6	0.10	39.7	4595	315.9	0.09	175	0.9
filter									

This impactor (along with an IMPROVEd DRUM) was deployed in the EPA/NPS IMPROVE BRAVO study in Big Bend NP, July - October 1999, and has been in almost continuous use in scores of EPA and NSF supported studies since that time. The time resolution was obtained by the size of the analytical beams used, and could be low as 1 hr when analyzed at the synchrotron x-ray fluorescence microprobe of the Advanced Light Source, Lawrence Berkley NL. Peer reviewed papers based upon this sampler, together with its analytical use, is summarized in Appendix C.

a. Sample collection versus FRM $PM_{2.5}$ and analysis for mass

Since the FRM standard is based on mass, the DELTA Group has developed mass analysis based on soft beta ray transmission through DRUM strips and filters. The 67 keV betas of Ni^{63} are a good match to the 500 $\mu g/cm^2$ Mylar® drum strips. The beta takes measurements every 0.5 mm, resulting in a time resolution of 3 hr when the DRUM is used in a continuous 5 week field study.

An example of the precision achieved for mass is shown in an inter-comparisons done as part of an extensive set of quality assurance tests under contract with the US EPA.

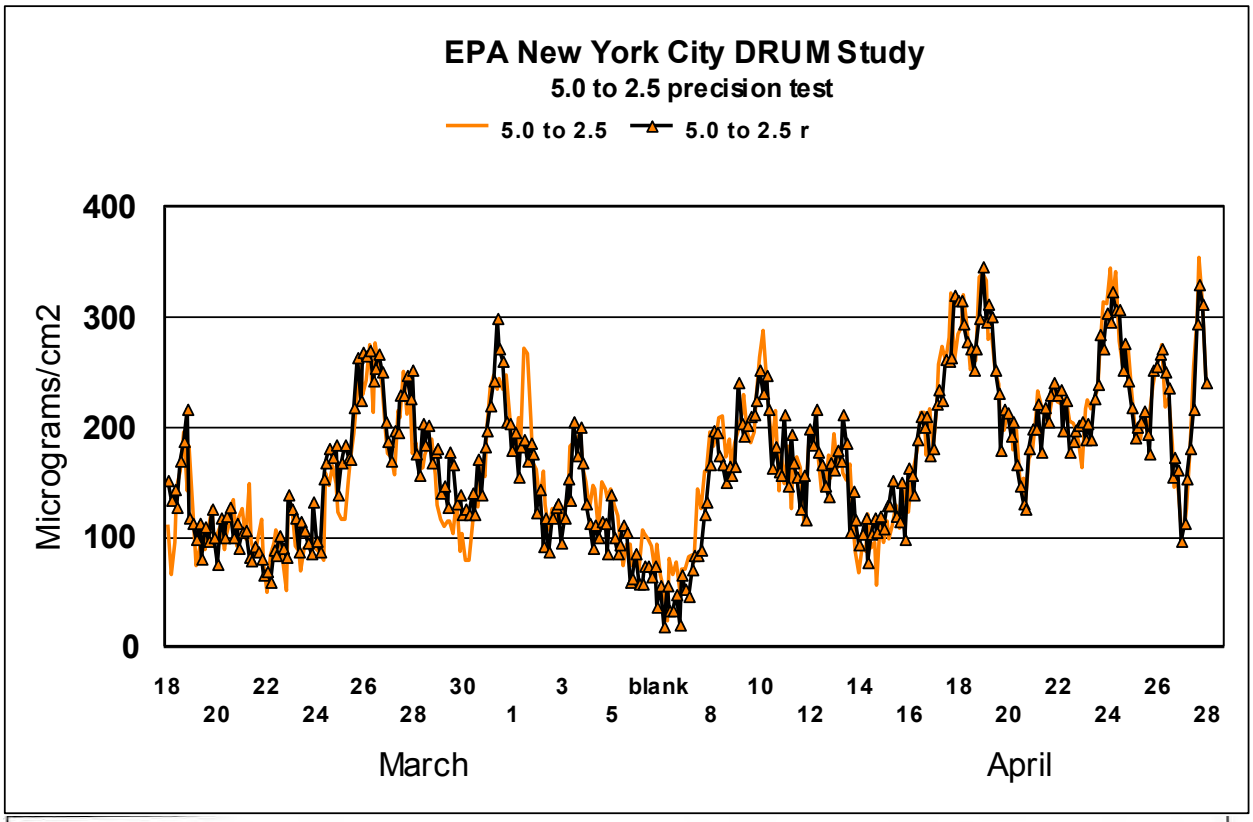

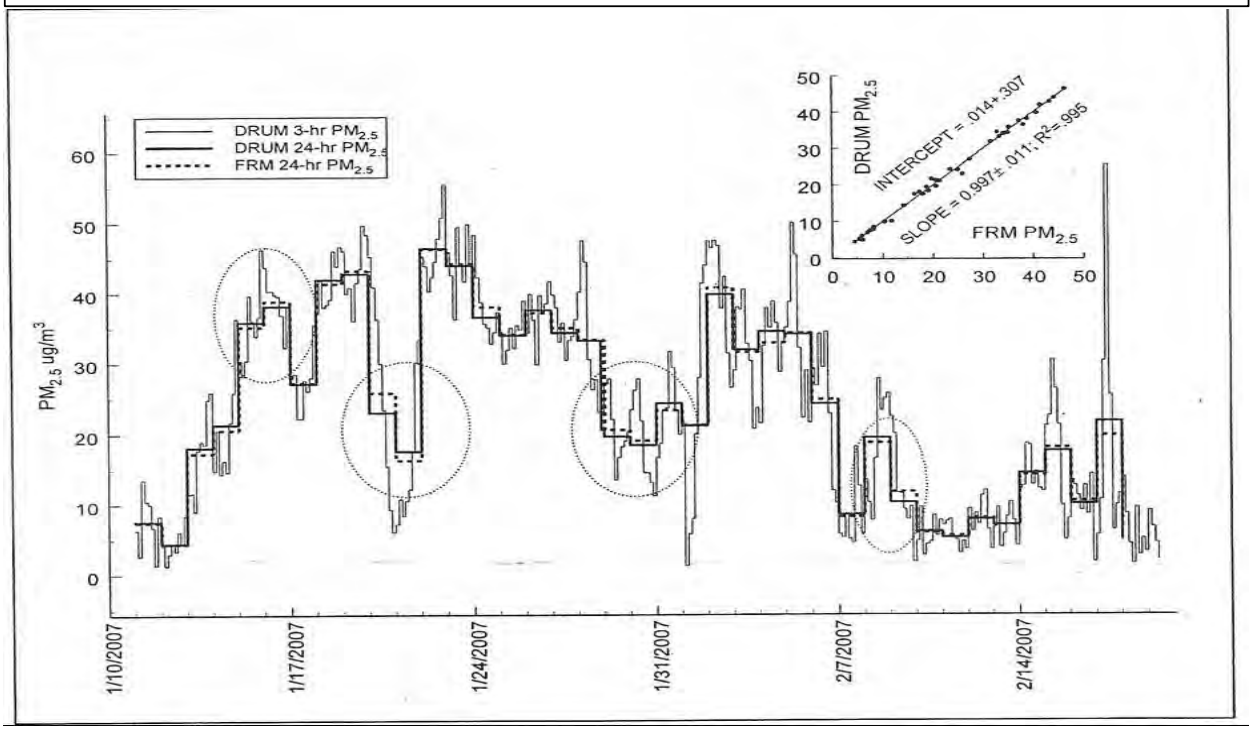

The most recent comparison of the DRUM sampling collection followed by mass analysis was done as part of a 1 year side by side study with the California Air resources Board. Below we show the results for the most polluted period, winter, as prepared by CVA Air Resources Board staff. The agreement was within 1 %, but for the entire year, better than ± 10%,

well superior to the EPA criterion of ± 15%. These results were peer reviewed and included in two papers in an EPA sponsored Special Issue of Aerosol Science and Technology.
Thomas A. Cahill, David E. Barnes, Nicholas J. Spada, Jonathan A. Lawton, and Thomas M. Cahill , Very Fine and Ultra-Fine Metals and Ischemic Heart Disease in the California Central Valley 1: 2003 – 2007**, Aerosol Science and Technology** 45**, 1125-1134 (2011)**
Thomas A. Cahill, Thomas M. Cahill, David E. Barnes, Nicholas J. Spada and Roger Miller , Inorganic and organic aerosols downwind of California's Roseville Railyard**, Aerosol Science and Technology** 45**, 1049-1059 (2011)**

b. Elements by XRF and S-XRF analysis

Although the FRM standard is based on mass, two major EPA-sponsored ambient aerosol programs also add elemental and chemical analysis, the non-urban IMPROVE program (which I started and ran 1977-1997), and the similar but urban Species Trends Network (STN). Both relay on protocols using x-ray analysis.

Our XRF protocols use NIST FRMs 1832 and 1833 (which we helped develop) and 65 thin elemental standards from Micromatter Corp., Seattle , WA. We participated in inter-comparisons with IMPROVE and major commercial and university laboratories, (below).

Table 2 Summary of intercomparisons, DELTA S-XRF versus other laboratories

Study and date	Methods	**Average ratio, Al to Fe**	Std. dev.	**Average ratio, Cu to Pb**	Std. dev.
BRAVO, 1999	PIXE vs S-XRF	**0.99**	0.04		
BRAVO, 1999	CNL XRF vs S-XRF			**1.24**	0.14
FACES, 2001	ARB XRF vs S-XRF	**0.93**	0.21	**1.02**	0.08
ARB LTAD 2005	DRI XRF vs S-XRF	**1.037**	0.085	**0.907**	0.009
All prior studies	**Average**	**0.984**	**0.15**	**0.977**	**0.115**

A recent inter-comparison is in a Table 7, in the Science issue of Dec 21, 2012, showing excellent agreement with XRF and ICP/MS laboratories, (1.005 ± 0.30) even to the ppb level. (Appendix B) For additional details, In Appendix C one can requisition the official US EPA QAPP/QC documentation supporting a recent study in Cleveland, Ohio.

c. Validation, mass versus sum of species

A key validation of any technique is comparison of diverse methods. As part of the side by side study with the CA ARB at 13th and T Street, the ultra-fine fraction was analyzed for mass (gravimetrically by weighing the filters) and then compared to the sum of all species. The organic matter was estimated using the technique developed by the DELTA Group and

extensively used in the IMPROVE Program, including 10s of thousands of comparisons, organic matter by combustion (DRI) versus organic matter by hydrogen.

Table 3 Mass closure for ultra-fine mass, D_p < 0.09 µm. Note the dominance of the non-soil iron, nickel, copper, and zinc in the transition metals.

Mass	ng/m3		Minor ultra-fine species	ng/m3
Mass (gravimetric)	**2,040 ± 200**		Phosphorus	2.4 ± 0.2
Mass (reconstructed)	**2,150 ± 350**		Vanadium	0.15 ± 0.01
			Chromium	0.45 ±0.04
Major ultra-fine species			**Iron (non-soil)**	**38.0 ± 6**
Organic mass (OMH)	1,720 ± 200		**Nickel**	**3.5 ± 0.4**
Ammonium Sulfate	340 ± 150		**Copper**	**8.3 ± 0.8**
Salt	40 ± 4		**Zinc**	**11.5 ± 1.2**
Soil (IMPROVE)	48 ± 5		Arsenic	0.6 ± 0.2
K non	53 ± 5		Selenium	0.3 ± 0.1
Metals (- iron)	0.035 ± 0.002		Bromine	3.7 ± 0.4
			Lead	4 ± 0.4

Cahill, T.A., R.A. Eldred, N. Motallebi, and W.C. Malm**. Indirect measurement of hydrocarbon aerosols across the United States by nonsulfate hydrogen-remaining gravimetric mass correlations.** *Aerosol Science and Technology.* 10:421-429 (1989).

Quality Control and Quality Assurance validations

The Quality Control and Quality Assurance protocols set the standard for all such groups around the world, as evidences by peer reviewed publications based on the techniques of the DELTA Group.

Overviews of aerosol compositional analysis:

Cahill, Thomas A. and Paul Wakabayashi. **Compositional analysis of size-segregated aerosol samples.** Chapter in the ACS book *Measurement Challenges in Atmospheric Chemistry*. Leonard Newman, Editor. Chapter 7, Pp. 211-228 (1993).

Cahill, Thomas A. **Compositional Analysis of Atmospheric Aerosols**. 1995 *Particle-Induced X-Ray Emission Spectrometry*, Edited by Sven A. E. Johansson, John L. Campbell, and Klas G. Malmqvist. *Chemical Analysis Series,* Vol. 133, pp. 237-311. John Wiley & Sons, Inc.

Publications using S-XRF (early - SSRL)

Cahill, Thomas A., Kent Wilkinson, and Russ Schnell**. Compositional analyses of size-resolved aerosol samples taken from aircraft downwind of Kuwait, Spring, 1991**. *Journal of Geophysical Research*. Vol. 97, No. D13, Paper no. 92JD01373, Pp. 14513-14520, September 20 (1992).

Cahill, Thomas A., Kent Wilkinson, Paul Wakabayashi, Robert Eldred, and William Malm**. Observation of oil smoke in the upper troposphere at Mauna Loa Observatory - a middle eastern source?** *CMDL No. 20 Summary Report 1991* Eldon E. Ferguson, Editor. Boulder, CO. pp. 89-90, December (1992).

Reid, Jeffrey S., Thomas A. Cahill, and Micheal R. Dunlap**. Geometric/aerodynamic equivalent diameter ratios of ash aggregate aerosols collected in burning Kuwaiti well fields.** 1994 *Atmospheric Environment*, Vol.28, No. 13, pp. 2227-2234

Reid, J.S., T.A. Cahill, E.A. Gearhart, R.G. Flocchini, J.S. Schweitzer, and C.A. Peterson. **Elemental analysis of Kuwaiti petroleum and combustion products**. *Journal of Nuclear Geophysics*. Vol. 7, No. 1, Pp. 81-86 (1993).

Publications using S-XRF (ALS)

14-1 Cahill, Thomas A., , David E. Barnes, Nicholas J. Spada, **Seasonal variability of ultra-fine metals downwind of a heavily traveled secondary road**, , Atmospheric Environment 94, 173 – 179 (2014)

13-2 Baldauf, Richard, Greg McPherson, Linda Wheaton, Max Zhabg, Tom Cahill, Chad Bailey, Christina Hemphill-Fuller, Earl Withycombe, and Kori Titus, **Integrating Vegetation and Green Infrastructure into Sustainable Transportation Planning**, Transportation Research Bulletin, National Academy of Sciences (2013**)**

13-1 Cahill, Thomas M., and Thomas A. Cahill. **Seasonal variability of particle-associated organic compounds near a heavily traveled secondary road**. *Aerosol Science and Technology* (2013) doi: 10.1080/02786826.2013.857757

12-2 VanCuren, Richard, Thomas Cahill, John Burkhart, David Barnes, Yongjing Zhao, Kevin Perry, Steven Cliff, and Joe Mcconnell, **Aerosols and their sources at Summit Greenland – First results of continuous size- and time-resolved sampling**. *Atmospheric Environment*, 52:82-97 (2012) doi:10.1016/j.atmosenv.2011.10.047

11-1 Thomas A. Cahill, David E. Barnes, Earl Withycombe, and Mitchell Watnik, **Very Fine and Ultra-Fine Metals and Ischemic Heart Disease in the California Central Valley 2: 1974 – 1991,** Aerosol Science and Technology 45, 1135-1142 (2011)

11.2 Thomas A. Cahill, David E. Barnes, Nicholas J. Spada, Jonathan A. Lawton, and Thomas M. Cahill , **Very Fine and Ultra-Fine Metals and Ischemic Heart Disease in the California Central Valley 1: 2003 – 2007**, Aerosol Science and Technology 45, 1125-1134 (2011)

11.3 Thomas A. Cahill, Thomas M. Cahill, David E. Barnes, Nicholas J. Spada, and Roger Miller, **Inorganic and organic aerosols downwind of California's Roseville Railyard**, Aerosol Science and Technology **45**, 1049-1059 (2011)

10-2 Cahill, Catherine F., Peter G. Rinkleff, Jonathan Dehn, Peter V. Webley, Thomas A. Cahill, and David E. Barnes, **Aerosol measurements from a recent Alaskan volcanic eruption: implications for ash transport predictions,** J. Volcanology and Geothermal Research 198, 76 - 80 (2010)

07-1 Emma Pere-Trepat, Eugene Kim, Pentti Taatero, and Philp k. Hopke**, Source Apportionment of time and size resolved ambient particulate matter measured with a rotating DRUM impactor,** *Atmospheric Environ.* 41: 5921–5933 (2007).

05-1 Perry, Kevin; Cliff, Steven S.; Jimenez-Cruz, Michael P**.; Evidence for hygroscopic mineral dust particles from the Intercontinental Transport and Chemical Transformation Experiment.** *Journal of Geophysical Research, Vol. 109, 2004*.

04-1 Thomas A. Cahill, Steven S. Cliff, Michael Jimenez-Cruz, James F. Shackelford[1], Michael Dunlap[1], Michael Meier[1],Peter B. Kelly[2], Sarah Riddle[2], Jodye Selco[3,*], Graham Bench[4], Patrick Grant[4], Dawn Ueda[4], Kevin D. Perry[5], and Robert Leifer[6]**, Analysis of Aerosols from the World Trade center Collapse Site, New York, October 2 to October 30, 2001**. *Aerosol Science and Technology* 38; 165–183 (2004)

04-2 Han, J.S, K.J. Moon, J.Y. Ahn, Y.D. Hong, Y.J Kim, S. Y. Rhu, Steven S. Cliff, and Thomas A. Cahill**, Characteristics of Ion Components and Trace Elements of Fine Particles at Gosan, Korea in Spring Time from 2002 to 2002,** *Environmental Monitoring and Assessment* 00: 1-21, 2003

04-3 Seinfeld, J.H., Carmichael, G.R., Arimoto, R, Conant, W. C., Brechtel, F. J., Bates, T. S., Cahill, T. A., Clarke, A.D., Flatau, B.J., Huebert, B.J., Kim, J., Markowicx, K.M., Masonis, S.J., Quinn, P.K., Russell, L.M., Russell, P.B., Shimizu, A., Shinozuka, Y., Song, C.H., Tang, Y., Uno, I., Vogelmann, A.M., Weber, R.J., Woo, J-H., Zhang, Y. **ACE-Asia: Regional Climatic and Atmospheric Chemical Effects of Asian Dust and Pollution**, *Bulletin American Meteorological Society* 85 (3): 367+ MARCH 2004

04-4 Cahill, T. A., Cliff, S. S., Shackelford, J. F., Meier, M., Perry, K. D., Bench, G., and Leifer, R. **Very Fine Aerosols from the World Trade Center Collapse Piles: Anaerobic Incineration?** Advances in Chemistry (2004)

03-1 Cahill, C.F. **Asian Aerosol Transport to Alaska during ACE-Asia.** J. Geophys. Res. *JGR Manuscript Number: 2002JD003271*

00-1 Miller, Alan E. and Thomas A. Cahill. **Size and compositional analyses of biologically active aerosols from a CO_2 and diode laser plume.** 2000 *International Journal of PIXE*. Vol. 9, Nos. 3 & 4.5

Publications using S-XRF (recent - SSRL)

14.1 Sean R. Barberie, Christopher R. Iceman, Catherine F. Cahill, and Thomas M. Cahill, **Evaluation of Different Synchrotron Beamline Configurations for S X‐ray Fluorescence Analysis of Environmental Samples** , in press, Analytical Chemistry (2014)

13.3 S.R. Barberie, T.A. Cahill, C.F. Cahill, T.M. Cahill, C.R. Iceman, D.E. Barnes**. UC Davis XIPline ("zipline") end-station at the Stanford Synchrotron Radiation Lightsource: Development and experimental results.** *Nucl. Instrum. Meth. Phys. Res. A: Accelerators, Spectrometers, Detectors and Associated Equipment* 729:930-933 (2013) oi:10.1016/j. nima. 2013.08.043

12-1 Peter Jenniskens, Marc D. Fries, Qing-Zhu Yin, Michael Zolensky, Alexander N. Krot, Scott A. Sandford, Derek Sears, Robert Beauford, Denton S. Ebel, Jon M. Friedrich, Kazuhide Nagashima, Josh Wimpenny, Akane Yamakawa, Kunihiko Nishiizumi, Yasunori Hamajima, Marc W. Caffee, Kees C. Welten, Matthias Laubenstein, Andrew M. Davis, Steven B. Simon, Philipp R. Heck, Edward D. Young, Issaku E. Kohl, Mark H. Thiemens, Morgan H. Nunn, Takashi Mikouchi, Kenji Hagiya, Kazumasa Ohsumi, Thomas A. Cahill, Jonathan A. Lawton, David Barnes, Andrew Steele, Pierre Rochette, Kenneth L. Verosub, Jérôme Gattacceca, George Cooper, Daniel P. Glavin, Aaron S. Burton, Jason P. Dworkin, Jamie E. Elsila, Sandra Pizzarello, Ryan Ogliore, Phillipe Schmitt-Kopplin, Mourad Harir, Norbert Hertkorn, Alexander Verchovsky, Monica Grady, Keisuke Nagao, Ryuji Okazaki, Hiroyuki Takechi, Takahiro Hiroi, Ken Smith, Elizabeth A. Silber, Peter G. Brown, Jim Albers, Doug Klotz, Mike Hankey, Robert Matson, Jeffrey A. Fries, Richard J. Walker, Igor Puchtel, Cin-Ty A. Lee, Monica E. Erdman, Gary R. Eppich, Sarah Roeske, Zelimir Gabelica, Michael Lerche, Michel Nuevo, Beverly Girten, Simon P. Worden. **Radar-enabled recovery of the Sutter's Mill Meteorite, a carbonaceous chondrite regolith breccia**. *Science*, 338:1583-1587 (2012) doi: 10.1126/science.1227163

Attachment 3: Summary Notes from Archiving and Beta Sample Analysis

OlDr, Dep 609	
Input Prog Start datetime	2/3/15 18:20
predicted gap start datetime	
Predicted end datetime	
*Apparent end datetime	
*Apparent marker date	
Timing:	Field Stop = 2/21/2015 5:15:00 PM
	Deployment ended before any protocol motions so no off-sets needed in analysis.
	Site Visit: 2/10/2015 15:45 System running well no problems.
	Flow measured 7.89 l/min.
	Ninth Stage stopped at 10.42 days, measured to center of end deposit.
	Ninth Stage stopped at (peak center) 2/14/15 04:25
	Data after ninth stage stopped has larger error due to variable flow restriction.
Measured Flow (l/min)	
7.89	After Ufine continuos after filter stalls, the flow is affected and variable.
	measured value at end of deployment is 6.4 l/m
Beta Background	
	Ninth Stage stopped after, 2/13/15 6:56 ~7AM
Stage	Notes
1	very clean hard to see
2	21.5-94
3	21.5-94
4	20-92
5	23.5-95+-0.25 tilt
6	20.5-92: Only 1st 7_8mm slight moisture time averaging
7	25-97
8	23.5-95 moistureafterout2 108mm
9	start ~37-38mm then heavy deposit centered at 41.5+-2.5
	notes Beta only
1	
2	
3	
4	
5	
6	
7	
8	
9	
* Apparent datetimes (after mid-gap) are /w protocol mid-gap time shift	
6mm mid-protocol gap (6mm @ 4mm/day is 36 hours offset after Midgap)	

Attachment 4: Photo record of the DRUM samples for Olive Drive

First with a black background that shows scattering aerosols, then with a white background which shows absorbing aerosols.

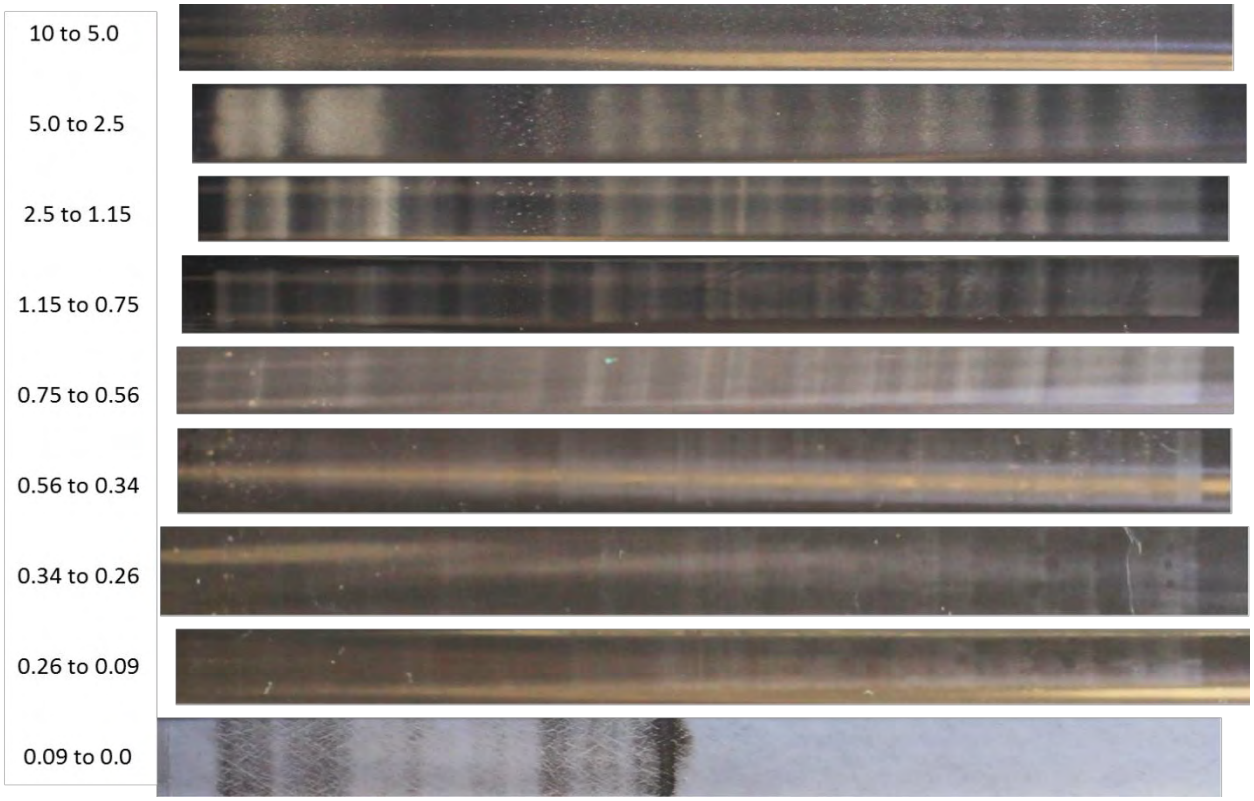

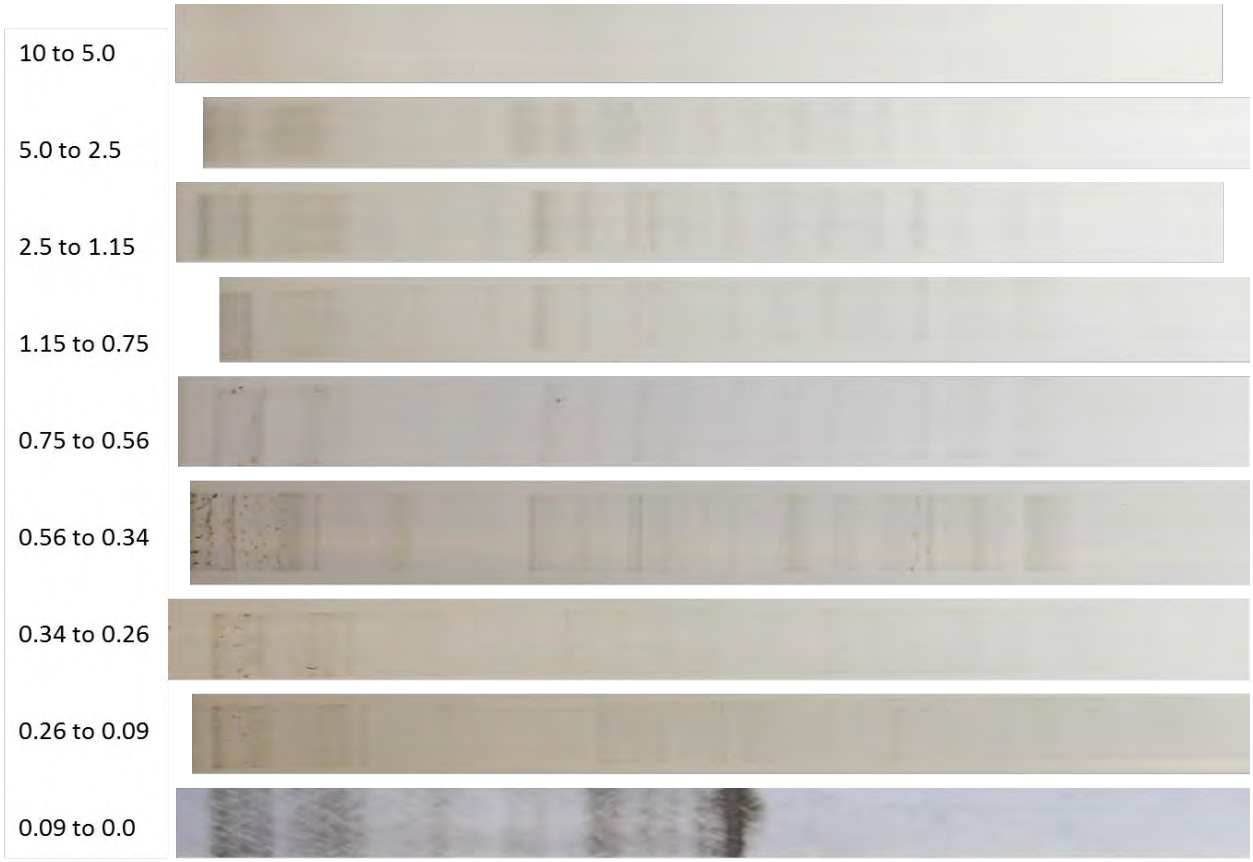
10 to 5.0
5.0 to 2.5
2.5 to 1.15
1.15 to 0.75
0.75 to 0.56
0.56 to 0.34
0.34 to 0.26
0.26 to 0.09
0.09 to 0.0

Attachment 5: Excerpt of Weather Underground Meteorological station data table

From Weather Underground, University AP site													
Date	Time PST	Temperature F	Dew Point F	Humidity	Sea Level Pressure In	Visibility MPH	Wind Direction	Wind Speed MPH	Gust Speed MPH	Precipitation In	Events	Conditions	WindDir Degrees
2/4/2015	12:00 AM	48.2	46.4	93	30.09	10	Calm	Calm	-	N/A		Clear	0
2/4/2015	12:20 AM	48.2	46.4	93	30.09	10	Calm	Calm	-	N/A		Clear	0
2/4/2015	12:40 AM	46.4	44.6	93	30.09	10	NW	3.5	-	N/A		Clear	320
2/4/2015	1:00 AM	48.2	46.4	93	30.09	10	Calm	Calm	-	N/A		Clear	0
2/4/2015	1:20 AM	48.2	46.4	93	30.09	10	Calm	Calm	-	N/A		Clear	0
2/4/2015	1:40 AM	48.2	46.4	93	30.08	10	Calm	Calm	-	N/A		Clear	0
2/4/2015	2:00 AM	46.4	46.4	100	30.08	10	Calm	Calm	-	N/A		Clear	0
2/4/2015	2:20 AM	48.2	46.4	93	30.08	10	Calm	Calm	-	N/A		Clear	0
2/4/2015	2:40 AM	46.4	44.6	93	30.08	10	Calm	Calm	-	N/A		Clear	0
2/4/2015	3:00 AM	46.4	46.4	100	30.08	10	Calm	Calm	-	N/A		Clear	0
2/4/2015	3:20 AM	48.2	46.4	93	30.08	10	Calm	Calm	-	N/A		Clear	0
2/4/2015	3:40 AM	46.4	44.6	93	30.07	10	Calm	Calm	-	N/A		Clear	0
2/4/2015	4:00 AM	44.6	44.6	100	30.07	10	Calm	Calm	-	N/A		Clear	0
2/4/2015	4:20 AM	44.6	44.6	100	30.07	9	Calm	Calm	-	N/A		Clear	0
2/4/2015	4:40 AM	44.6	44.6	100	30.08	10	Calm	Calm	-	N/A		Clear	0
2/4/2015	5:00 AM	46.4	44.6	93	30.07	10	NNW	3.5	-	N/A		Clear	340
2/4/2015	5:20 AM	46.4	44.6	93	30.07	10	North	3.5	-	N/A		Clear	350
2/4/2015	5:40 AM	46.4	46.4	100	30.07	10	North	3.5	-	N/A		Clear	350
2/4/2015	6:00 AM	46.4	44.6	93	30.07	10	North	3.5	-	N/A		Clear	350
2/4/2015	6:20 AM	46.4	44.6	93	30.08	8	NNW	3.5	-	N/A		Clear	340
2/4/2015	6:40 AM	44.6	44.6	100	30.08	8	Calm	Calm	-	N/A		Clear	0
2/4/2015	7:00 AM	46.4	44.6	93	30.09	9	NNW	3.5	-	N/A		Clear	340
2/4/2015	7:20 AM	44.6	44.6	100	30.1	7	North	3.5	-	N/A		Clear	360
2/4/2015	7:40 AM	44.6	44.6	100	30.1	7	Calm	Calm	-	N/A		Clear	0
2/4/2015	8:00 AM	46.4	44.6	93	30.1	8	North	3.5	-	N/A		Clear	360
2/4/2015	8:20 AM	48.2	46.4	93	30.11	7	NNW	3.5	-	N/A		Clear	330
2/4/2015	8:40 AM	48.2	46.4	93	30.11	8	North	3.5	-	N/A		Clear	360
2/4/2015	9:00 AM	48.2	46.4	93	30.1	7	North	3.5	-	N/A		Clear	360
2/4/2015	9:20 AM	48.2	48.2	100	30.11	8	North	3.5	-	N/A		Clear	350
2/4/2015	9:40 AM	50	48.2	94	30.11	10	North	3.5	-	N/A		Clear	350
2/4/2015	10:00 AM	53.6	50	88	30.11	10	NNW	3.5	-	N/A		Clear	340
2/4/2015	10:20 AM	55.4	50	82	30.11	9	Calm	Calm	-	N/A		Clear	0
2/4/2015	10:40 AM	57.2	51.8	82	30.11	6	Calm	Calm	-	N/A		Clear	0
2/4/2015	11:00 AM	59	51.8	77	30.11	5	East	3.5	-	N/A		Clear	100
2/4/2015	11:20 AM	59	51.8	77	30.1	4	ESE	5.8	-	N/A		Clear	120
2/4/2015	11:40 AM	59	51.8	77	30.09	5	ENE	3.5	-	N/A		Clear	70
2/4/2015	12:00 PM	59	51.8	77	30.09	4	SE	3.5	-	N/A		Clear	140
2/4/2015	12:20 PM	60.8	53.6	77	30.09	4	SE	3.5	-	N/A		Clear	130
2/4/2015	12:40 PM	60.8	51.8	72	30.08	4	SE	5.8	-	N/A		Clear	130
2/4/2015	1:00 PM	60.8	51.8	72	30.07	4	South	4.6	-	N/A		Clear	190
2/4/2015	1:20 PM	60.8	51.8	72	30.06	4	South	4.6	-	N/A		Clear	170
2/4/2015	1:40 PM	60.8	51.8	72	30.04	4	SSE	6.9	-	N/A		Clear	150
2/4/2015	2:00 PM	62.6	51.8	68	30.04	4	South	6.9	-	N/A		Clear	190
2/4/2015	2:20 PM	62.6	51.8	68	30.03	4	SSE	4.6	-	N/A		Clear	160
2/4/2015	2:40 PM	62.6	51.8	68	30.03	4	Calm	Calm	-	N/A		Clear	0
2/4/2015	3:00 PM	64.4	51.8	64	30.03	4	Calm	Calm	-	N/A		Clear	0
2/4/2015	3:20 PM	62.6	53.6	72	30.03	4	South	3.5	-	N/A		Clear	170
2/4/2015	3:40 PM	64.4	51.8	64	30.03	4	Calm	Calm	-	N/A		Clear	0
2/4/2015	4:00 PM	62.6	51.8	68	30.02	4	Calm	Calm	-	N/A		Clear	0
2/4/2015	4:20 PM	62.6	53.6	72	30.01	4	ESE	3.5	-	N/A		Clear	120
2/4/2015	4:40 PM	62.6	51.8	68	30.01	4	SSE	3.5	-	N/A		Clear	150
2/4/2015	5:00 PM	62.6	51.8	68	30.01	4	Calm	Calm	-	N/A		Clear	0

Attachment 6: HYSPLIT Analyses of upwind sources/downwind receptors
HYSPLIT trajectory analyses

While local meteorology is very useful to determine on-to-site wind direction, regional wind patterns are also important to identify potential upwind sources, or establish downwind impacts. For this we used HTSPLIT.

Hybrid Single-Particle Lagrangian Integrated Trajectory — (HYSPLIT) Model

---

Description

The HYSPLIT model is a complete system for computing simple air parcel trajectories to complex dispersion and deposition simulations. The initial development was a result of a joint effort between NOAA and Australia's Bureau of Meteorology. Recent upgrades include enhancements provided by a number of different contributors. Some new features include improved advection algorithms, updated stability and dispersion equations, continued improvements to the graphical user interface, and the option to include modules for chemical transformations. Without the additional dispersion modules, Hysplit computes the advection of a single pollutant particle, or simply its trajectory.

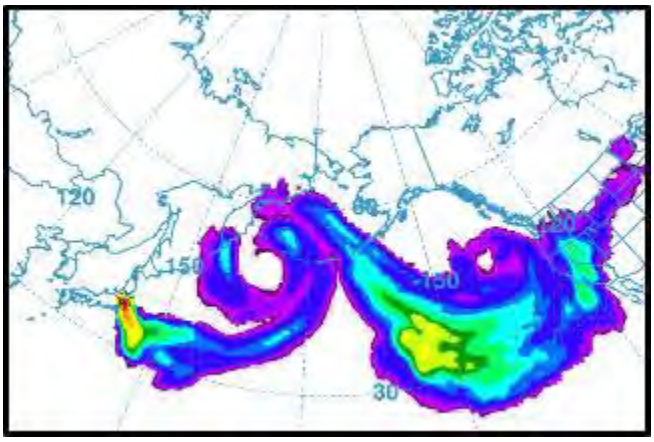

The dispersion of a pollutant is calculated by assuming either puff or particle dispersion. In the puff model, puffs expand until they exceed the size of the meteorological grid cell (either horizontally or vertically) and then split into several new puffs, each with it's share of the pollutant mass. In the particle model, a fixed number of particles are advected about the model domain by the mean wind field and spread by a turbulent component. The model's default configuration assumes a 3-dimensional particle distribution (horizontal and vertical).

The model can be run interactively on the Web through the READY system on our site or the code executable and meteorological data can be downloaded to a Windows or Mac PC. The web version has been configured with some limitations to avoid computational saturation of our web server. The registered PC version is complete with no computational restrictions, except that user's must obtain their own meteorological data files. The unregistered version is identical to the registered version except that plume concentrations cannot be calculated with with forecast meteorology data files. The trajectory-only model has no restrictions and forecast or archive trajectories may be computed with either version

Publications using HYSPLIT results, maps or other READY products provided by NOAA ARL are requested to include an acknowledgement of, and citation to, the NOAA Air Resources Laboratory. Appropriate versions of the following are recommended:

Citation

Draxler, R.R. and Rolph, G.D., 2013. HYSPLIT (HYbrid Single-Particle Lagrangian Integrated Trajectory) Model access via NOAA ARL READY Website (http://www.arl.noaa.gov/HYSPLIT.php). NOAA Air Resources Laboratory, College Park, MD.

Rolph, G.D., 2013. Real-time Environmental Applications and Display sYstem (READY) Website (http://www.ready.noaa.gov). NOAA Air Resources Laboratory, College Park, MD.

Acknowledgment

The authors gratefully acknowledge the NOAA Air Resources Laboratory (ARL) for the provision of the HYSPLIT transport and dispersion model and/or READY website (http://www.ready.noaa.gov) used in this publication.

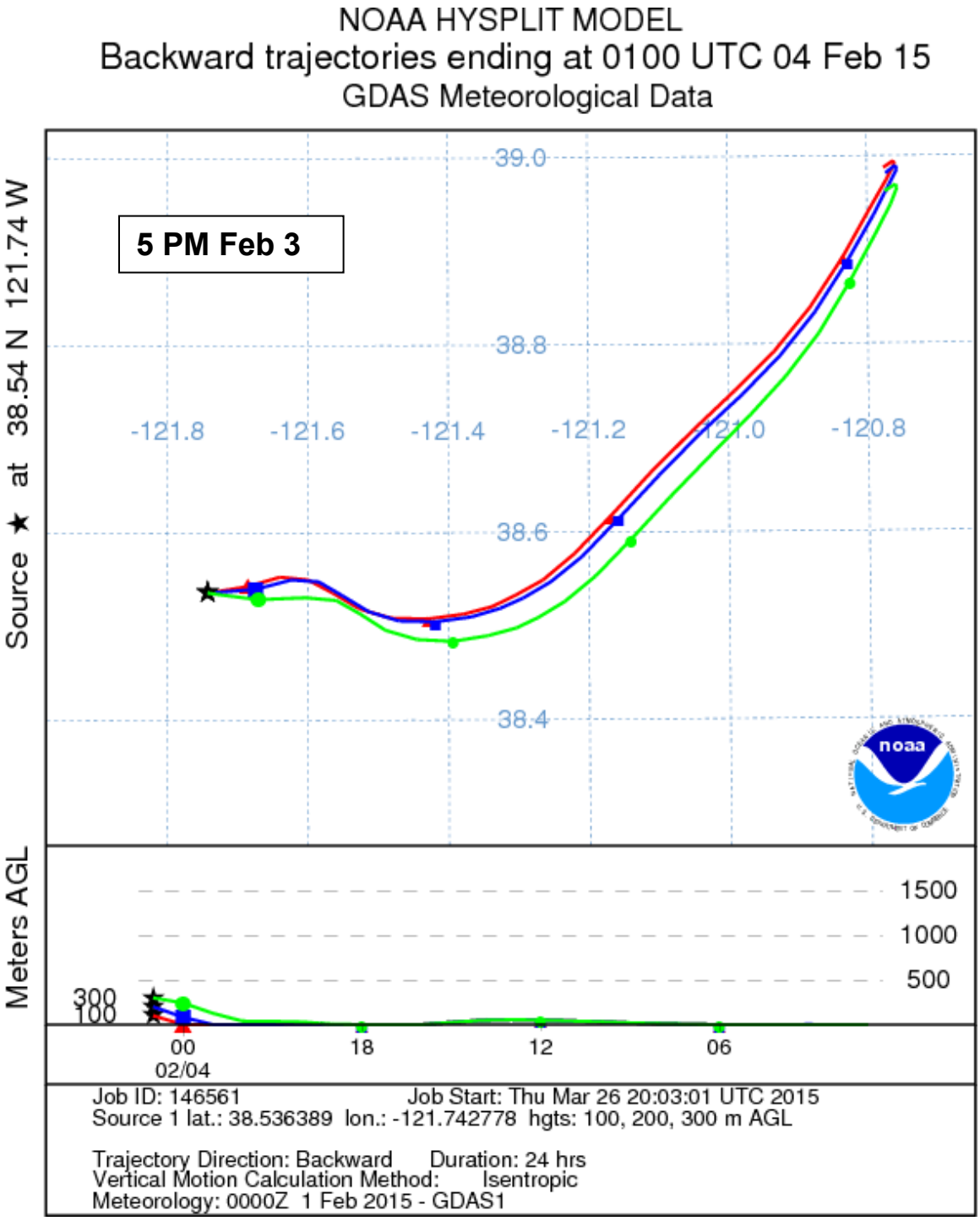

HYSPLIT Trajectory to February 3rd at 5 PM

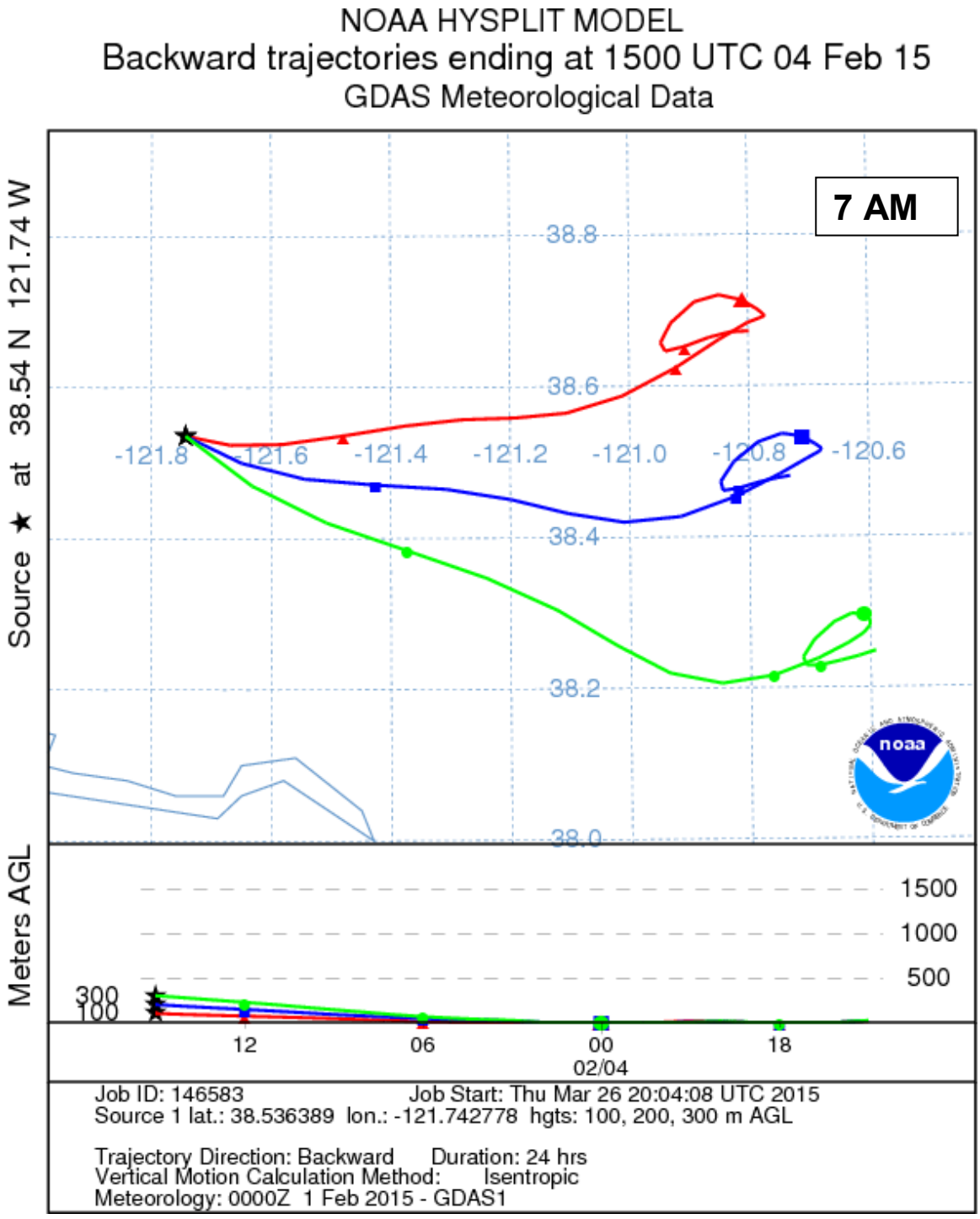
NOAA HYSPLIT MODEL
Backward trajectories ending at 1500 UTC 04 Feb 15
GDAS Meteorological Data
7 AM
Source ★ at 38.54 N 121.74 W
38.8
38.6
38.4
38.2
38.0
-121.8
-121.6
-121.4
-121.2
-121.0
-120.8
-120.6
noaa
Meters AGL
1500
1000
500
300
100
12
06
00
18
02/04
Job ID: 146583
Job Start: Thu Mar 26 20:04:08 UTC 2015
Source 1 lat.: 38.536389 lon.: -121.742778 hgts: 100, 200, 300 m AGL
Trajectory Direction: Backward
Duration: 24 hrs
Vertical Motion Calculation Method:
Isentropic
Meteorology: 0000Z 1 Feb 2015 - GDAS1

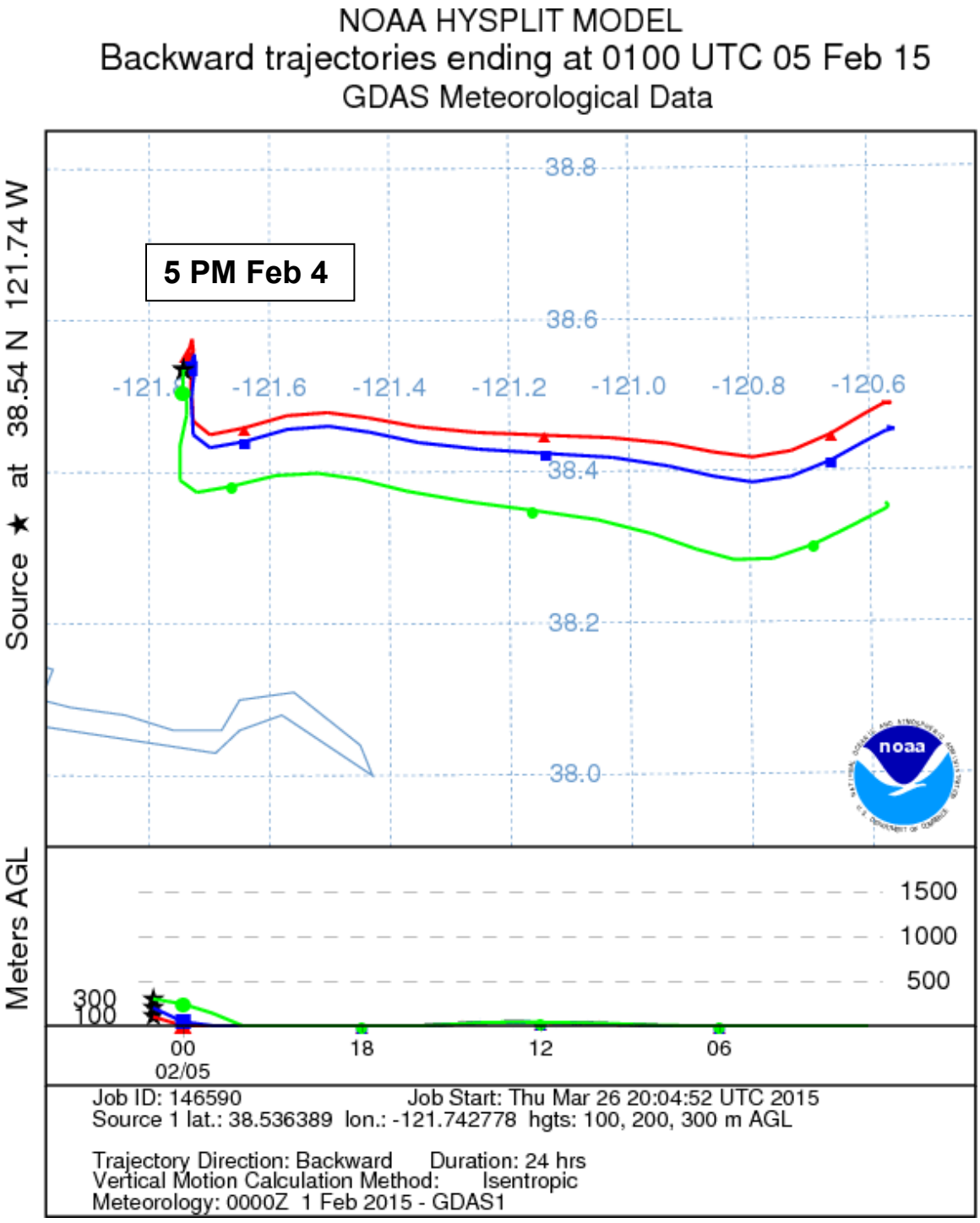
NOAA HYSPLIT MODEL
Backward trajectories ending at 0100 UTC 05 Feb 15
GDAS Meteorological Data
5 PM Feb 4
Source ★ at 38.54 N 121.74 W
38.8
38.6
38.4
38.2
38.0
-121.8
-121.6
-121.4
-121.2
-121.0
-120.8
-120.6
noaa
Meters AGL
1500
1000
500
300
100
00
02/05
18
12
06
Job ID: 146590
Job Start: Thu Mar 26 20:04:52 UTC 2015
Source 1 lat.: 38.536389 lon.: -121.742778 hgts: 100, 200, 300 m AGL
Trajectory Direction: Backward
Duration: 24 hrs
Vertical Motion Calculation Method:
Isentropic
Meteorology: 0000Z 1 Feb 2015 - GDAS1

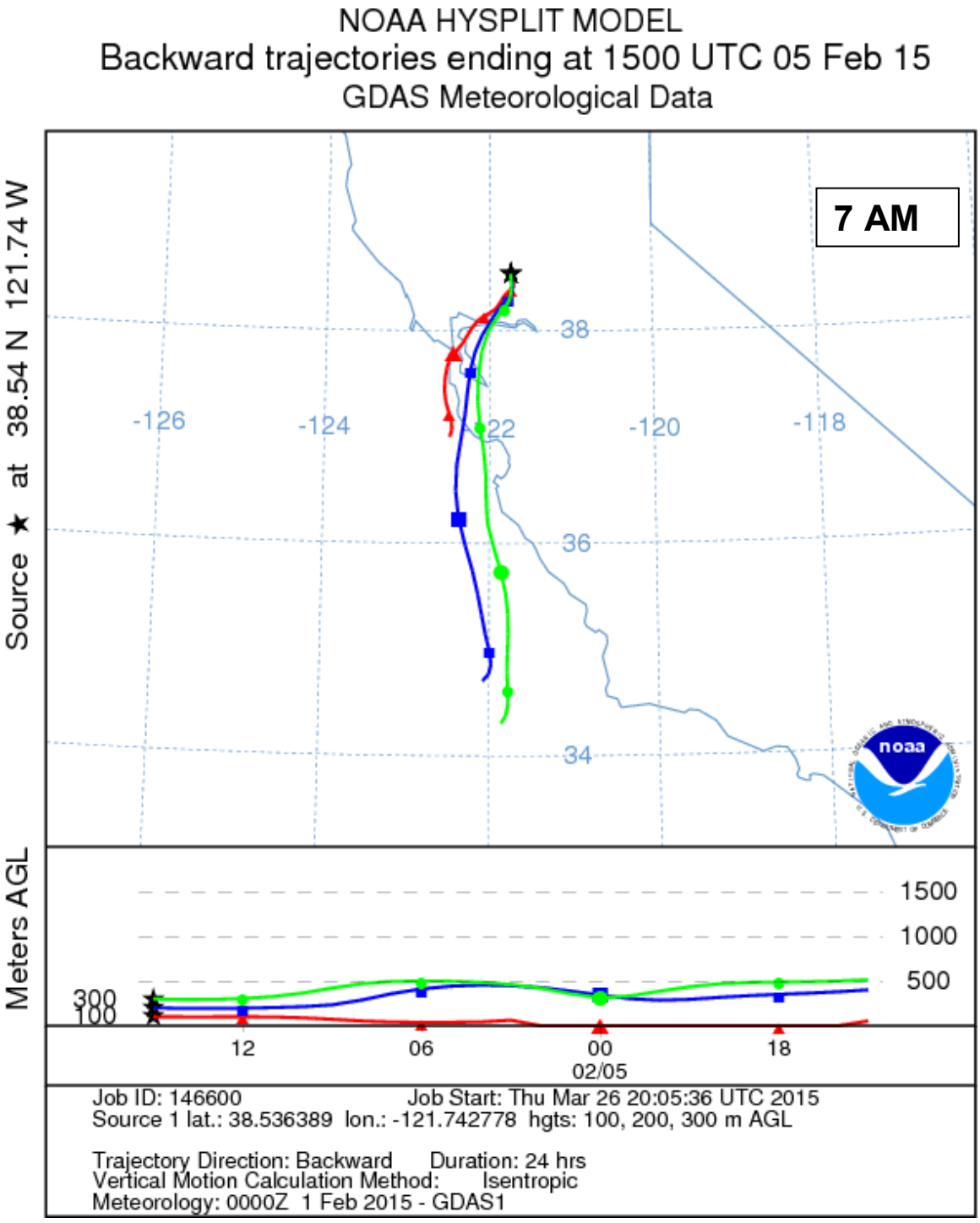
NOAA HYSPLIT MODEL
Backward trajectories ending at 1500 UTC 05 Feb 15
GDAS Meteorological Data
7 AM
Source ★ at 38.54 N 121.74 W
38
36
34
-126
-124
-122
-120
-118
noaa
Meters AGL
1500
1000
500
300
100
12
06
00
18
02/05
Job ID: 146600
Job Start: Thu Mar 26 20:05:36 UTC 2015
Source 1 lat.: 38.536389 lon.: -121.742778 hgts: 100, 200, 300 m AGL
Trajectory Direction: Backward
Duration: 24 hrs
Vertical Motion Calculation Method:
Isentropic
Meteorology: 0000Z 1 Feb 2015 - GDAS1

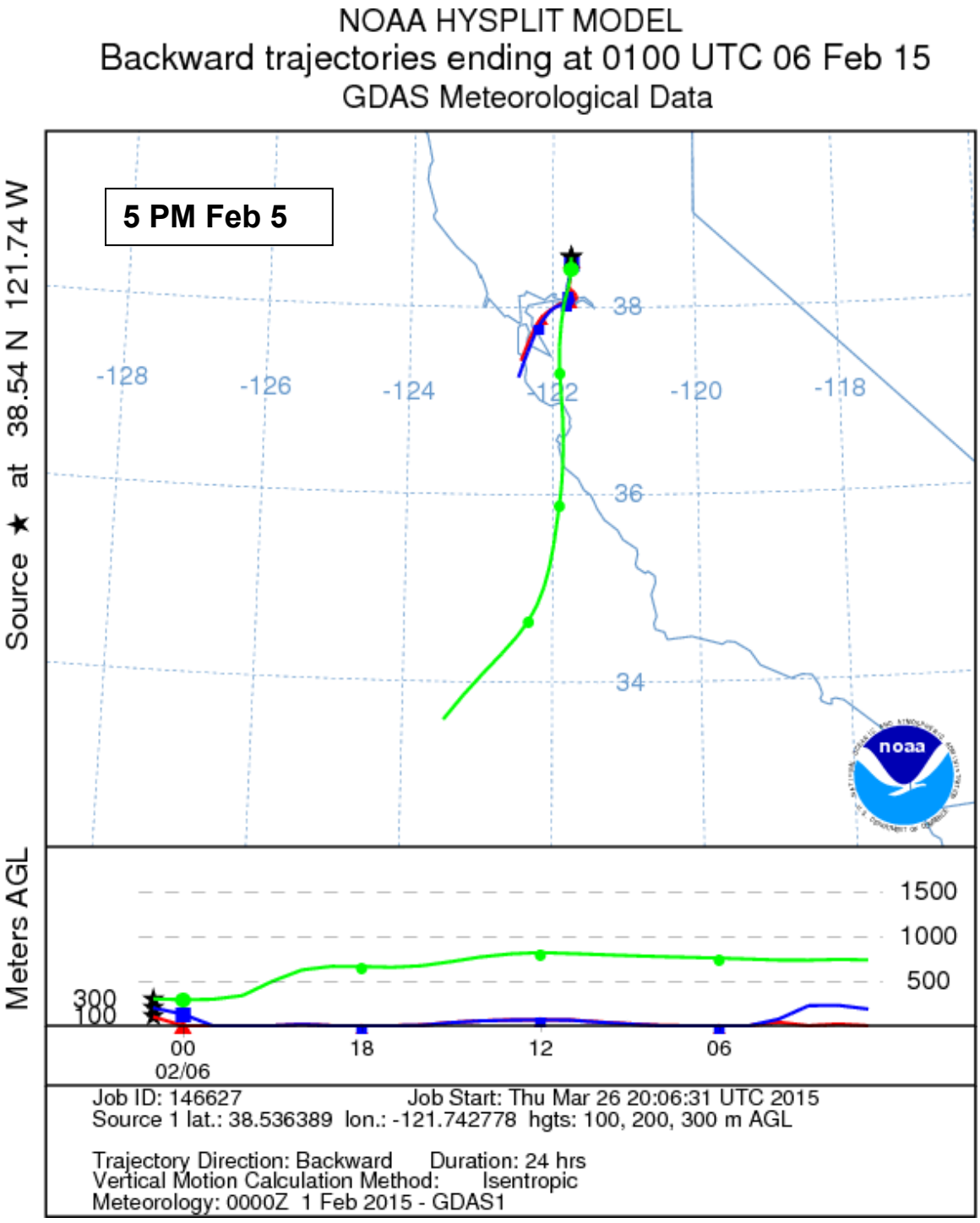
NOAA HYSPLIT MODEL
Backward trajectories ending at 0100 UTC 06 Feb 15
GDAS Meteorological Data
5 PM Feb 5
Source ★ at 38.54 N 121.74 W
38
36
34
-128
-126
-124
-122
-120
-118
noaa
Meters AGL
1500
1000
500
300
100
00
02/06
18
12
06
Job ID: 146627
Job Start: Thu Mar 26 20:06:31 UTC 2015
Source 1 lat.: 38.536389 lon.: -121.742778 hgts: 100, 200, 300 m AGL
Trajectory Direction: Backward
Duration: 24 hrs
Vertical Motion Calculation Method:
Isentropic
Meteorology: 0000Z 1 Feb 2015 - GDAS1

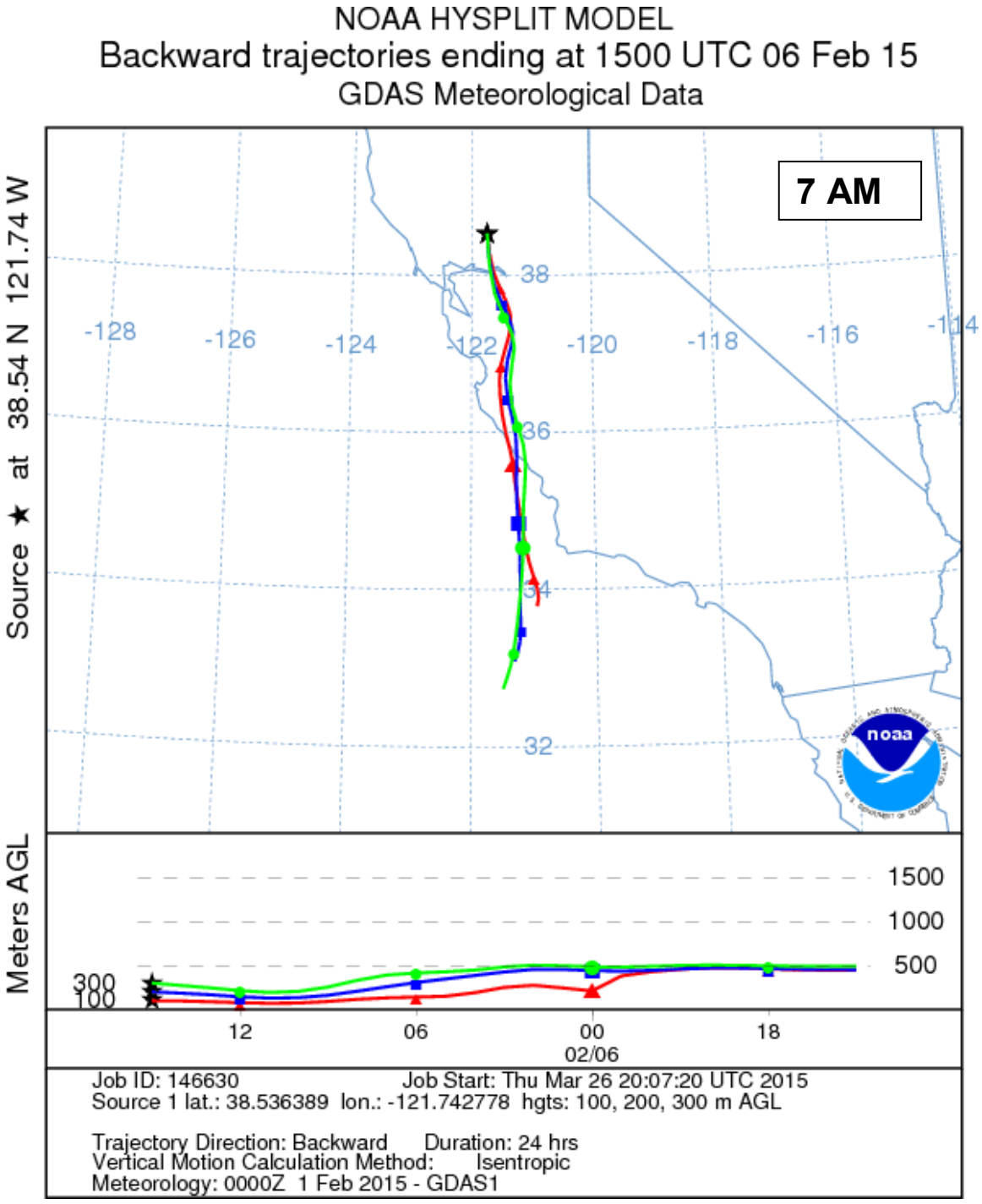
NOAA HYSPLIT MODEL
Backward trajectories ending at 1500 UTC 06 Feb 15
GDAS Meteorological Data
7 AM
Source ★ at 38.54 N 121.74 W
-128
-126
-124
-122
-120
-118
-116
-114
38
36
34
32
noaa
Meters AGL
1500
1000
500
300
100
12
06
00
18
02/06
Job ID: 146630 Job Start: Thu Mar 26 20:07:20 UTC 2015
Source 1 lat.: 38.536389 lon.: -121.742778 hgts: 100, 200, 300 m AGL
Trajectory Direction: Backward Duration: 24 hrs
Vertical Motion Calculation Method: Isentropic
Meteorology: 0000Z 1 Feb 2015 - GDAS1

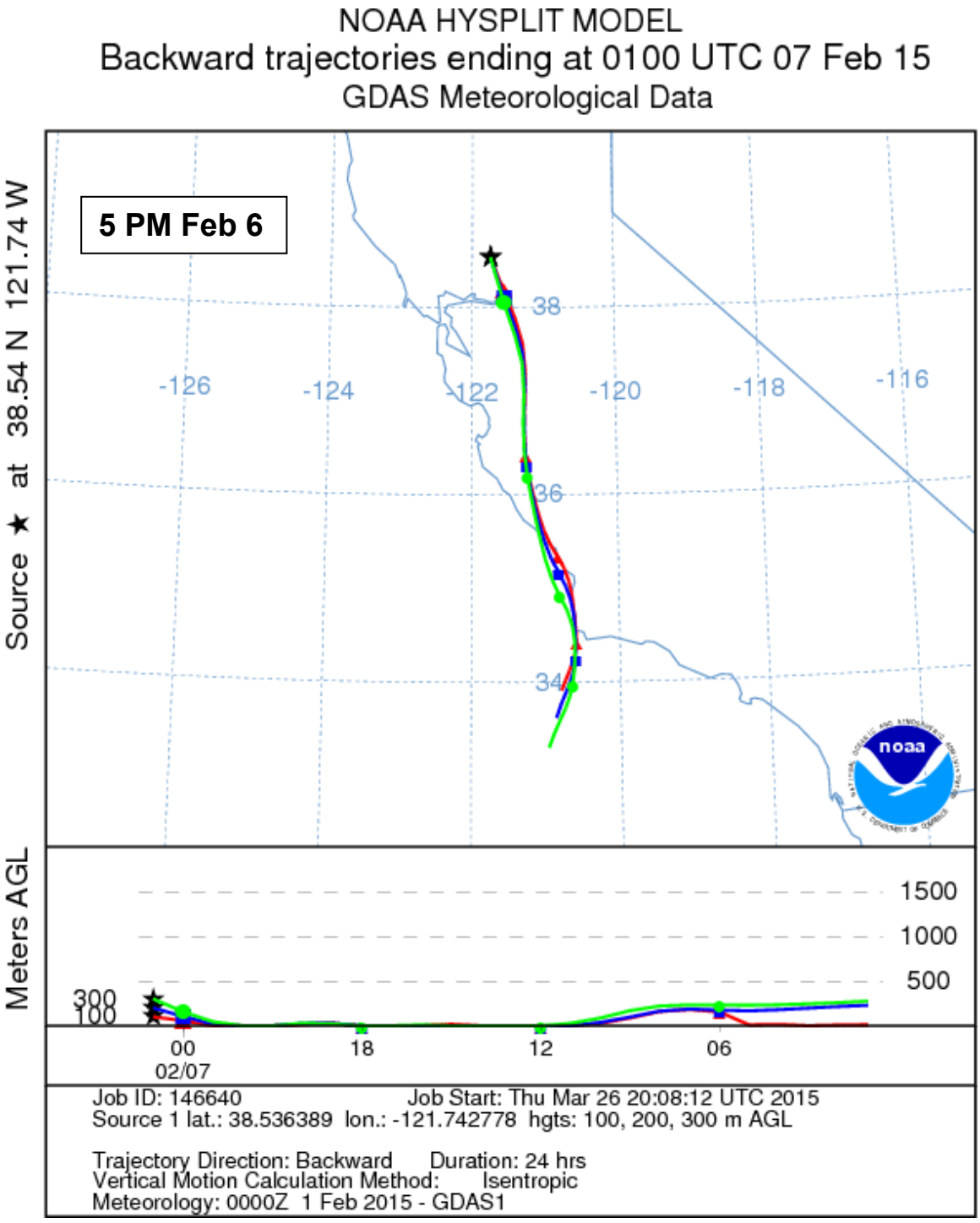
NOAA HYSPLIT MODEL
Backward trajectories ending at 0100 UTC 07 Feb 15
GDAS Meteorological Data
5 PM Feb 6
Source ★ at 38.54 N 121.74 W
-126
-124
-122
-120
-118
-116
38
36
34
noaa
Meters AGL
1500
1000
500
300
100
00
02/07
18
12
06
Job ID: 146640
Job Start: Thu Mar 26 20:08:12 UTC 2015
Source 1 lat.: 38.536389 lon.: -121.742778 hgts: 100, 200, 300 m AGL
Trajectory Direction: Backward
Duration: 24 hrs
Vertical Motion Calculation Method:
Isentropic
Meteorology: 0000Z 1 Feb 2015 - GDAS1

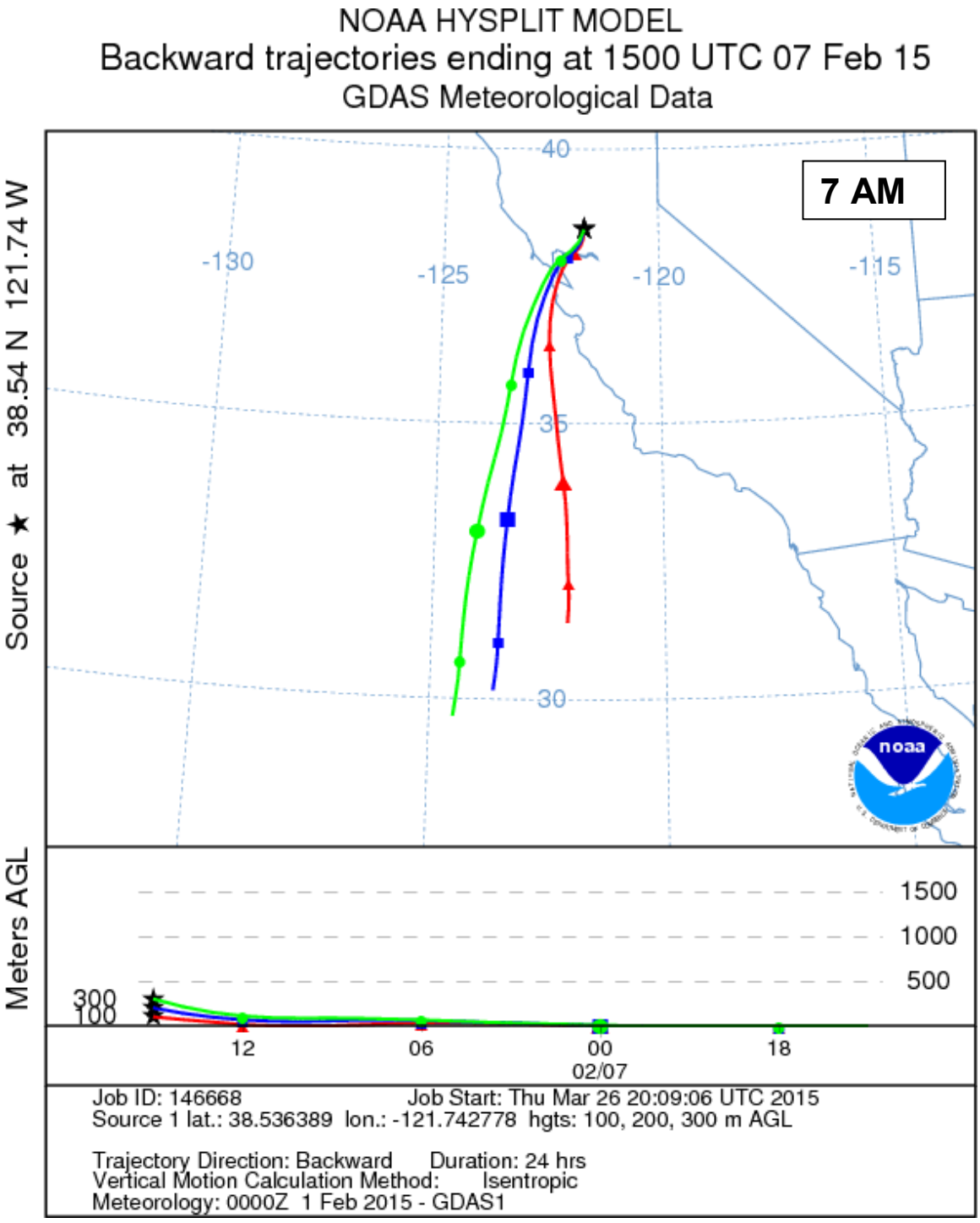
NOAA HYSPLIT MODEL
Backward trajectories ending at 1500 UTC 07 Feb 15
GDAS Meteorological Data
7 AM
Source ★ at 38.54 N 121.74 W
40
-130
-125
-120
-115
35
30
noaa
Meters AGL
1500
1000
500
300
100
12
06
00
02/07
18
Job ID: 146668
Job Start: Thu Mar 26 20:09:06 UTC 2015
Source 1 lat.: 38.536389 lon.: -121.742778 hgts: 100, 200, 300 m AGL
Trajectory Direction: Backward
Duration: 24 hrs
Vertical Motion Calculation Method:
Isentropic
Meteorology: 0000Z 1 Feb 2015 - GDAS1

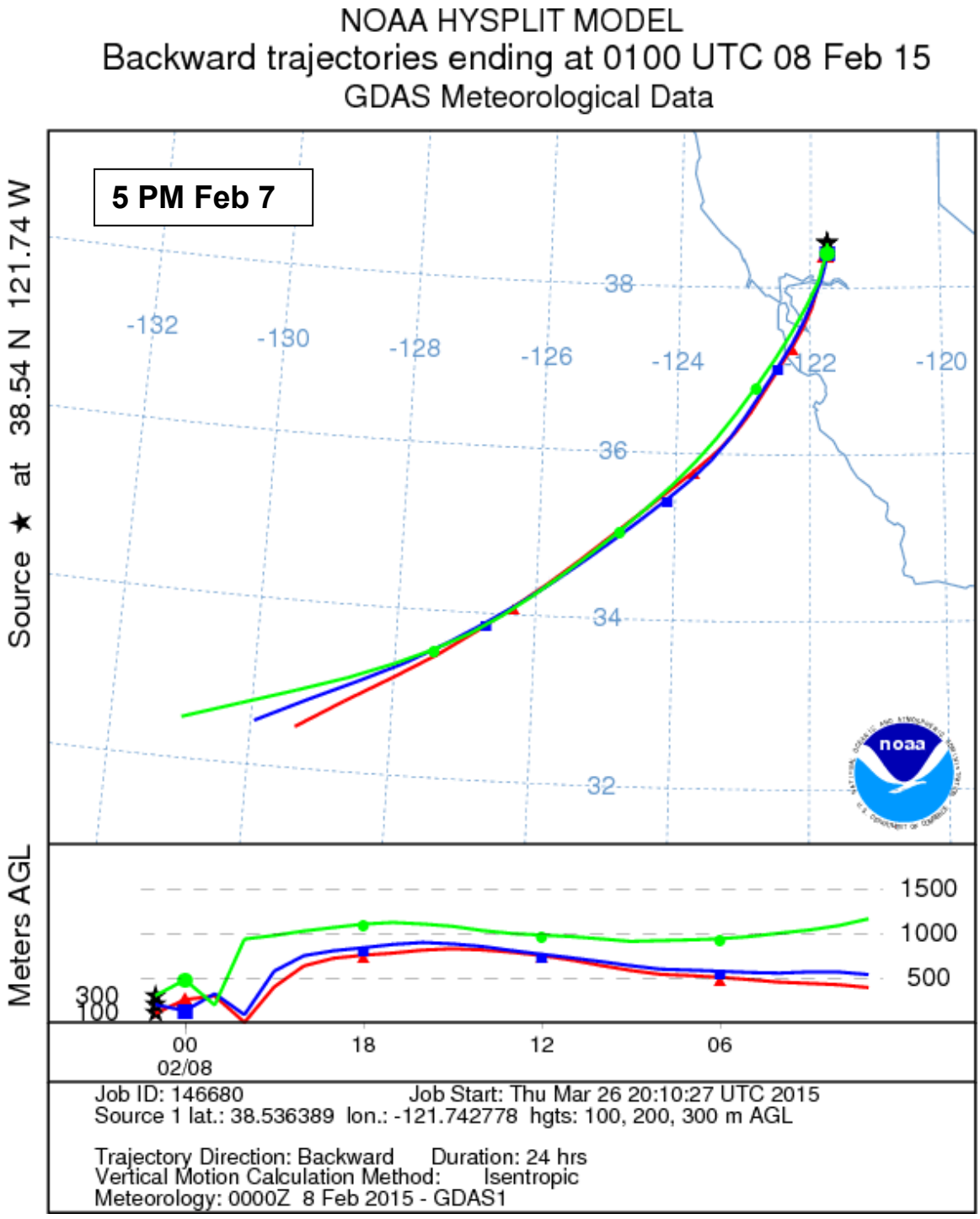
NOAA HYSPLIT MODEL
Backward trajectories ending at 0100 UTC 08 Feb 15
GDAS Meteorological Data
5 PM Feb 7
Source ★ at 38.54 N 121.74 W
-132
-130
-128
-126
-124
-122
-120
38
36
34
32
noaa
Meters AGL
1500
1000
500
300
100
00
02/08
18
12
06
Job ID: 146680
Job Start: Thu Mar 26 20:10:27 UTC 2015
Source 1 lat.: 38.536389 lon.: -121.742778 hgts: 100, 200, 300 m AGL
Trajectory Direction: Backward
Duration: 24 hrs
Vertical Motion Calculation Method:
Isentropic
Meteorology: 0000Z 8 Feb 2015 - GDAS1

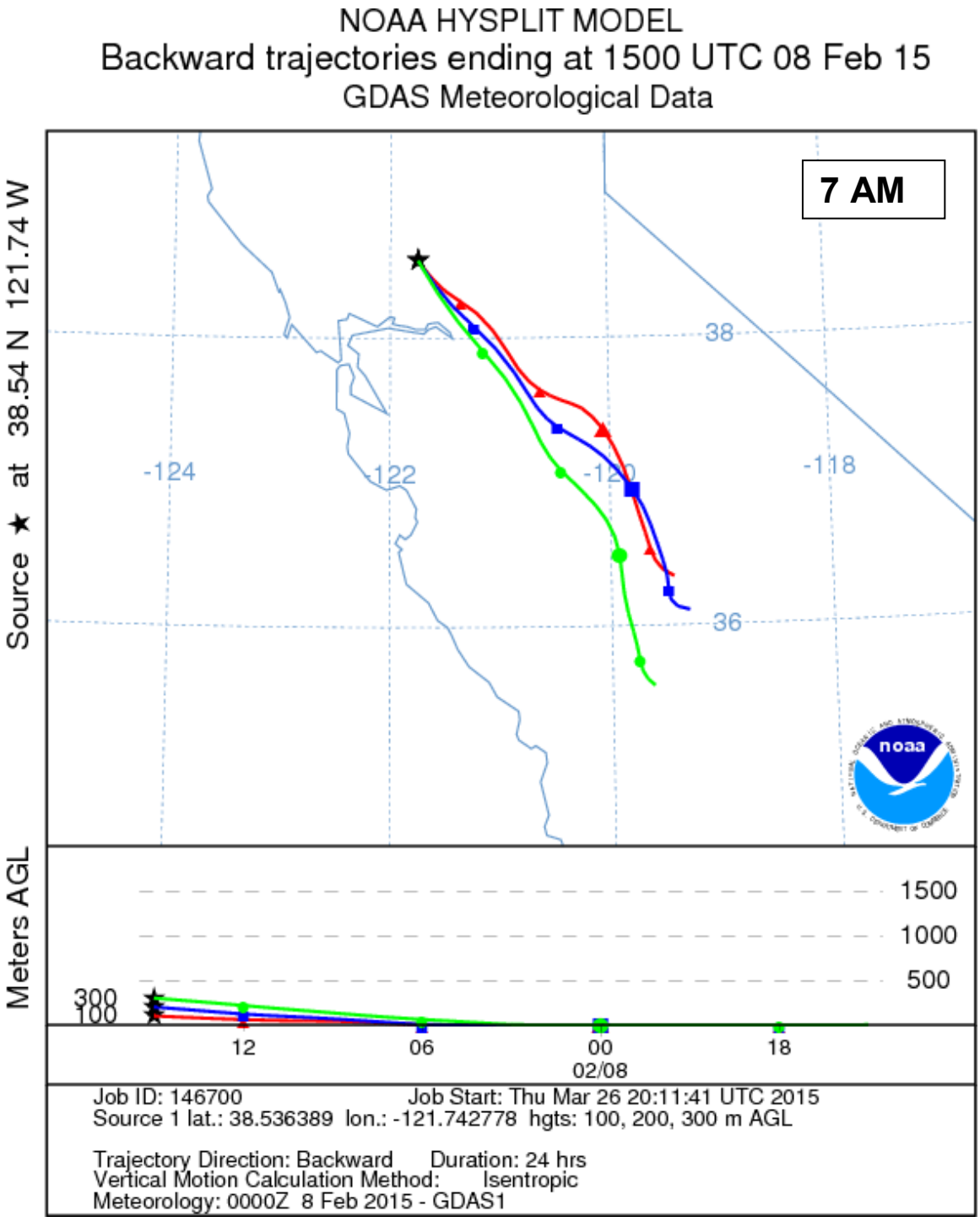
NOAA HYSPLIT MODEL
Backward trajectories ending at 1500 UTC 08 Feb 15
GDAS Meteorological Data
7 AM
Source ★ at 38.54 N 121.74 W
38
36
-124
-122
-120
-118
noaa
Meters AGL
1500
1000
500
300
100
12
06
00
18
02/08
Job ID: 146700
Job Start: Thu Mar 26 20:11:41 UTC 2015
Source 1 lat.: 38.536389 lon.: -121.742778 hgts: 100, 200, 300 m AGL
Trajectory Direction: Backward
Duration: 24 hrs
Vertical Motion Calculation Method:
Isentropic
Meteorology: 0000Z 8 Feb 2015 - GDAS1

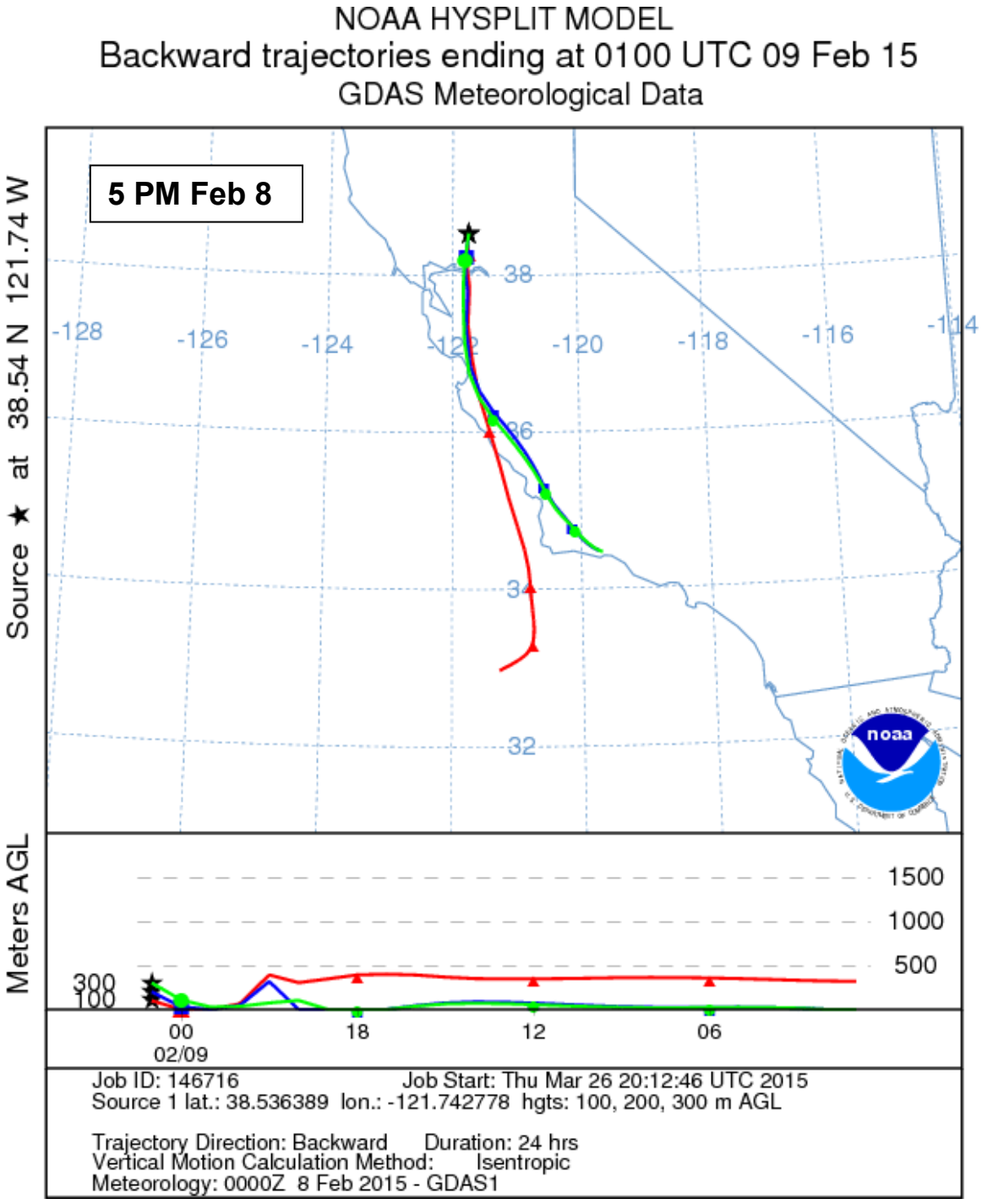
NOAA HYSPLIT MODEL
Backward trajectories ending at 0100 UTC 09 Feb 15
GDAS Meteorological Data
5 PM Feb 8
Source ★ at 38.54 N 121.74 W
-128
-126
-124
-122
-120
-118
-116
-114
38
36
34
32
noaa
Meters AGL
1500
1000
500
300
100
00
02/09
18
12
06
Job ID: 146716
Job Start: Thu Mar 26 20:12:46 UTC 2015
Source 1 lat.: 38.536389 lon.: -121.742778 hgts: 100, 200, 300 m AGL
Trajectory Direction: Backward
Duration: 24 hrs
Vertical Motion Calculation Method:
Isentropic
Meteorology: 0000Z 8 Feb 2015 - GDAS1

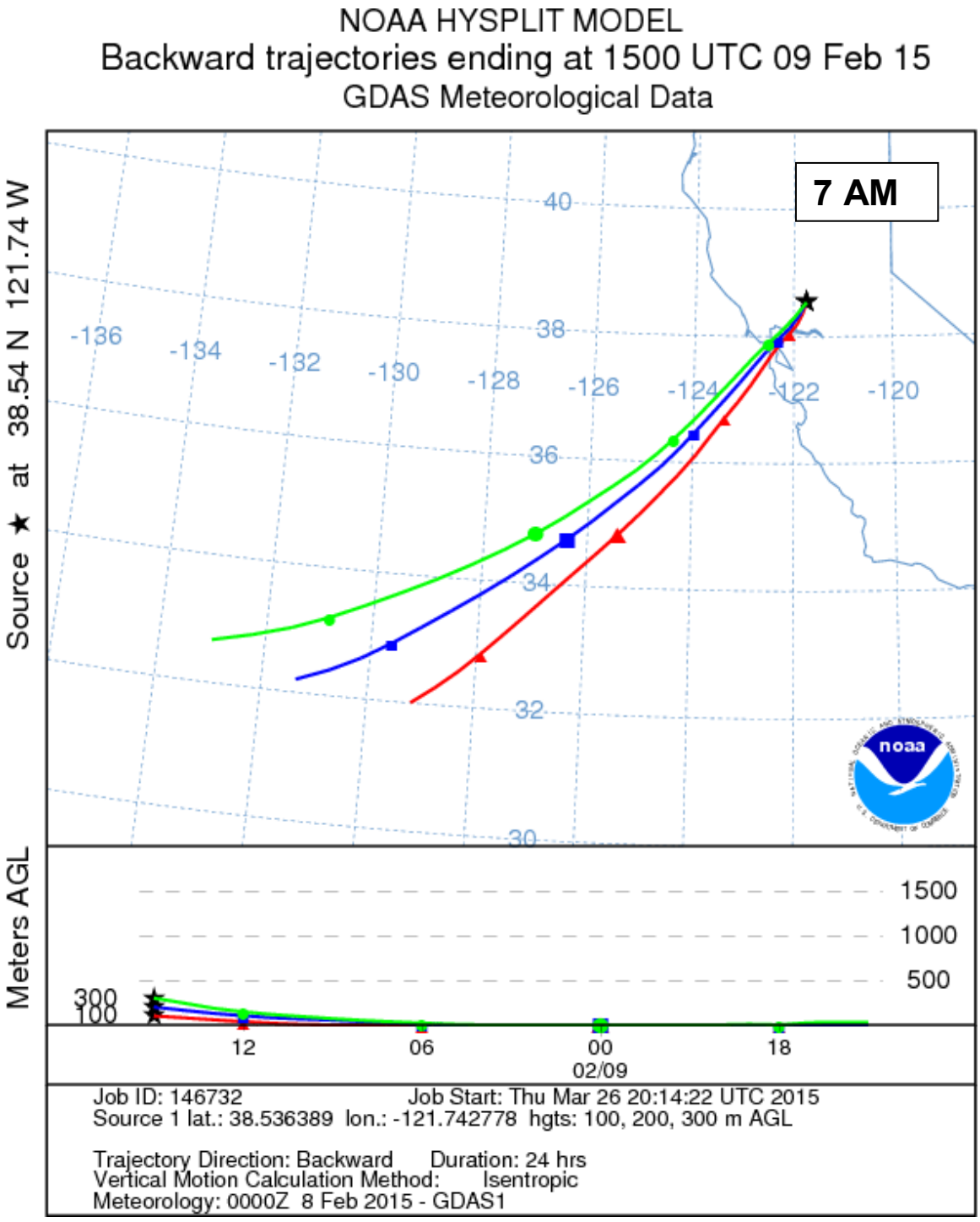
NOAA HYSPLIT MODEL
Backward trajectories ending at 1500 UTC 09 Feb 15
GDAS Meteorological Data
7 AM
Source ★ at 38.54 N 121.74 W
40
38
36
34
32
30
-136
-134
-132
-130
-128
-126
-124
-122
-120
noaa
Meters AGL
1500
1000
500
300
100
12
06
00
18
02/09
Job ID: 146732
Job Start: Thu Mar 26 20:14:22 UTC 2015
Source 1 lat.: 38.536389 lon.: -121.742778 hgts: 100, 200, 300 m AGL
Trajectory Direction: Backward
Duration: 24 hrs
Vertical Motion Calculation Method:
Isentropic
Meteorology: 0000Z 8 Feb 2015 - GDAS1

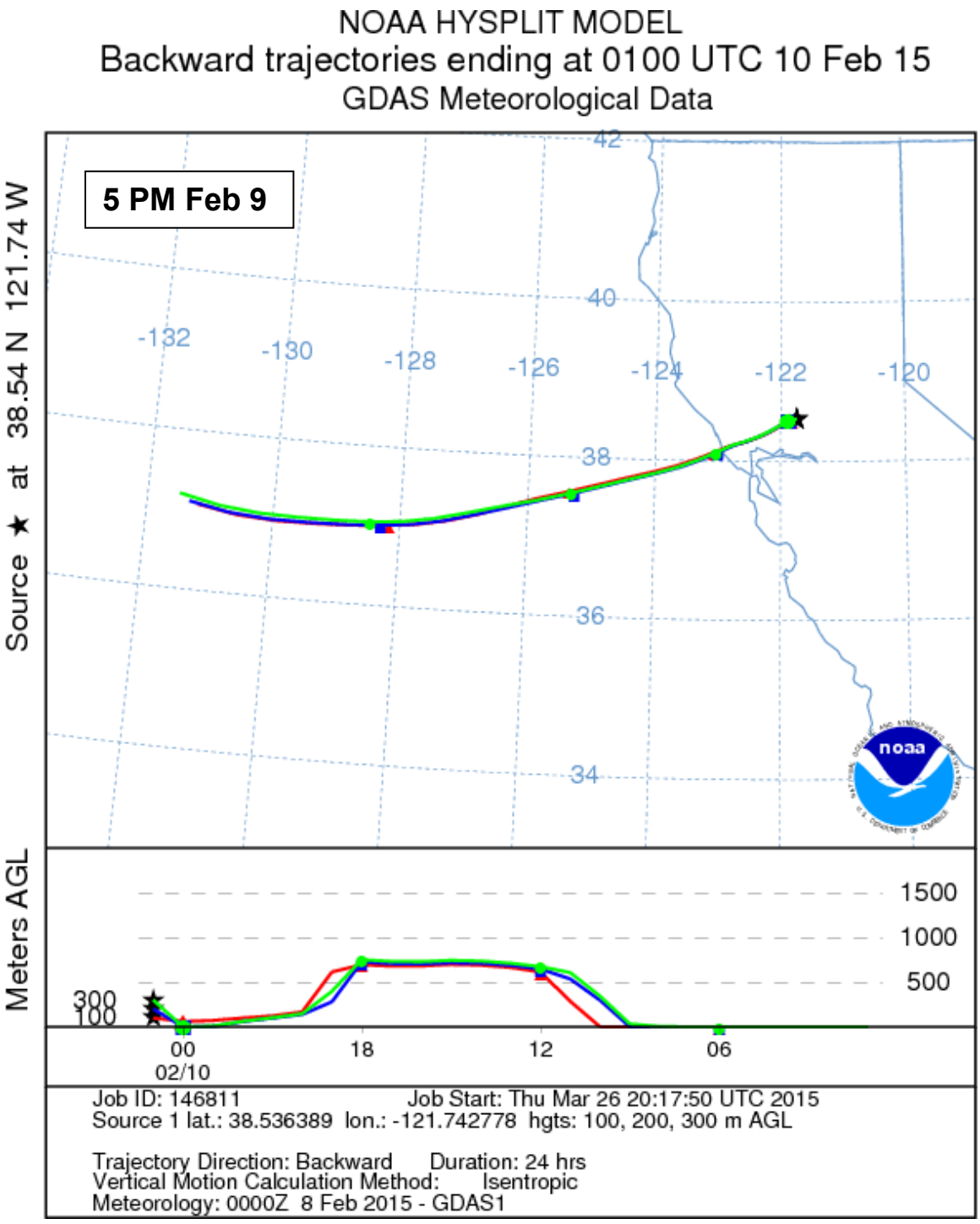
NOAA HYSPLIT MODEL
Backward trajectories ending at 0100 UTC 10 Feb 15
GDAS Meteorological Data
5 PM Feb 9
Source ★ at 38.54 N 121.74 W
42
40
38
36
34
-132
-130
-128
-126
-124
-122
-120
noaa
Meters AGL
1500
1000
500
300
100
00
02/10
18
12
06
Job ID: 146811
Job Start: Thu Mar 26 20:17:50 UTC 2015
Source 1 lat.: 38.536389 lon.: -121.742778 hgts: 100, 200, 300 m AGL
Trajectory Direction: Backward
Duration: 24 hrs
Vertical Motion Calculation Method:
Isentropic
Meteorology: 0000Z 8 Feb 2015 - GDAS1

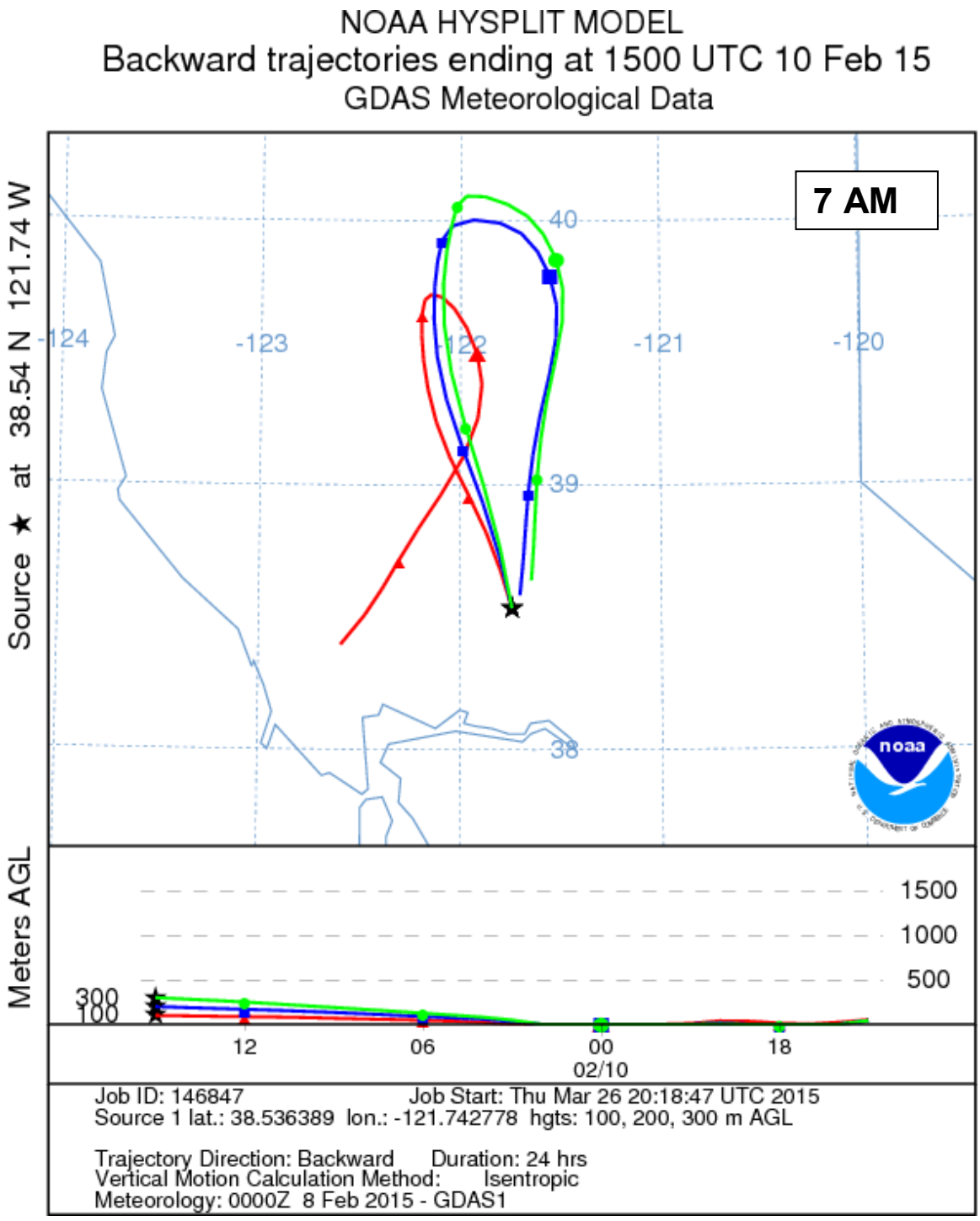
NOAA HYSPLIT MODEL
Backward trajectories ending at 1500 UTC 10 Feb 15
GDAS Meteorological Data
7 AM
Source ★ at 38.54 N 121.74 W
-124
-123
-122
-121
-120
40
39
38
noaa
Meters AGL
1500
1000
500
300
100
12
06
00
18
02/10
Job ID: 146847
Job Start: Thu Mar 26 20:18:47 UTC 2015
Source 1 lat.: 38.536389 lon.: -121.742778 hgts: 100, 200, 300 m AGL
Trajectory Direction: Backward
Duration: 24 hrs
Vertical Motion Calculation Method:
Isentropic
Meteorology: 0000Z 8 Feb 2015 - GDAS1

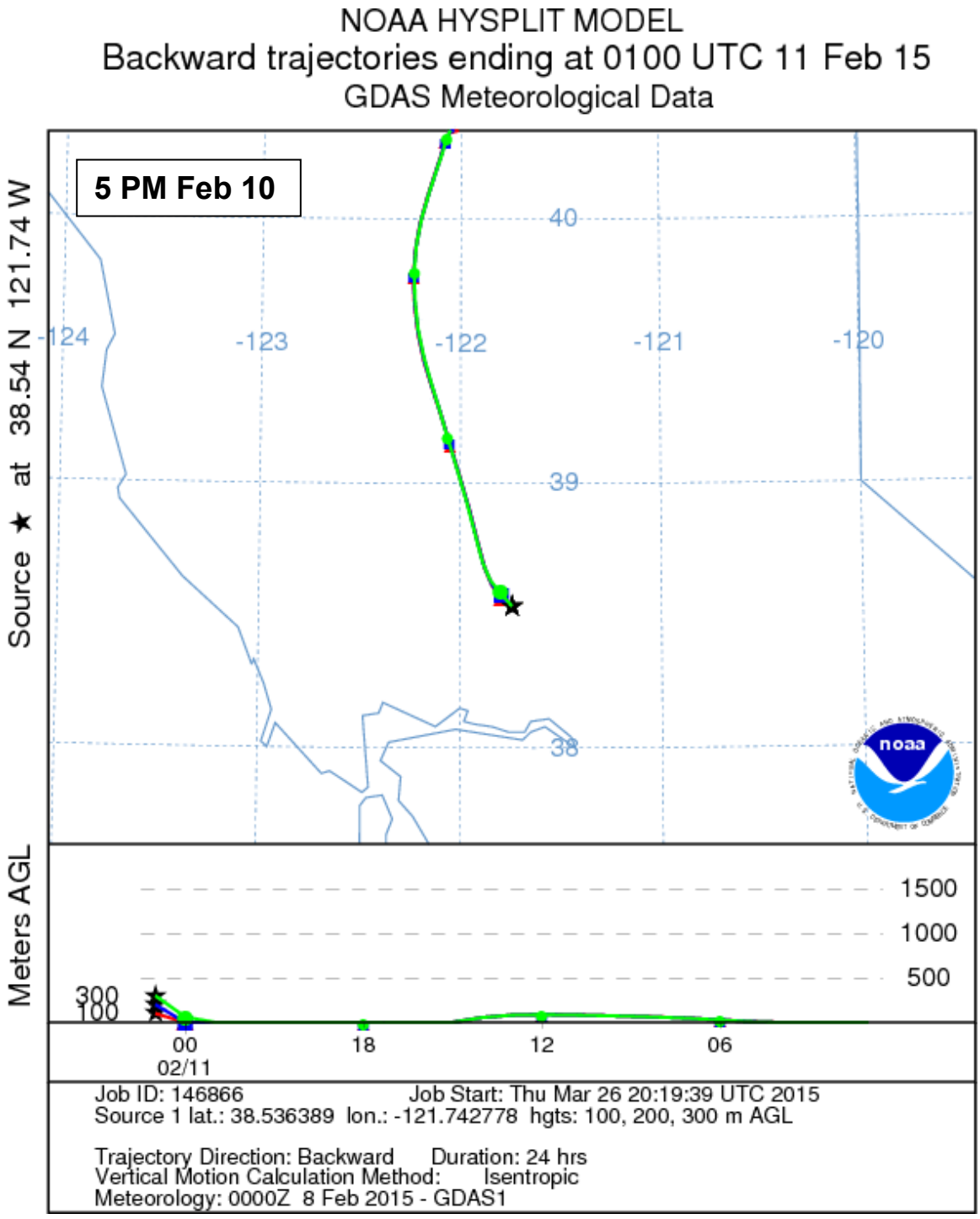
NOAA HYSPLIT MODEL
Backward trajectories ending at 0100 UTC 11 Feb 15
GDAS Meteorological Data
5 PM Feb 10
Source ★ at 38.54 N 121.74 W
40
39
38
-124
-123
-122
-121
-120
noaa
Meters AGL
1500
1000
500
300
100
00
02/11
18
12
06
Job ID: 146866
Job Start: Thu Mar 26 20:19:39 UTC 2015
Source 1 lat.: 38.536389 lon.: -121.742778 hgts: 100, 200, 300 m AGL
Trajectory Direction: Backward
Duration: 24 hrs
Vertical Motion Calculation Method:
Isentropic
Meteorology: 0000Z 8 Feb 2015 - GDAS1

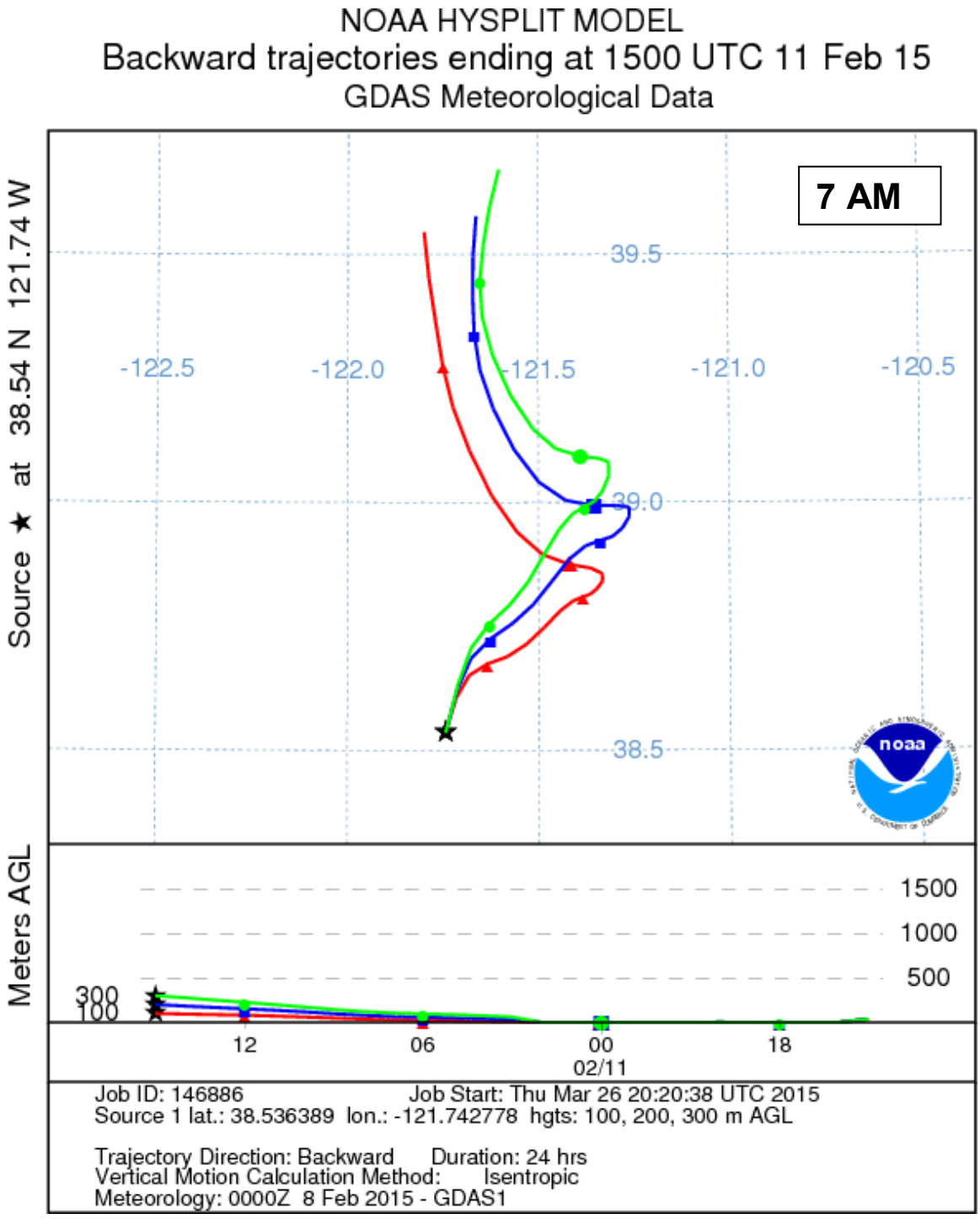
NOAA HYSPLIT MODEL
Backward trajectories ending at 1500 UTC 11 Feb 15
GDAS Meteorological Data
7 AM
Source ★ at 38.54 N 121.74 W
39.5
39.0
38.5
-122.5
-122.0
-121.5
-121.0
-120.5
noaa
Meters AGL
1500
1000
500
300
100
12
06
00
18
02/11
Job ID: 146886
Job Start: Thu Mar 26 20:20:38 UTC 2015
Source 1 lat.: 38.536389 lon.: -121.742778 hgts: 100, 200, 300 m AGL
Trajectory Direction: Backward
Duration: 24 hrs
Vertical Motion Calculation Method:
Isentropic
Meteorology: 0000Z 8 Feb 2015 - GDAS1

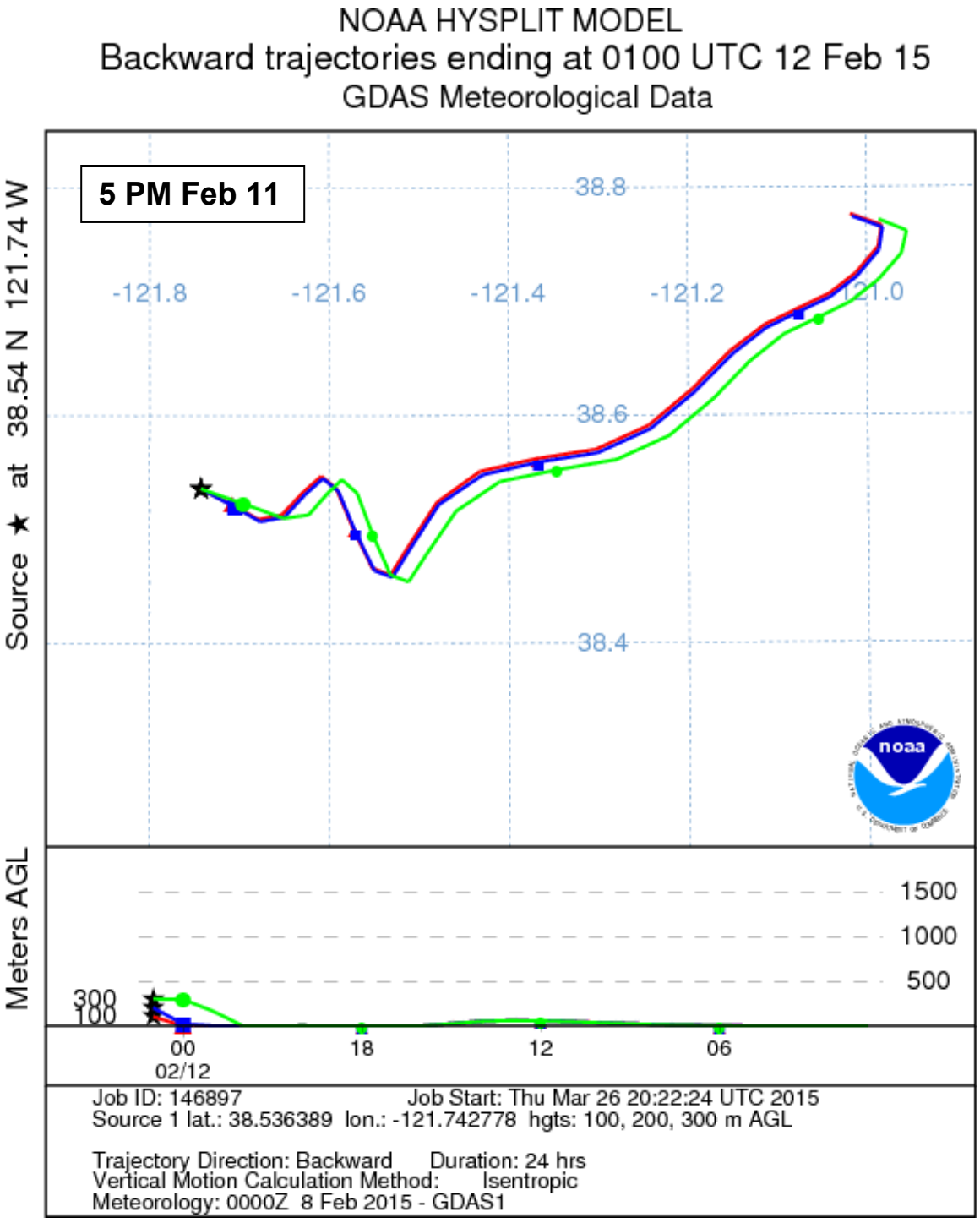
NOAA HYSPLIT MODEL
Backward trajectories ending at 0100 UTC 12 Feb 15
GDAS Meteorological Data
5 PM Feb 11
Source ★ at 38.54 N 121.74 W
38.8
38.6
38.4
-121.8
-121.6
-121.4
-121.2
-121.0
noaa
Meters AGL
1500
1000
500
300
100
00
02/12
18
12
06
Job ID: 146897
Job Start: Thu Mar 26 20:22:24 UTC 2015
Source 1 lat.: 38.536389 lon.: -121.742778 hgts: 100, 200, 300 m AGL
Trajectory Direction: Backward
Duration: 24 hrs
Vertical Motion Calculation Method:
Isentropic
Meteorology: 0000Z 8 Feb 2015 - GDAS1

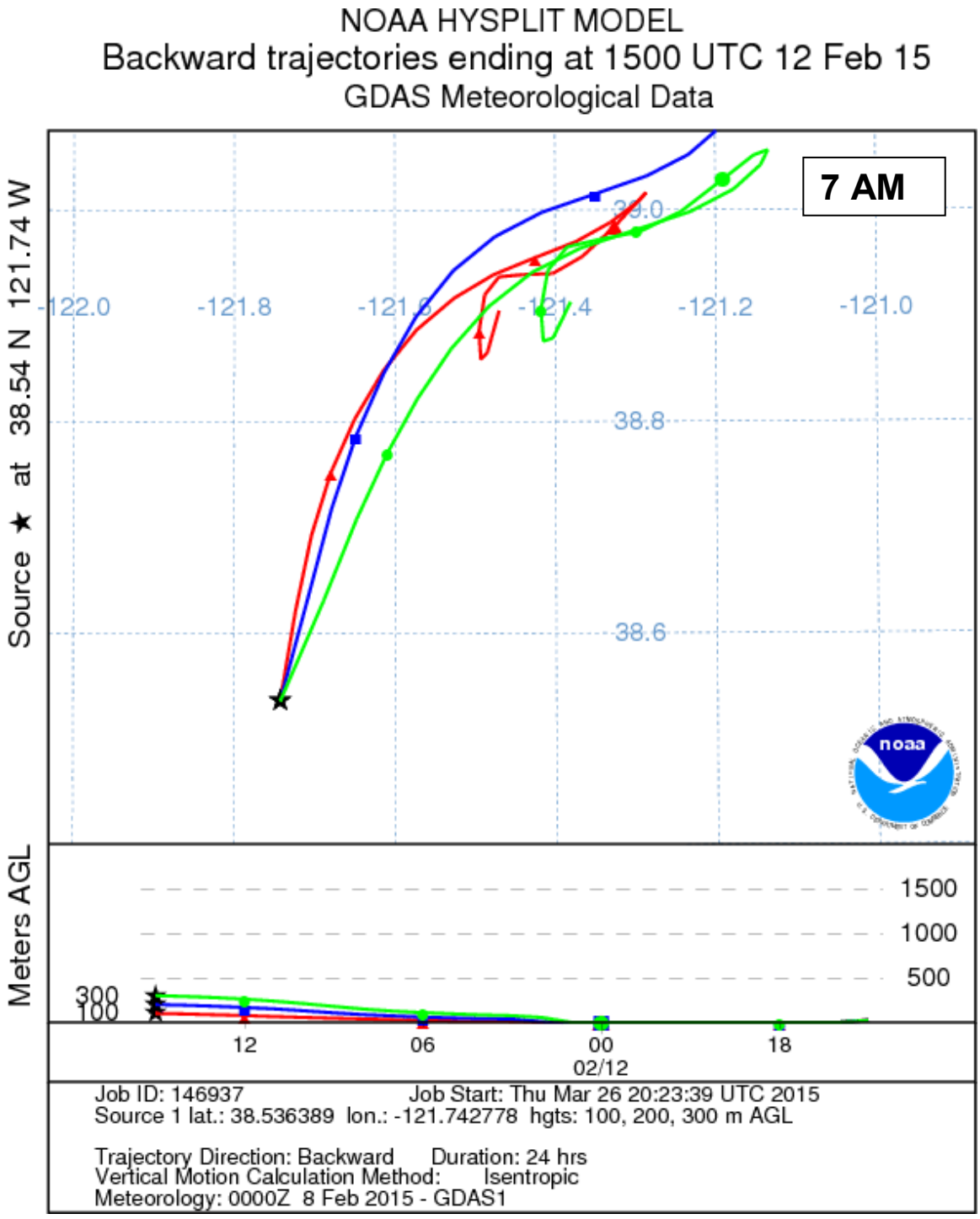
NOAA HYSPLIT MODEL
Backward trajectories ending at 1500 UTC 12 Feb 15
GDAS Meteorological Data
7 AM
Source ★ at 38.54 N 121.74 W
-122.0
-121.8
-121.6
-121.4
-121.2
-121.0
39.0
38.8
38.6
noaa
Meters AGL
1500
1000
500
300
100
12
06
00
18
02/12
Job ID: 146937
Job Start: Thu Mar 26 20:23:39 UTC 2015
Source 1 lat.: 38.536389 lon.: -121.742778 hgts: 100, 200, 300 m AGL
Trajectory Direction: Backward
Duration: 24 hrs
Vertical Motion Calculation Method:
Isentropic
Meteorology: 0000Z 8 Feb 2015 - GDAS1

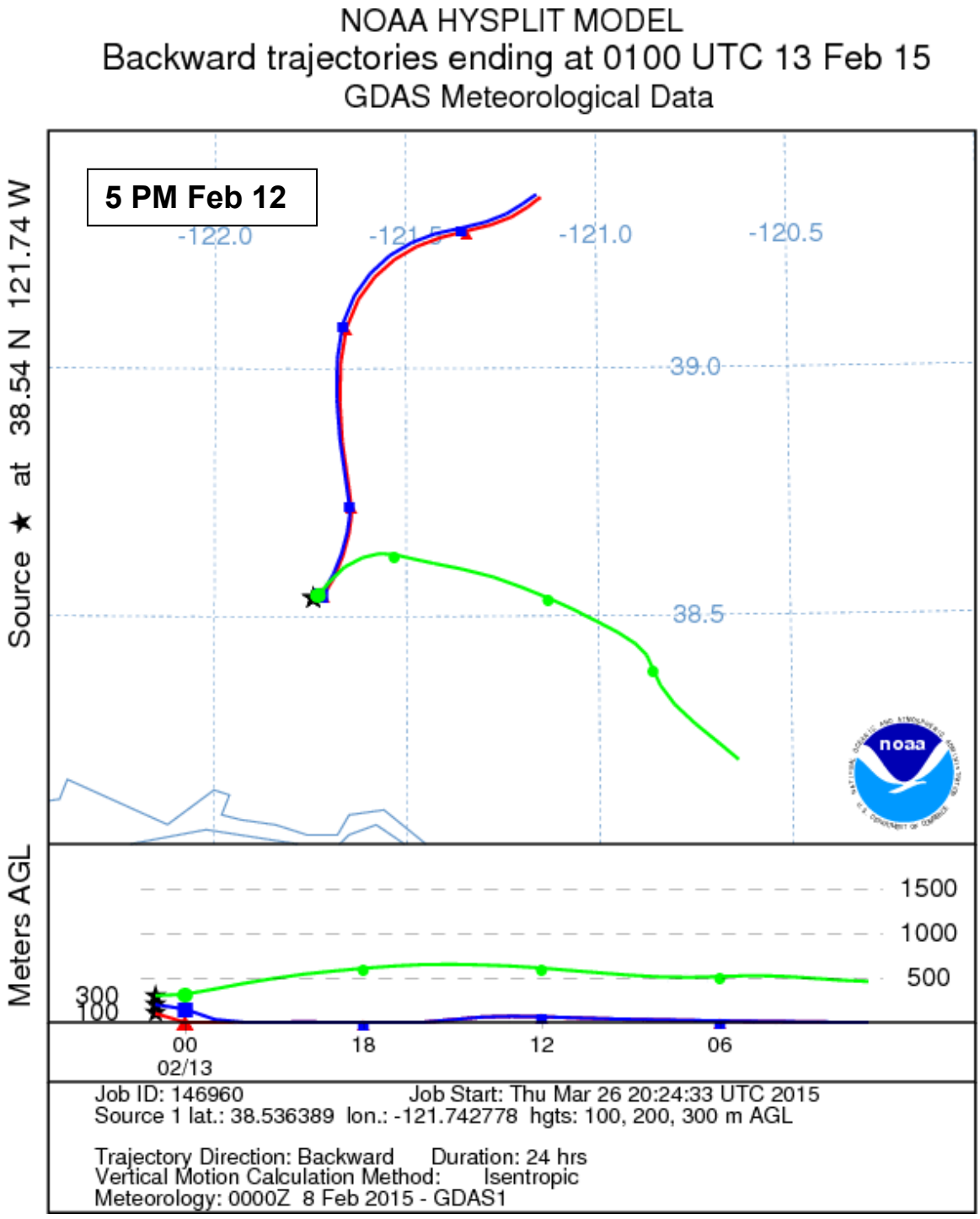
NOAA HYSPLIT MODEL
Backward trajectories ending at 0100 UTC 13 Feb 15
GDAS Meteorological Data
5 PM Feb 12
Source ★ at 38.54 N 121.74 W
-122.0
-121.5
-121.0
-120.5
39.0
38.5
noaa
Meters AGL
1500
1000
500
300
100
00
02/13
18
12
06
Job ID: 146960
Job Start: Thu Mar 26 20:24:33 UTC 2015
Source 1 lat.: 38.536389 lon.: -121.742778 hgts: 100, 200, 300 m AGL
Trajectory Direction: Backward
Duration: 24 hrs
Vertical Motion Calculation Method:
Isentropic
Meteorology: 0000Z 8 Feb 2015 - GDAS1

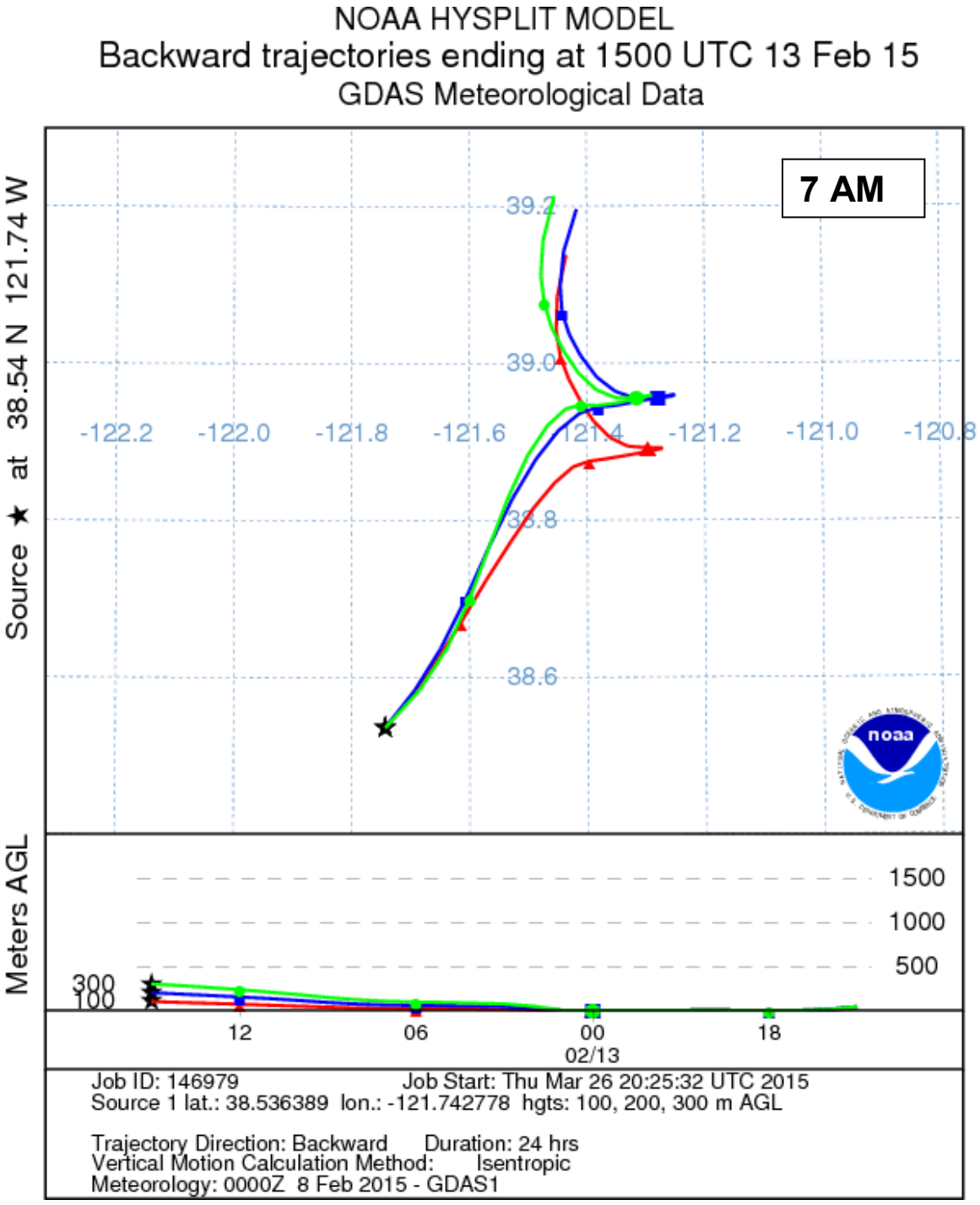
NOAA HYSPLIT MODEL
Backward trajectories ending at 1500 UTC 13 Feb 15
GDAS Meteorological Data
7 AM
Source ★ at 38.54 N 121.74 W
39.2
39.0
38.8
38.6
-122.2
-122.0
-121.8
-121.6
-121.4
-121.2
-121.0
-120.8
noaa
Meters AGL
1500
1000
500
300
100
12
06
00
18
02/13
Job ID: 146979
Job Start: Thu Mar 26 20:25:32 UTC 2015
Source 1 lat.: 38.536389 lon.: -121.742778 hgts: 100, 200, 300 m AGL
Trajectory Direction: Backward
Duration: 24 hrs
Vertical Motion Calculation Method:
Isentropic
Meteorology: 0000Z 8 Feb 2015 - GDAS1

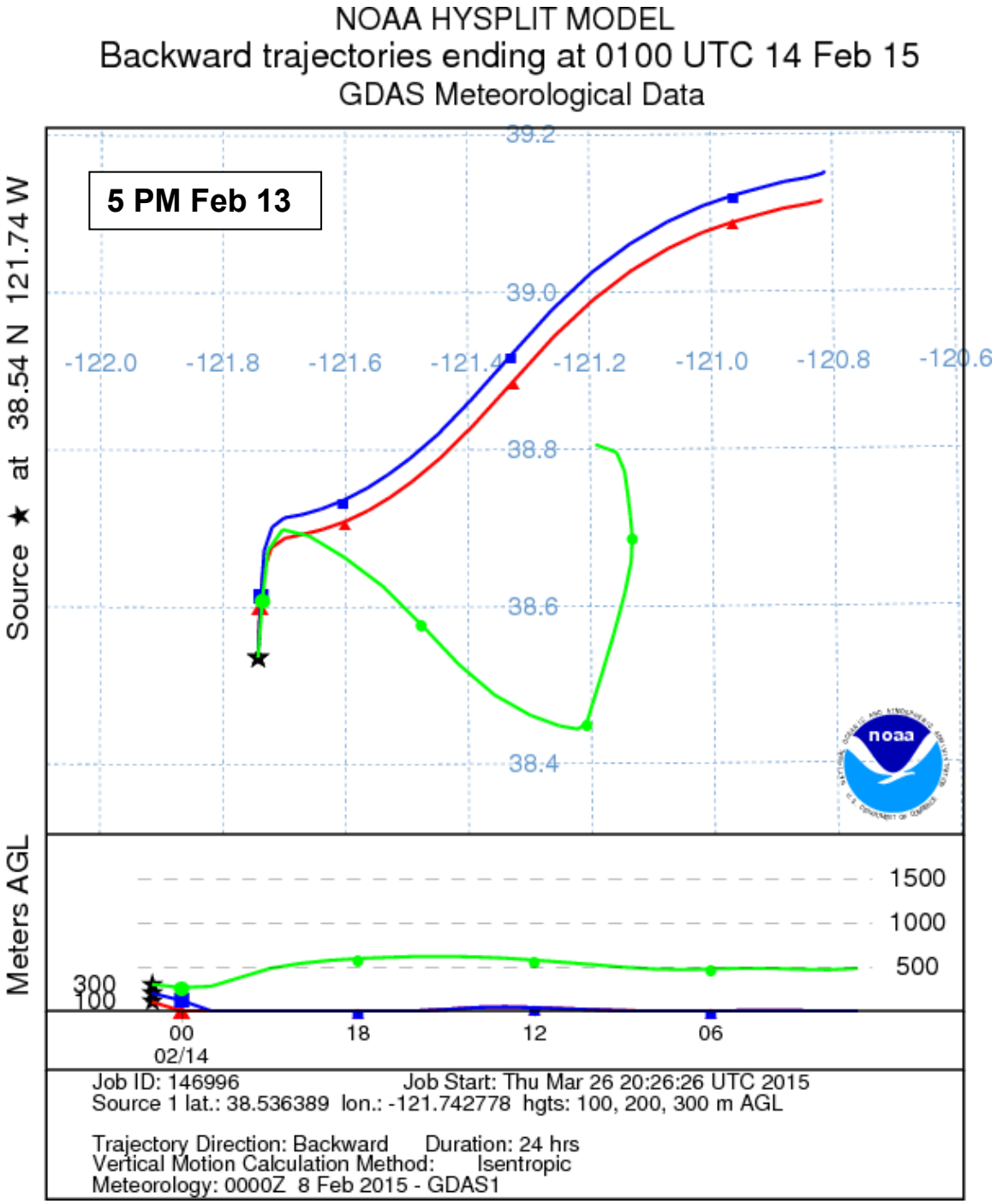
NOAA HYSPLIT MODEL
Backward trajectories ending at 0100 UTC 14 Feb 15
GDAS Meteorological Data
5 PM Feb 13
Source ★ at 38.54 N 121.74 W
39.2
39.0
38.8
38.6
38.4
-122.0
-121.8
-121.6
-121.4
-121.2
-121.0
-120.8
-120.6
noaa
Meters AGL
1500
1000
500
300
100
00
02/14
18
12
06
Job ID: 146996 Job Start: Thu Mar 26 20:26:26 UTC 2015
Source 1 lat.: 38.536389 lon.: -121.742778 hgts: 100, 200, 300 m AGL
Trajectory Direction: Backward Duration: 24 hrs
Vertical Motion Calculation Method: Isentropic
Meteorology: 0000Z 8 Feb 2015 - GDAS1

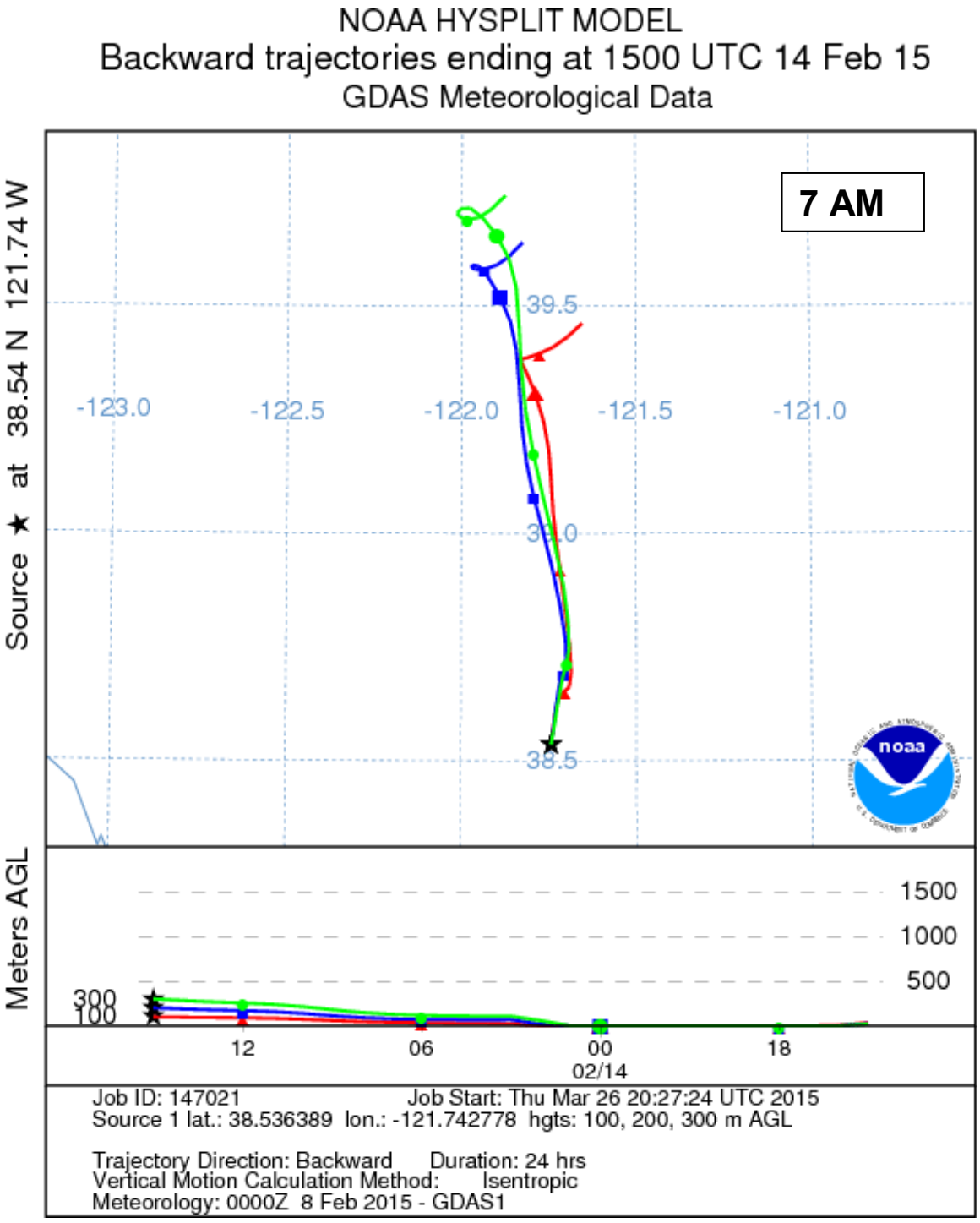
NOAA HYSPLIT MODEL
Backward trajectories ending at 1500 UTC 14 Feb 15
GDAS Meteorological Data
7 AM
Source ★ at 38.54 N 121.74 W
-123.0
-122.5
-122.0
-121.5
-121.0
39.5
38.5
noaa
Meters AGL
1500
1000
500
300
100
12
06
00
18
02/14
Job ID: 147021
Job Start: Thu Mar 26 20:27:24 UTC 2015
Source 1 lat.: 38.536389 lon.: -121.742778 hgts: 100, 200, 300 m AGL
Trajectory Direction: Backward
Duration: 24 hrs
Vertical Motion Calculation Method:
Isentropic
Meteorology: 0000Z 8 Feb 2015 - GDAS1

UTC (Zulu) Time Conversion Chart

UTC (Zulu)	PST/ ALDT	PDT/ MST	MDT/ CST	CDT/ EST	EDT/ AST	ALST	HST
0000*	1600	1700	1800	1900	2000	1500	1400
0100	1700	1800	1900	2000	2100	1600	1500
0200	1800	1900	2000	2100	2200	1700	1600
0300	1900	2000	2100	2200	2300	1800	1700
0400	2000	2100	2200	2300	0000*	1900	1800
0500	2100	2200	2300	0000*	0100	2000	1900
0600	2200	2300	0000*	0100	0200	2100	2000
0700	2300	0000*	0100	0200	0300	2200	2100
0800	0000*	0100	0200	0300	0400	2300	2200
0900	0100	0200	0300	0400	0500	0000*	2300
1000	0200	0300	0400	0500	0600	0100	0000*
1100	0300	0400	0500	0600	0700	0200	0100
1200	0400	0500	0600	0700	0800	0300	0200

UTC (Zulu)	PST/ ALDT	PDT/ MST	MDT/ CST	CDT/ EST	EDT/ AST	ALST	HST
1300	0500	0600	0700	0800	0900	0400	0300
1400	0600	0700	0800	0900	1000	0500	0400
1500	0700	0800	0900	1000	1100	0600	0500
1600	0800	0900	1000	1100	1200	0700	0600
1700	0900	1000	1100	1200	1300	0800	0700
1800	1000	1100	1200	1300	1400	0900	0800
1900	1100	1200	1300	1400	1500	1000	0900
2000	1200	1300	1400	1500	1600	1100	1000
2100	1300	1400	1500	1600	1700	1200	1100
2200	1400	1500	1600	1700	1800	1300	1200
2300	1500	1600	1700	1800	1900	1400	1300
2400	1600	1700	1800	1900	2000	1500	1400

***0000 and 2400 are interchangeable.**
2400 is associated with the date of the day ending, 0000 with the day just starting.

UTC = Coordinated Universal Time, or **Zulu**
PST = Pacific Standard Time (UTC - 8 hours)
ALDT = Alaskan Daylight Time (UTC - 8 hours)
PDT = Pacific Daylight Time (UTC - 7 hours)
MST = Mountain Standard Time (UTC - 7 hours)
MDT = Mountain Daylight Time (UTC - 6 hours)
CST = Central Standard Time (UTC - 6 hours)
CDT = Central Daylight Time (UTC - 5 hours)
EST = Eastern Standard Time (UTC - 5 hours)
EDT = Eastern Daylight Time (UTC - 4 hours)
AST = Atlantic Standard Time (UTC - 4 hours)
ALST = Alaskan Standard Time (UTC - 9 hours)
HST = Hawaiian Standard Time (UTC - 10 hours)

Attachment 7: File list for extended data in digital report only

The following files are a part of this report but not included in the hard document. The files include complete sets of data generated from the analyses, and a full version of the DELTA quality assurance document, and a pdf of the paper used for the ultra-fine species comparison. These files will be provided with the softcopy of this report.

Excel files:
S-XRF elemental analyses concentrations filename, OlDr 609 Elements Data.xlsx
Full Beta Mass analyses concentrations for site Olive Drive: OlDr 609 Beta Data.xlsx
Data are from Norcal project site: Site 1, Olive Drive.

Documents:
Full DELTA Group DRUM Quality Assurance Protocols: DQAP.pdf

Recent paper (.pdf) used in ultra-fine elemental comparison:
Seasonal variability of ultra-fine metals downwind of a heavily traveled secondary road, Atmospheric Environment, 94 (2014)173-179, doi:10.1016/j.atmosenv.2014.05.025